The Institute of Paper Chemistry

Appleton, Wisconsin

Doctor's Dissertation

Polymer Adsorption and Flocculation of Particles in Turbulent Flow

Anders L. Wigsten

June, 1983

POLYMER ADSORPTION AND FLOCCULATION OF PARTICLES IN TURBULENT FLOW

A thesis submitted by

Anders L. Wigsten

M.S. 1975, Chalmers University of Technology
Goteborg, Sweden

M.S. 1980, Lawrence University

in partial fulfillment of the requirements
of The Institute of Paper Chemistry
for the degree of Doctor of Philosophy
from Lawrence University,
Appleton, Wisconsin

June, 1983

TABLE OF CONTENTS

ABSTRACT

Polymers are commonly used in the paper industry as retention aids and flocculants. Simple electrolytes can also aid retention and flocculation if added in sufficient amounts. Reports in the literature on the effects of polymers on colloidal flocculation rates vary from slower to faster compared to coagulation with simple electrolytes. The present work was designed to study the relationship between the kinetics of polymer adsorption and particle flocculation under nonquiescent conditions.

Simultaneous polymer adsorption and particle flocculation rates were measured for a dilute system in turbulent pipe flow. The particles were negatively charged polystyrene latex, diameter 1.07 μm, and the polymer was a linear high molecular weight polyamine. The charge degree of the polymer was varied from 95% at pH 3 to 3% at pH 10. Reaction times ranged from 0.16 to 2.4 seconds. Flocculation rates were compared with rates obtained by destabilizing the suspension with a simple electrolyte. Polymer induced flocculation was considerably slower. Concentrations of unadsorbed polymer measured at the end of the pipe were rarely below 75% of the initial dose.

It was concluded that polymer adsorption was the rate determining step in the overall flocculation process in this system. Although restabilization did occur at high polymer doses, the amounts adsorbed never exceeded fifty per cent of maximum adsorption under equilibrium conditions. This suggests that the effective surface coverage is higher under nonequilibrium conditions than at equilibrium for a given amount of adsorbed polymer. The high charge density polymer was more effective as a flocculant than the low charge density polymer. This was explained as the result of its higher adsorption rate and its ability to form stronger flocs.

The measured adsorption and flocculation rates are discussed in terms of collision rate theories, where the shear rate in the system and the hydrodynamic sizes of the particles and the polymer molecules are taken into consideration.

INTRODUCTION

Flocculation phenomena are of vital interest in many industrial situations. In the paper industry the wet end of a paper machine and the waste water treatment plant are examples of process segments where flocculation is of importance.

Aqueous colloidal suspensions are generally stabilized by electrostatic surface charges, and destabilization can occur via several mechanisms. Sufficiently high concentrations of inorganic (simple) electrolytes will screen out the electrostatic repulsive forces, allowing the attractive van der Waals forces to cause aggregation, i.e., coagulation in the classical sense (1). Synthetic polymers, especially those of high molecular weight, have proven to be very effective destabilizing agents or flocculants and they are now commonly used in the industry.

Two mechanisms have been proposed for flocculation with polymers: bridging and electrostatic patch. In the former mechanism, charge neutralization is not necessary as long as the polymer is capable of forming a bridge between two particles, spanning a gap wider than the range dominated by the electrostatic repulsive forces. In the latter the polymer has to have high charge density and opposite charge to the colloidal particles; flocculation occurs as a result of electrostatic attraction between patches of opposite charge on colliding particles.

When polymers are used as flocculants, adsorption of these polymers onto the colloidal particles is required before flocculation can occur. The adsorption time is of consequence not only for flocculation but also for processes where adsorption alone is the desired result of a polymer addition. An example of this would be the addition of sizing and strength agents to a paper furnish.

The concentrations, mixing conditions and hydrodynamic sizes of the colloidal particles and the polymer molecules will determine adsorption and flocculation rates. A knowledge of the relations between these variables is necessary to optimize any adsorption and flocculation process.

POLYMER ADSORPTION AND PARTICLE FLOCCULATION

The effect of polymers on colloid destabilization has received much attention in recent years and good presentations of the topic can be found in review papers (2,3) and proceedings from recent symposia (4,5). The present study is focused on the relationship between the kinetics of polymer adsorption and particle flocculation.

In this study the kinetics of polymer adsorption are treated in close analogy to coagulation rate theories. A review of the latter is therefore given before polymer adsorption and polymer-aided flocculation are discussed. Following the terminology of earlier workers (6) destabilization and aggregation is defined as coagulation when caused by a simple electrolyte and flocculation when caused by a polymer. Rapid coagulation is defined as the case where the effects of the electrostatic repulsive forces are completely eliminated by high concentrations of simple electrolyte. A process - coagulation, adsorption or flocculation - is further defined as perikinetic if the transport mechanism is solely due to Brownian motion and orthokinetic if solely due to shear.

COAGULATION

Smoluchowski Theory

The classical work of von Smoluchowski (7,8) is the base case against which modern and more sophisticated analyses are compared. A complete derivation of the Smoluchowski theory is given in (1) and a review including recent advances in coagulation theory is given by Schowalter in (5).

Von Smoluchowski analyzed two cases of coagulation in the absence of repulsive forces. He assumed that every collision was successful and that the coagulating

particles were spherical. In the first case particle transport was solely due to Brownian motion, i.e., perikinetic coagulation. The rate of change of the number concentration of particles of size k can then be written

$$dn_k/dt = 0.5 \sum_{\substack{i=1 \\ j=k-i}}^{i=k-1} 4\pi D_{ij} (a_i + a_j) n_i n_j - \sum_{i=1}^{\infty} 4\pi D_{ik} (a_i + a_k) n_i n_k \qquad (1)$$

where

n_k = number concentration of particles containing k singlets, m^{-3}

t = time, s

$D_{ij} = D_i + D_j$ = relative diffusion coefficient, m^2/s

a_i = particle radius, m

The first term on the right hand side of Eq. (1) describes the appearance rate of k-particles and the second term describes the disappearance rate.

The second case treated by von Smoluchowski dealt with coagulation in laminar shear flow, i.e., orthokinetic coagulation. As a starting point for this analysis he considered the flux of particles into a "collision sphere" surrounding a central reference particle. The radius of the collision sphere is the sum of the radius of the central particle, a_1, and the radius of the approaching particle, a_2, see Fig. 1. The resulting coagulation rate equation is

$$dn_k/dt = 0.5 \sum_{\substack{i=1 \\ j=k-i}}^{i=k-1} (4G/3)(a_i + a_j)^3 n_i n_j - \sum_{i=1}^{\infty} (4G/3)(a_i + a_k)^3 n_i n_k \qquad (2)$$

where

G = shear rate, s^{-1}

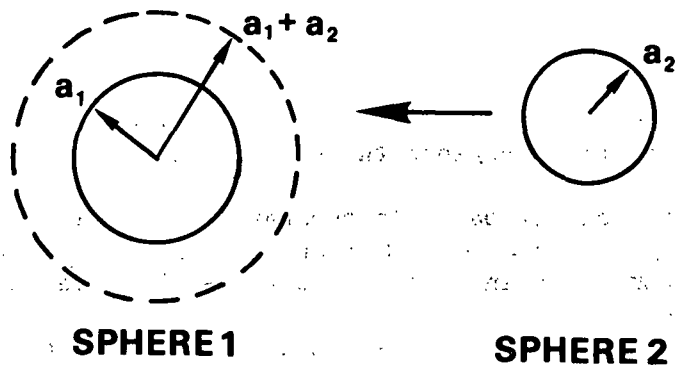

Figure 1. Definition of collision sphere with radius $a_1 + a_2$.

Camp and Stein (9) extended the Smoluchowski approach to turbulent conditions. They derived an expression for an average shear rate, $\overline{G}$, which should be substituted for the laminar shear rate, G, in Eq. (2):

$$\overline{G} = (\varepsilon/\nu)^{1/2} \tag{3}$$

where

ε = energy dissipation, J/(kgs)

ν = kinematic viscosity, m^2/s

Saffman and Turner (10) analyzed the collision rates in isotropic turbulence of equal sized particles smaller than the Kolmogorov microscale. They arrived at a rate constant of

$$k = 1.294\ (\varepsilon/\nu)^{1/2} \tag{4}$$

This is in very close agreement with the Camp and Stein rate constant

$$k = (4\overline{G}/3) = 1.333\ (\varepsilon/\nu)^{1/2} \tag{5}$$

Delichatsios and Probstein (11), developing an approach suggested by Levich (12), obtained a theoretical rate constant that was 40% lower than the values given above.

Hydrodynamic Effects

Perikinetic Coagulation

The analyses outlined above neglect the hydrodynamic and viscous effects that occur at very small distances of particle separation. Spielman (13) and Honig et al. (14) analyzed the case of Brownian coagulation. The relative diffusion coefficient D_{ij} tends to zero when the distance of separation between particles tends to zero. Without an attractive force like the London-van der Waals force, which increases rapidly as the gap narrows, the coagulation rate would be vanishingly small even in the absence of repulsive forces. A collision efficiency, α, for rapid coagulation can then be defined as

$$\alpha = J/J_s \tag{6}$$

where

J = observed rapid coagulation rate

J_s = rapid coagulation rate according to von Smoluchowski

Including both viscous interactions and attractive London-van der Waals forces in the analysis, but excluding repulsion, leads to a collision efficiency of order unity for equal sized particles. This result is rather insensitive to the value of the Hamaker constant, A. A twentyfold change in A produces only a 60% change in α, which can be either smaller or larger than one. This explains the success of the Smoluchowski theory, which by definition gives a collision efficiency of unity. Experimentally determined collision efficiencies for rapid perikinetic coagulation are of order unity, which confirms the validity of the detailed theory. Spherical particles with a radius of 0.5 μm and a Hamaker constant of $5 \cdot 10^{-21}$ J [as for polystyrene latex (15)] take on a theoretical collision efficiency of

$$\alpha = 0.5 \qquad (7)$$

Orthokinetic Coagulation

The Smoluchowski equation for laminar shear flow (2) is based on the assumption that the particles move along rectilinear paths. Modern analyses of orthokinetic coagulation take into account the curvilinear nature of streamlines around solid spheres (16,17). Touching collisions are altogether impossible in the absence of attractive forces. Closed streamlines around the particles determine the distance of closest approach, d_{min}, see Fig. 2. Values of d_{min}/a_1, vary from $4.2 \cdot 10^{-5}$ for $\lambda = 1$, to 0.16 for $\lambda \to \infty$, where $\lambda = a_1/a_2$ (16).

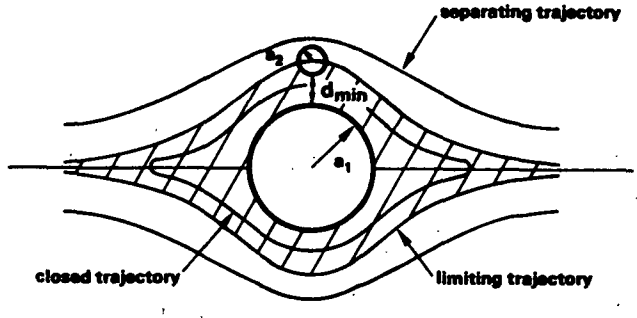

Figure 2. Equatorial trajectories of two spheres in simple shear (schematic). The solid lines are possible trajectories of a sphere of radius a_2 with respect to a central reference sphere of radius a_1. Two kinds of trajectory exist: separating (or open) and closed ones, separated by a limiting trajectory. The shaded region is the region of the closed trajectories. Adapted from (16) by permission of the copyright owner.

A collision efficiency for rapid orthokinetic coagulation can be defined in analogy to Eq. (6), as the observed rate divided by the Smoluchowski rate. Van de Ven and Mason (17) obtained the following functional form for the collision efficiency:

$$\alpha_{ii} = g(\lambda_L/a_i)C_A^{0.18}; \qquad 10^{-5} < C_A < 10^{-1} \qquad (8)$$

where

λ_L = London retardation wavelength, nm

$C_A = A/(36\pi\mu\ G\ a_i^3)^{0.18}$

$$C_A = \frac{A}{36\pi\eta G a_i^3}$$

The double index ii denotes collisions between equal sized particles; the index ij would stand for collisions between particles of different sizes. For conditions typical of this study, $A = 5 \cdot 10^{-21} J$, $G = 1800\ s^{-1}$ and $a_1 = 0.535\ \mu m$, the value of C_A is $1.6 \cdot 10^{-4}$. Polystyrene latex particles with a radius of 0.5 μm and a retardation wavelength of 100 nm give a value of 0.95 for $g(\lambda_L/a_1)$ (17), resulting in the following expression for the collision efficiency.

$$\alpha_{11} = 0.788 G^{0.18} \qquad (9)$$

For a shear rate of $1800 s^{-1}$, typical of the present study, the collision efficiency would be

$$\alpha_{11} = 0.204 \qquad (10)$$

Adler (19) and Higashitani et al. (20) extended the analysis to include collision efficiencies, α_{ij}, for unequal sized particles. Figure 3, reproduced from (20), shows the dependence of the collision efficiency on the parameter N_s, which is the ratio of hydrodynamic forces to attractive colloidal forces.

$$N_s = 6\pi\mu\ a_{ij}^3\ G/A \qquad (11)$$

where

$$a_{ij} = (a_i + a_j)/2$$

For a shear rate typical of the present study, $1800\ s^{-1}$, the value of N_s is 1040.

Note the strong effect on collision efficiency of the particle size ratio λ in Fig. 3. The authors (20) speculated that the collision efficiency for large particles and large λ values may set an upper practical limit to aggregate size under a

given set of coagulation conditions. They suggested this as an alternative mechanism to breakup, in explaining the maximum limit of aggregate sizes often seen experimentally.

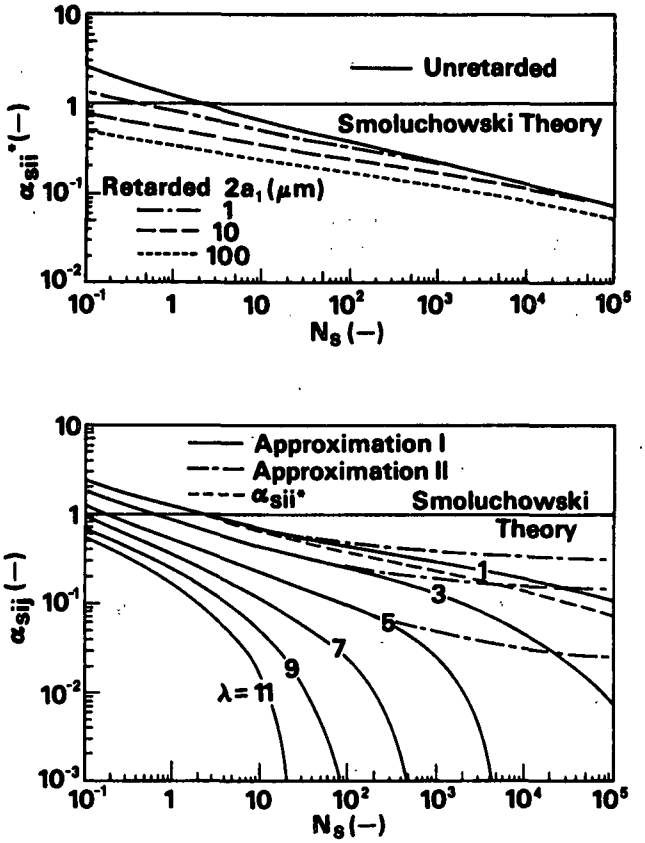

Figure 3. Collision efficienies of equal spheres, α_{sii}^*, and of unequal spheres, α_{sij}. Reprinted from Higashitani et al. (20) by permission of the copyright owner.

Only rapid coagulation has been considered in the discussion above. Modern coagulation theories provide the means of also including electrostatic repulsive effects in the collision efficiency ("slow coagulation"). This aspect will, however, not be reviewed here, see, e.g., (16,18,19).

Finally it should be mentioned that additivity of perikinetic and orthokinetic coagulation rates is not theoretically justified (16,18). For high shear rates and large particles the perikinetic contribution can often be neglected. However, a significant error can result if additivity is assumed when Brownian motion is dominating.

KINETICS OF POLYMER ADSORPTION

It has been proposed (21,22,15) that the kinetics of polymer adsorption onto dispersed colloidal particles could be theoretically treated in close analogy with coagulation theory. The adsorption rate would then be calculated from a collision rate using equations similar to (1) and (2). This approach obviously requires the knowledge of the hydrodynamic size of a polymer molecule.

The dimensions of a linear, uncharged polymer in solution can be estimated with random flight statistics (23)

$$\langle r^2 \rangle = g(b) n l^2 \tag{12}$$

$\langle r^2 \rangle$ = mean square end-to-end distance, m^2

$g(b)$ = function of bond stiffness and excluded volume

n = number of bonds in a polymer chain

l = bond length, m

The polymer molecule behaves as a random coil in solution, with a time averaged shape of a spheroid (23). The root mean square radius of gyration, $\langle s^2 \rangle^{1/2}$, is related to the end-to-end distance according to Eq. (13).

$$\langle s^2 \rangle^{1/2} = (\langle r^2 \rangle / 6)^{1/2} \tag{13}$$

The radius of gyration can be determined with light scattering methods (23). A hydrodynamic diameter, "Stokes diameter", can also be obtained from direct measurements of Brownian diffusion coefficients (23).

A charged polymer, a polyelectrolyte, will have an expanded coil size due to electrostatic interactions. Expansion factors for use in Eq. (12) and (13) can be estimated from experimental data (24,25). Theoretical calculations of the expansion factor have also been attempted (26,27). A polymer of high charge density, i.e., a polymer with a large fraction of charged monomer units, can have a radius of gyration several times the radius of the same polymer in an uncharged state, see also Appendix I.

It has been proposed (28) that the rate of adsorption of a polymer onto a smooth solid surface should be proportional to the available free surface area. This can be written

$$\text{adsorption rate} \propto 1-\theta \tag{14}$$

where

θ = fractional surface coverage.

This approach was shown experimentally to be valid up to a certain degree of surface coverage, a "crowd" point (28). At this point additional polymer molecules can no longer be adsorbed without interaction with already adsorbed polymer.

It is proposed in the present study that the same dependence on surface coverage should also apply to adsorption onto a dispersed phase. Fractional surface coverage, θ, for different polymer doses can be determined under equilibrium conditions (29). However, it is not obvious how the fractional surface coverage should be defined

under nonequilibrium conditions. Gregory and Sheiham (30) inferred from flocculation experiments with a high molecular weight, high charge density polymer that the reconformation time was of the order of several seconds. The reconformation time is defined as the time elapsed from the first attachment of a polymer segment onto the surface till a state of equilibrium is reached.

A high charge density polymer adsorbing on an oppositely charged surface will take on a flat conformation at equilibrium (29). On the other extreme, the thickness of the adsorbed polymer layer may approach the dimensions of the coil in solution, when the energy of interaction between the polymer and the surface is low (29). This would be the case for adsorption on a charged surface by a low charge density or nonionic polymer.

Polymer adsorption is virtually irreversible (31). Even for low energies of interaction, the polymer may still be attached to the surface at multiple points. Even though each attached segment is in equilibrium with the liquid phase, the probability of simultaneous desorption of all segments may be negligible.

To the present author's knowledge the only attempt to link experimental adsorption data to a theoretical treatment according to collision rate theory was made by Kasper (21). By applying von Smoluchowski's equations, (1) and (2), for initial adsorption conditions, he concluded that polymer adsorption should be fast compared with flocculation in a low shear rate system. The experimental adsorption rates were judged as being high, but no clear attempt was made to compare measured rates with theoretical predictions. The shear rate in his agitated system was not given (100 RPM for 10 minutes) and flocculation rates were only qualitatively inferred from turbidity measurements and literature data [from (41)].

FLOCCULATION

The two major theories of flocculation, the bridging model (6) and the electrostatic patch model (21,33), were briefly described in the Introduction. These theories provide the conceptual framework for the understanding of polymer-aided flocculation, but they do not directly address the kinetics of the process.

Smellie and La Mer (32) incorporated the bridging concept into a kinetic model of flocculation. They proposed that the collision efficiency in the flocculation process should be a function of the fractional surface coverage. Using a modified Smoluchowski equation they wrote for the initial flocculation rate

$$dn_o/dt = k\theta(1-\theta)n_o^2 \qquad (15)$$

Equation (15) is based on the assumption that adsorption is fast ("instantaneous") compared with flocculation. In other words, the surface coverage is taken to be constant during the flocculation process. Equation (15) states that the flocculation rate tends to 0 when θ tends to 0 or 1. The maximum rate occurs at θ = 0.5, i.e., at 50% surface coverage.

Perikinetic Flocculation

Very few studies have been done to evaluate Eq. (15). Uriarte (34) found qualitative agreement but the predicted flocculation rates were too high. Singer et al. (35) concluded that the maximum flocculation rate occured at a fractional surface coverage of less than 50%. Absolute flocculation rates were not reported.

Gregory (33,36) and Gregory and Sheiham (30) used high charge density cationic polymers to flocculate negatively charged polystyrene latexes. They measured flocculation rates that were about twice as high as rapid coagulation rates. This was

tentatively explained as the result of electrostatic attraction between polymer covered and polymer free patches on colliding latex particles. They also noted an increase in initial flocculation rate with increasing polymer molecular weight, although the final extent of flocculation remained the same.

Enhanced flocculation rates, compared with rapid coagulation, have also been found for nonionic polymers (37), and anionic polymers adsorbed on negatively charged surfaces (38). The explanations referred to possible changes in the hydrodynamic interactions between polymer covered particles and increased effective collision diameters due to polymer adsorption.

There are indications that the assumption of "instant" polymer adsorption should be used with care for high particle concentrations. Gregory and Sheiham (30) concluded that high charge density cationic polymers flocculate negatively charged particles according to the electrostatic patch mechanism at low particle concentrations. However, at high particle concentrations, using a high molecular weight polymer, bridging may also occur. From the experimental results it was inferred that the reconformation step was slow compared to the particle-particle collision frequency at high particle concentrations. This results in floc formation with the adsorbed polymer in an extended, nonequilibrium, configuration. They called this phenomenon "nonequilibrium flocculation".

Walles (39) found a strong effect of molecular weight on flocculation rates, when the contour length of the polymer was equal to or larger than the particle radius. He referred to experiments with clay suspensions of high concentration, 10%, where the flocculation rate increased 150 times for an increase in polymer molecular weight from $0.5 \cdot 10^6$ to $8 \cdot 10^6$. He modified the Smoluchowski theory to account for these observations by introducing an increase in effective particle collision radius due to polymer adsorption.

Orthokinetic Flocculation

Black, Birkner and Morgan (40) flocculated colloidal clay with a radioactive cationic polymer. The samples were stirred for 20 minutes at 100 rpm plus 20 minutes at 15 rpm. Extent of flocculation was evaluated from residual turbidity after a 15 minute settling period. Polymer adsorption was found to be 85% complete after 30 seconds, a short period of time compared to the duration of the flocculation experiments. It was concluded that polymer adsorption should not be rate determining for the overall flocculation process. However, no comparison was made with simple electrolyte induced coagulation.

Birkner and Morgan (41) flocculated polystyrene latex particles, diameter 1.3 μm, with a cationic polymer (PEI), molecular weight $3.5 \cdot 10^4$. They used a stirred reactor and the average shear rate, calculated from the energy input, varied from 11 s^{-1} to 120 s^{-1}. They found that coagulation with NaCl was twice as fast as flocculation with polymer at a shear rate of 11 s^{-1}. At higher shear rates coagulation was considerably faster than twice the floccuation rate. Polymer adsorption rates were not determined, but based on their previous study (40) they assumed that adsorption would not be rate limiting in the flocculation process. The apparently low flocculation rates at higher shear rates were attributed to floc breakup. At low shear rates steric effects due to adsorbed polymer were assumed to be the reason for slower flocculation compared to coagulation.

Klute and Hahn (42) compared the effect of different stirrer types on coagulation and flocculation rates of colloidal clay. Aggregation rates varied with stirrer type for a given energy dissipation and a given destabilizer. It was concluded that the effective shear rate at a constant energy dissipation was strongly dependent on stirrer type. The two coagulants, $CaCl_2$ and NaCl, and the

flocculant, a high molecular weight anionic polymer, gave significantly different aggregation rates. The ranking of the destabilizers with respect to aggregation rate varied with stirrer type and energy dissipation. This result was attributed to different floc strengths, with NaCl producing the strongest flocs and the polymer giving the weakest flocs.

Franco (43) flocculated TiO_2 particles, average diameter 0.15 μm, with cationic polymers in turbulent pipe flow. He found that flocculation was faster than coagulation with NaCl. The highest flocculation rate was obtained with a high molecular weight, low charge density polymer. The high flocculation rates were explained as being caused by an increase in the effective particle radius due to polymer adsorption.

Graham (44) used cationic polymers to flocculate large porous silica spheres, diameter 7.6 μm, in a paddle stirred vessel. The average shear rate was calculated to be 100 s^{-1}. An inorganic salt, $Mg(NO_3)_2$, produced a coagulation rate that was only 1.7% of the predicted Smoluchowski rate [cf. Eq. (2)]. The lowest molecular weight polymer, $5 \cdot 10^4$, was about twice as effective. The highest flocculation rate was 51.4% of the Smoluchowski rate or 30 times the measured coagulation rate and was obtained for a medium charge density polymer with a molecular weight of $7 \cdot 10^6$.

Gregory (15,22), using the Smoluchowski equations, predicted that polymer adsorption may be rate limiting in orthokinetic flocculation. He found very erratic flocculation results for low concentrations of polystyrene latex, diameter 1.68 μm, in laminar tube flow (15). This was attributed to low polymer adsorption rates. Pretreating half of the particles with the same polymer gave reproducible flocculation results with collision efficiencies that were more than twice as high as those for

rapid coagulation. High charge density polymers were used, and increasing the molecular weight had only a slightly beneficial effect on the collision efficiency.

In summary, it seems to be the concensus in the literature that polymer adsorption should not be rate limiting in perikinetic flocculation. On the contrary, a rate enhancement compared with rapid coagulation is generally seen. The picture is more ambiguous for orthokinetic flocculation. Applying the Smoluchowski equations predicts the distinct possibility that flocculation may be rate limited due to slow polymer adsorption. Reported experimental flocculation rates are seemingly in conflict, with observations of both increases and decreases compared with rapid coagulation. This situation warrants further analysis and the present study is aimed at elucidating the relationship between polymer adsorption rates and particle flocculation rates, using new experimental results and theoretical considerations.

PRESENTATION OF THE PROBLEM AND THESIS OBJECTIVES

The kinetics of colloidal coagulation in the classical sense, where the coagulant is a simple electrolyte and the only attractive forces are London-van der Waals forces, have received much attention since von Smoluchowski's classical theory on coagulation (7,8). Recent extensions to this theory (16,18) have included hydrodynamic effects originally neglected.

Flocculation with polymers is now accepted in the industry as an efficient means of destabilizing colloidal suspensions (45). Many studies have been concerned with floc strength and bonding mechanisms (46,22,45). Some investigations have also dealt with the kinetics of polymer induced flocculation (22,3). However, no conclusive evidence has been presented to account for the observed effects of polymers on flocculation rates. Adsorption of polymer onto colloidal particles, which is a prerequisite for polymer-aided flocculation, has been extensively studied for Brownian-motion dominated processes (29,47). Virtually no studies have been performed on adsorption in turbulent flows, a more practical situation.

The purpose of this thesis was to elucidate the kinetics of polymer adsorption and polymer induced flocculation under turbulent flow conditions. The specific objectives of this work were

1. To measure polymer adsorption rates in a flocculating system
2. To compare flocculation rates for a colloidal suspension destabilized by a polymer and coagulation rates for a suspension destabilized by a simple electrolyte
3. To discuss the results in light of existing adsorption and flocculation rate theories

APPROACH

To solve the problem presented above, it was decided that a model system meeting certain requirements had to be set up.

Uniform polystyrene latex particles with a diameter of 1 μm were chosen as a suitable model colloid. Flocculation rates of particles of this size or larger would be a function of the shear rate in the system rather than a function of Brownian motion. The resulting flocs would be large enough for convenient measurements of floc size distributions using a Coulter Counter. The particles would, on the other hand, be small enough to represent the upper range of colloidal particles typically encountered in papermaking operations.

The polymer, a linear polyamine, was chosen because of its high molecular weight and the possibility of varying the charge degree by changing the pH. This particular polymer had also been characterized and used in a previous study (48).

Adsorption and flocculation experiments were performed in turbulent tube flow. The experimental apparatus permitted effective initial mixing and easy sampling. Floc breakup was not of interest in this study; therefore, reaction times were kept short in order to minimize this phenomenon.

Flocculation and adsorption were stopped at the end of the tube by collecting samples in concentrated surfactant solutions. Floc size distributions could then be measured with a Coulter Counter. The adsorption rates were determined by measuring the concentrations of unadsorbed polymer in the samples.

Coagulation rates were also measured for the case of destabilization with a simple electrolyte, $AlCl_3$ at pH 3. This provided the rate values for rapid coagulation in the classical sense, needed for comparison with polymer-aided flocculation.

EXPERIMENTAL MATERIALS, EQUIPMENT AND PROCEDURES

MATERIALS

The uniform polystyrene latex, PSL, was purchased from Dow Diagnostics. The mean particle diameter given by Dow was 1.091 μm. The particle size was remeasured using the Institute's transmission electron microscope (model JEM-100CX by JEOL Ltd.), see Appendix II. The reevaluated mean diameter, 1.070 μm, was used in the calculations throughout this study.

Emulsifier from the polymerization step had to be removed from the latex to give a well defined colloid stabilized by surface sulfate groups carrying negative charges (49). Two cleaning procedures were tested: ion exchange (50) and serum replacement (51). Both methods gave identical results. The surface charge density, determined by conductometric titration, was 0.53 ± 0.02 charges/$Å^2$ or 8.5 ± 0.3 $\mu C/cm^2$. Details about latex cleaning and characterization are given in Appendix II.

The polymer, polyvinylamine or PVAm, was generously donated by Dynapol Corp., California. Two different molecular weights were obtained, $1 \cdot 10^6$ and $1.3 \cdot 10^5$. The repeating unit in the linear polymer is shown below.

$$\left[CH_2 - CHNH_2 \right]_n$$

The amine group is easily protonated and the charge density of the polymer varies from 0 to 100% in the pH interval 10.5 to 2.5 (48), Fig. 4. At the pH values chosen for this study, pH 3 and pH 10, the charge densities were 95% and 3% respectively.

Aluminum chloride solutions at pH 3 were used for the rapid coagulation studies. A trivalent ion like Al^{3+} was chosen because of the relatively low concentrations

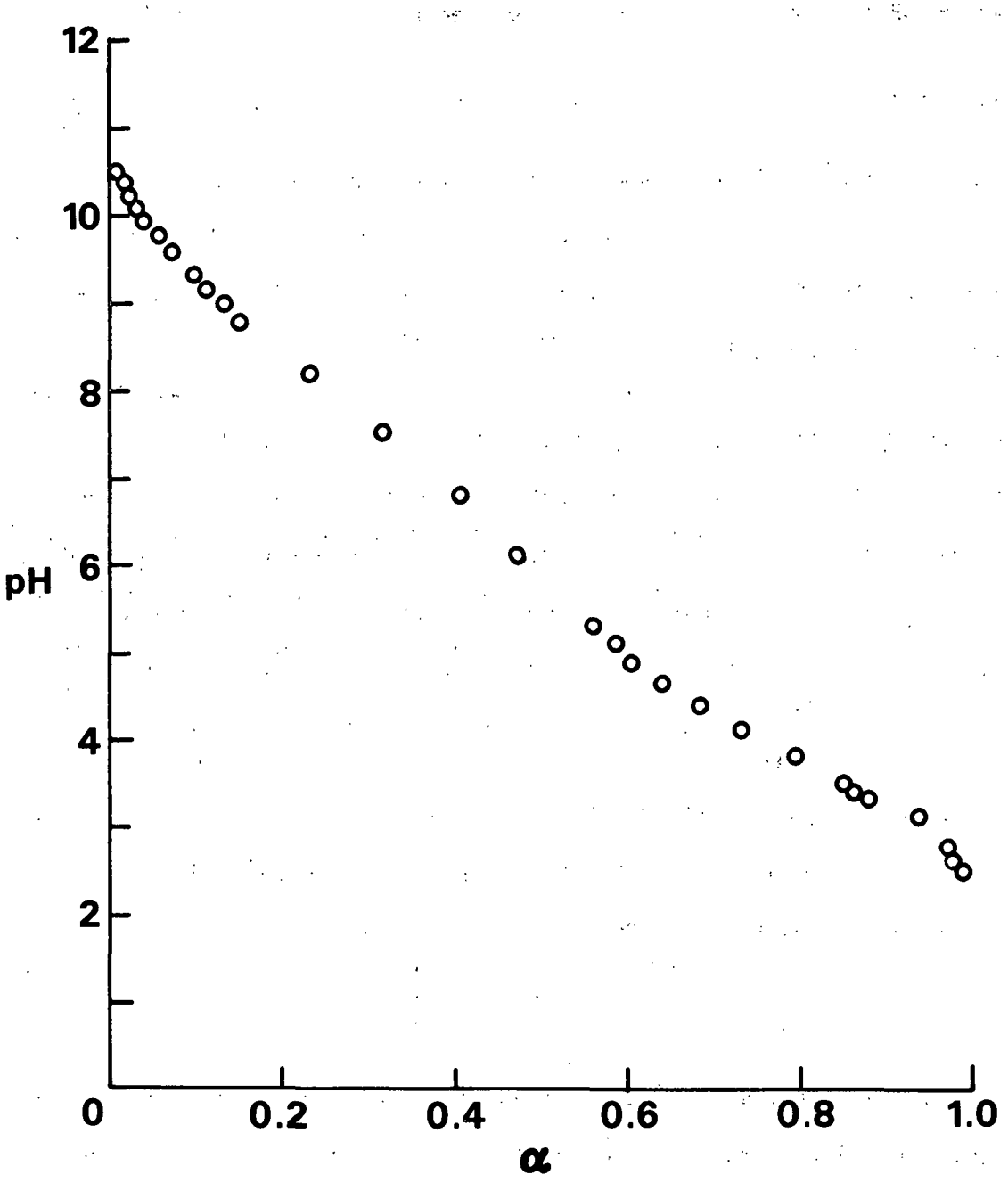

Figure 4. Degree of protonation of PVAm with pH. Reprinted from (48) by permission of the copyright owner.

needed for destabilization (1). The aluminum ion shows a very complex hydrolyzation pattern above pH 4, but $AlCl_3$ can safely be used as a simple electrolyte at pH 3 (52).

The surfactant employed to stop flocculation and adsorption was dodecyltrimethylammonium bromide, DTABr, (Sigma).

EQUIPMENT

All glassware in contact with polymer had first been equilibrated with an excess of PVAm and then thoroughly rinsed. Samples were collected in Teflon beakers and transferred to polypropylene bottles.

A schematic of the adsorption-flocculation apparatus is shown in Fig. 5. The funnels were of glass and had a volume of 1 L. All tubing used in the apparatus was transparent. The mixing tee, the reaction tube and the 3-way solenoid sample valve were made of Teflon (Fluorocarbon Corp., California). The inner diameter of the reaction tube was 4.76 mm (3/16 inch). The tube length was varied from 420 to 1960 mm. The lowest flow rate, 0.7 m/s, was generated by gravity. Higher flow rates, maximum 2.6 m/s, were obtained by applying a moderate nitrogen pressure (maximum 14 psi). Reaction times ranged from 0.16 to 2.4 seconds.

PROCEDURES

Nonequilibrium Adsorption and Flocculation

A typical experimental run is described below. The polystyrene latex, at a concentration ranging from 2 to 9 g/L, was loaded in one funnel and an equal volume of polymer solution was loaded in the other funnel. The solutions were transferred through the 3-way stopcocks by suction to minimize air entrainment. The flush valve timer was set to flush out a threefold turnover of the volume between the sample

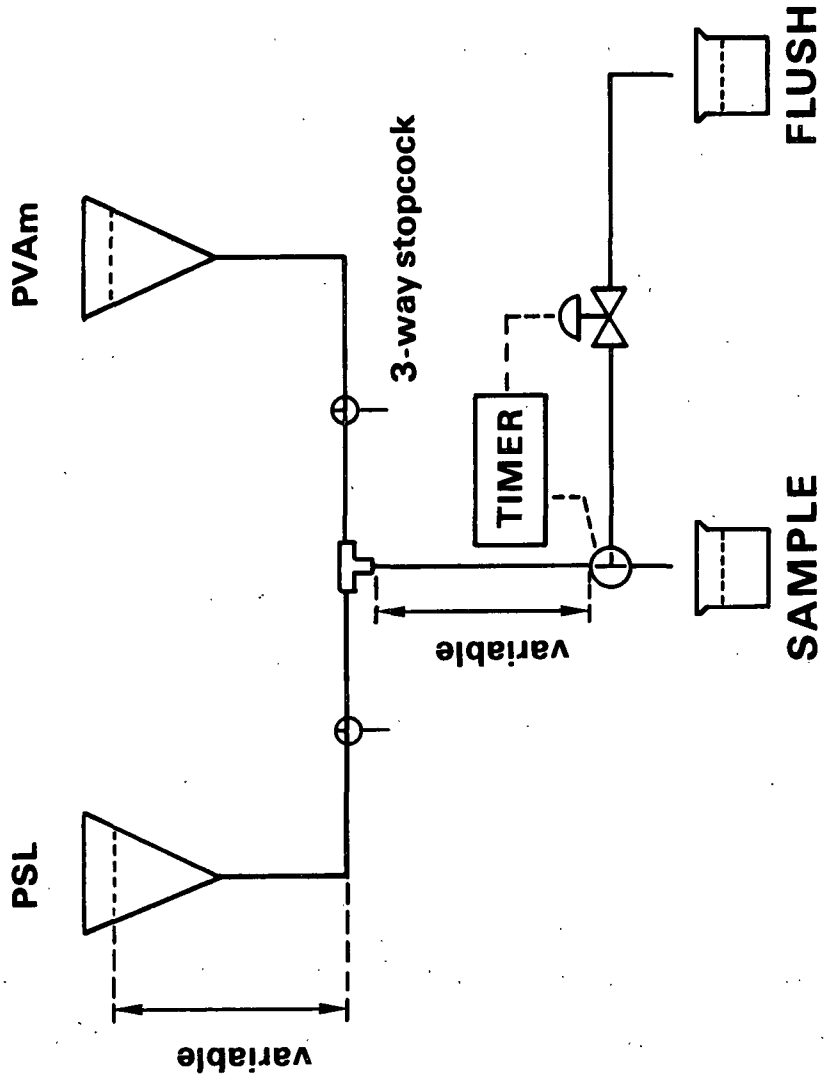

Figure 5. The experimental apparatus.

valve and the stopcocks. The sequentially operated sample valve timer was set to give a sample volume of 15 mL. The samples were collected in a Teflon beaker containing 15 mL of a surfactant solution, which immediately stopped further flocculation and adsorption. The samples were transferred to polypropylene bottles and taken to a Coulter Counter for determination of floc size distributions. The latex and the surfactant were then removed from the samples in order that the concentrations of unadsorbed polymer could be measured.

The efficiency of the surfactant solution to quench the flocculation (or coagulation) process was determined by measuring the apparent rate of flocculation (or coagulation) for various volumes and concentrations of the surfactant solution. Higher concentrations than $2 \cdot 10^{-3}$M were not used in order not to exceed the critical micelle concentration (53). Instantaneous quenching was assumed to occur when an increase in volume or concentration of the surfactant solution did not lead to a decrease in the apparent rate of flocculation (or coagulation).

Adsorption and flocculation experiments were carried out at pH 3, where the polymer is 95% charged, and at pH 10, where the charge density is 3%. All solutions at pH 3 contained $1 \cdot 10^{-4}$M NaCl and were pH adjusted with HCl. The Debye-Huckel length or electrical double layer thickness at pH 3 was 90 Å. The solutions at pH 10 contained $5 \cdot 10^{-4}$M $NaHCO_3$, which gave a slight buffering capacity. The dilution water had been deaerated under vacuum. The pH adjustment was made with carbonate-free 0.1M NaOH. The solutions were then blanketed with N_2 during handling to avoid pickup of CO_2 from the air. The Debye-Huckel length at pH 10 was also 90 Å (taking into account the equilibrium between HCO_3^- and CO_3^{2-}). After final pH adjustment the polystyrene latex was treated in an ultrasonic bath for twenty minutes to ensure minimum preaggregation.

Equilibrium Adsorption and Flocculation

To determine the equilibrium adsorption isotherms equal volumes of latex and polymer were mixed in polypropylene bottles. The bottles were left for 24 hours with occasional mild stirring. The latex was then separated from the solution by filtration and the concentration of unadsorbed polymer was measured.

The optimum flocculation concentration of polymer, OFC, under "equilibrium" conditions was determined as follows. Equal volumes of latex and polymer were mixed in a Teflon beaker, which was left without stirring for 10 minutes. The sample was then quenched with a surfactant solution and the floc size distribution was measured using a Coulter Counter. Two mixing modes were tested: sequential addition with pipette (first latex and then polymer) and simultaneous mixing with a syringe pump. The minimum concentration of $AlCl_3$ at pH 3, needed to ensure rapid coagulation, was arrived at using a method similar to the OFC determination.

Analytical Methods

The floc size distributions were measured using a Coulter Counter Model TA II equipped with a 30 μm aperture tube. The complete procedure is given in Appendix III.

Before the polymer concentration could be determined the latex had to be removed from the sample. This was accomplished by filtration through a 0.4 μm polycarbonate filter (Nuclepore) on a polycarbonate filter holder (Millipore). To analyze the low polymer concentrations used at pH 3 it was also necessary to remove the surfactant. This was done in a 200 mL stirred Amicon ultrafiltration cell equipped with a YM-10 membrane, which has a nominal molecular weight cut-off of 10,000 and low adsorption characteristics.

The polymer concentration was determined with a colorimetric method (54). The reagents were an anionic polymer, the potassium salt of polyvinylsulfate (PVSK), and a cationic dye, o-toluidine blue (OTB). The two reagents formed a complex in solution. The cationic polymer to be measured, PVAm in this case, formed a stronger complex with the anionic polymer, thereby releasing an equivalent amount of dye. The absorbance of the free dye was measured at 625 nm with a Perkin-Elmer Model 320 UV-Visible Spectrophotometer using a 10 cm cuvette.

To minimize scatter in the concentration measurements, precautions had to be taken to avoid polymer adsorption losses. Polycarbonate filters and ultrafiltration membranes had to be conditioned with polymer before use. Sample bottles must be rigorously cleaned. Samples were weighed whenever possible, rather than measured with pipettes and graduated cylinders to minimize adsorption losses. A more complete description of the method of polymer concentration analysis and associated problems is given in Appendix IV.

The polystyrene latex concentrations were determined by drying at 45°C (Dow recommends a temperature below 50°C) until constant weight was obtained, minimum 24 hours.

Electrophoretic mobilities were measured on a Zeta-Meter (Zeta Meter Inc.) and converted to zeta-potentials by the Helmholtz-Smoluchowski equation.

RESULTS

EQUILIBRIUM POLYMER ADSORPTION AND PARTICLE FLOCCULATION

Adsorption isotherms and zeta potential curves are presented in Fig. 6 and 7. The amount of polymer adsorbed and corresponding zeta potential have been plotted *vs.* the initial polymer concentration. The optimum flocculation concentrations, OFC, under quiescent conditions (Brownian flocculation) are determined from Fig. 8 and 9.

The OFC at pH 3 is the same for both molecular weights, *viz.*, 0.4 mg/L for a PSL concentration of 1.5 g/L. The OFC for a high charge density polymer, causing flocculation according to the electrostatic patch model, is not sensitive to molecular weight according to the literature (55,56), which is in agreement with the present findings. The mode of mixing (sequential or simultaneous) of the latex and the polymer does not influence the determination of the OFC, which is also in agreement with the literature (56).

At pH 10, where the polymer is only 3% charged, the bridging mechanism of flocculation is dominant (48). As a requirement for bridging to occur, the polymer should be able to span a gap of at least twice the thickness of the electrical double layer (22). This condition was satisfied, since the double layer thickness was 90 Å and the radii of gyration (see Appendix I) for the low and the high molecular weight polymer were 140 and 380 Å, respectively, at pH 10. The OFC for both polymers at pH 10 was 3.4 mg/L or 8.5 times greater than the value at pH 3. The increased adsorption at pH 10 is due to the fact that a low charge density polymer forms a much thicker adsorbed layer than does a high charge density polymer (29). However, the relationship between molecular weight and optimum flocculation concentration for bridging-type polymers is not well addressed in the literature.

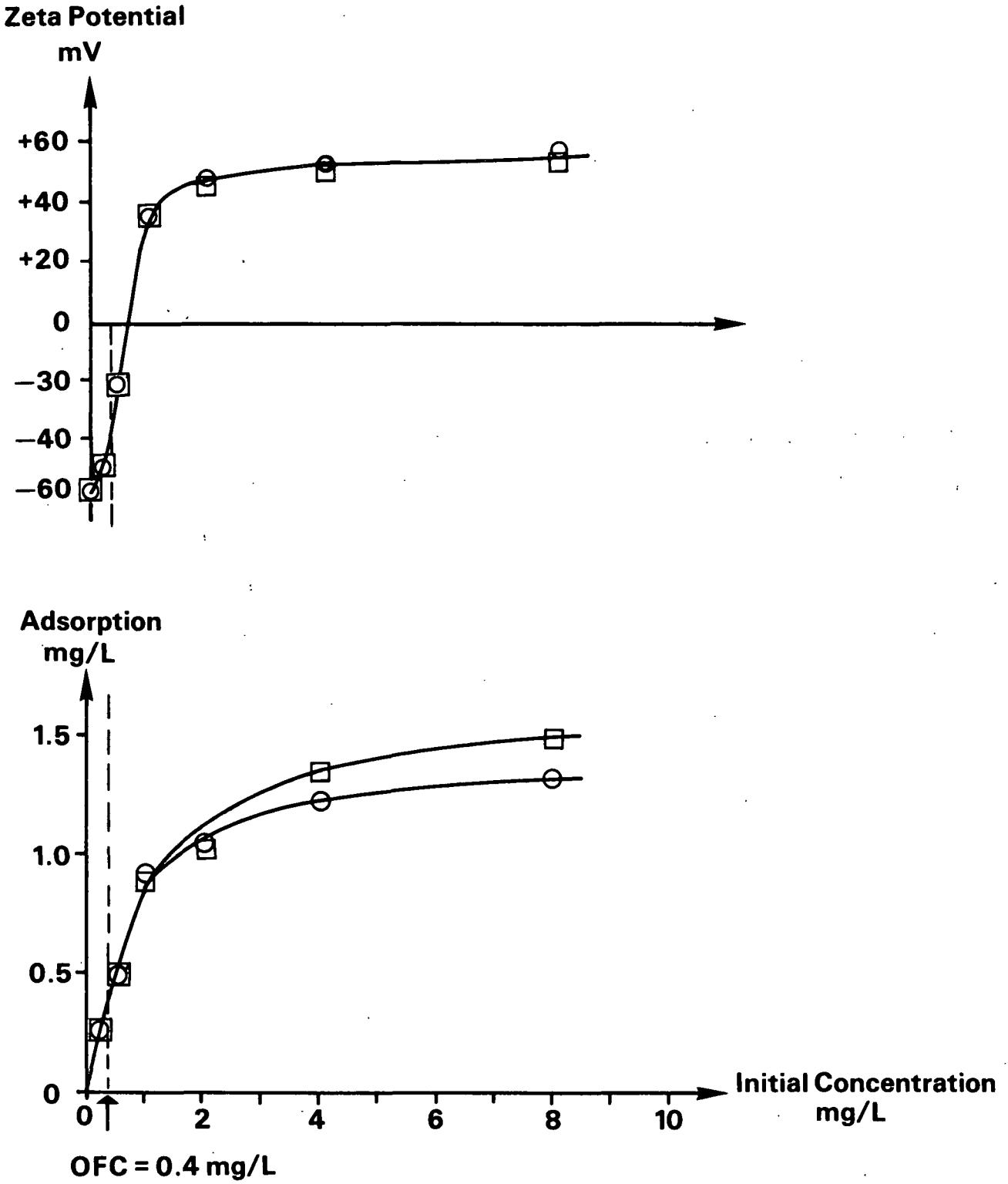

Figure 6. Zeta potential and equilibrium adsorption at pH 3. Polystyrene latex concentration 1.5 g/L. ○ molecular weight $1 \cdot 10^6$, □ molecular weight $1.3 \cdot 10^5$.

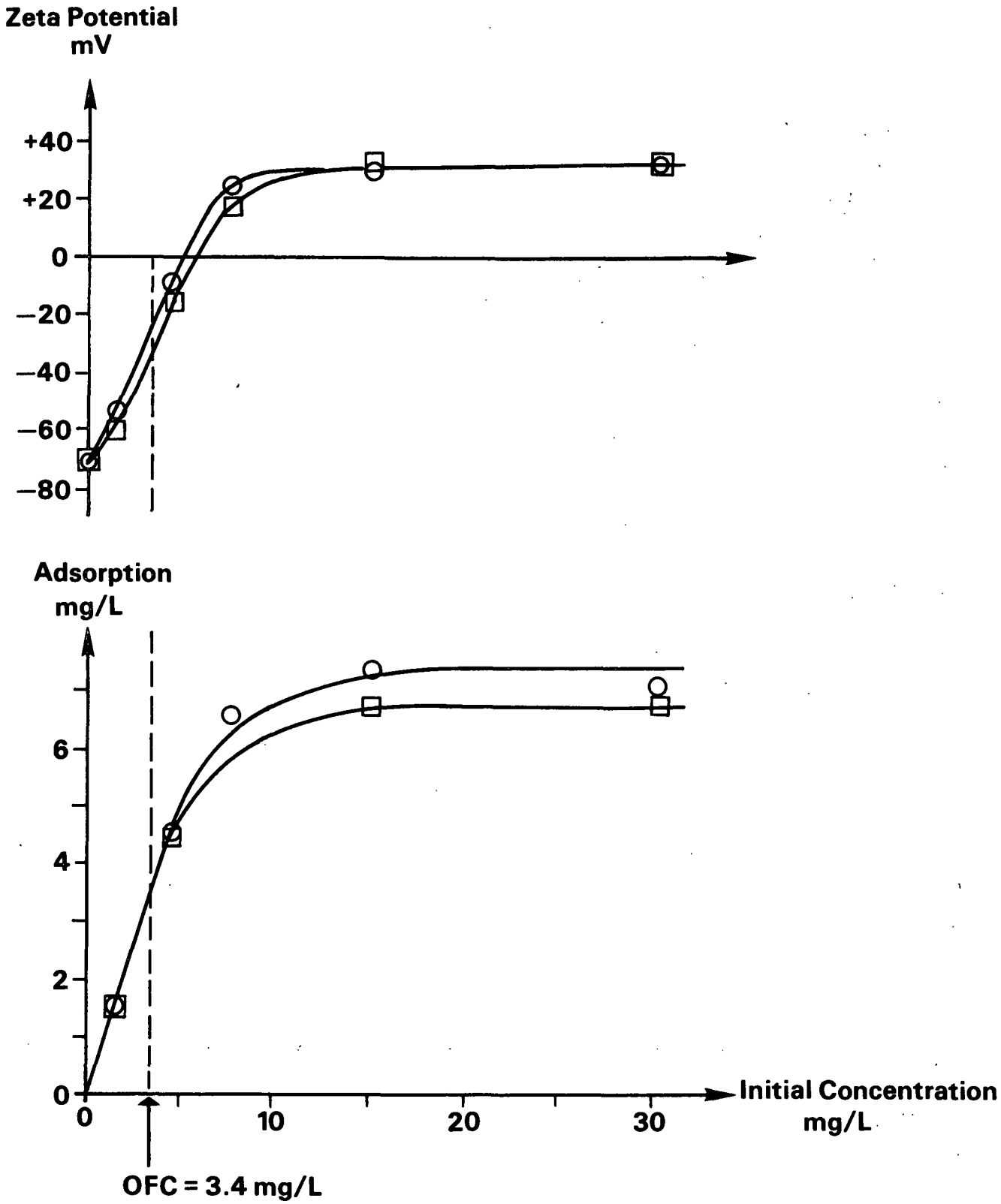

Figure 7. Zeta potential and equilibrium adsorption at pH 10. Polystyrene latex concentration 1.5 g/L. ○ molecular weight $1 \cdot 10^6$, □ molecular weight $1.3 \cdot 10^5$.

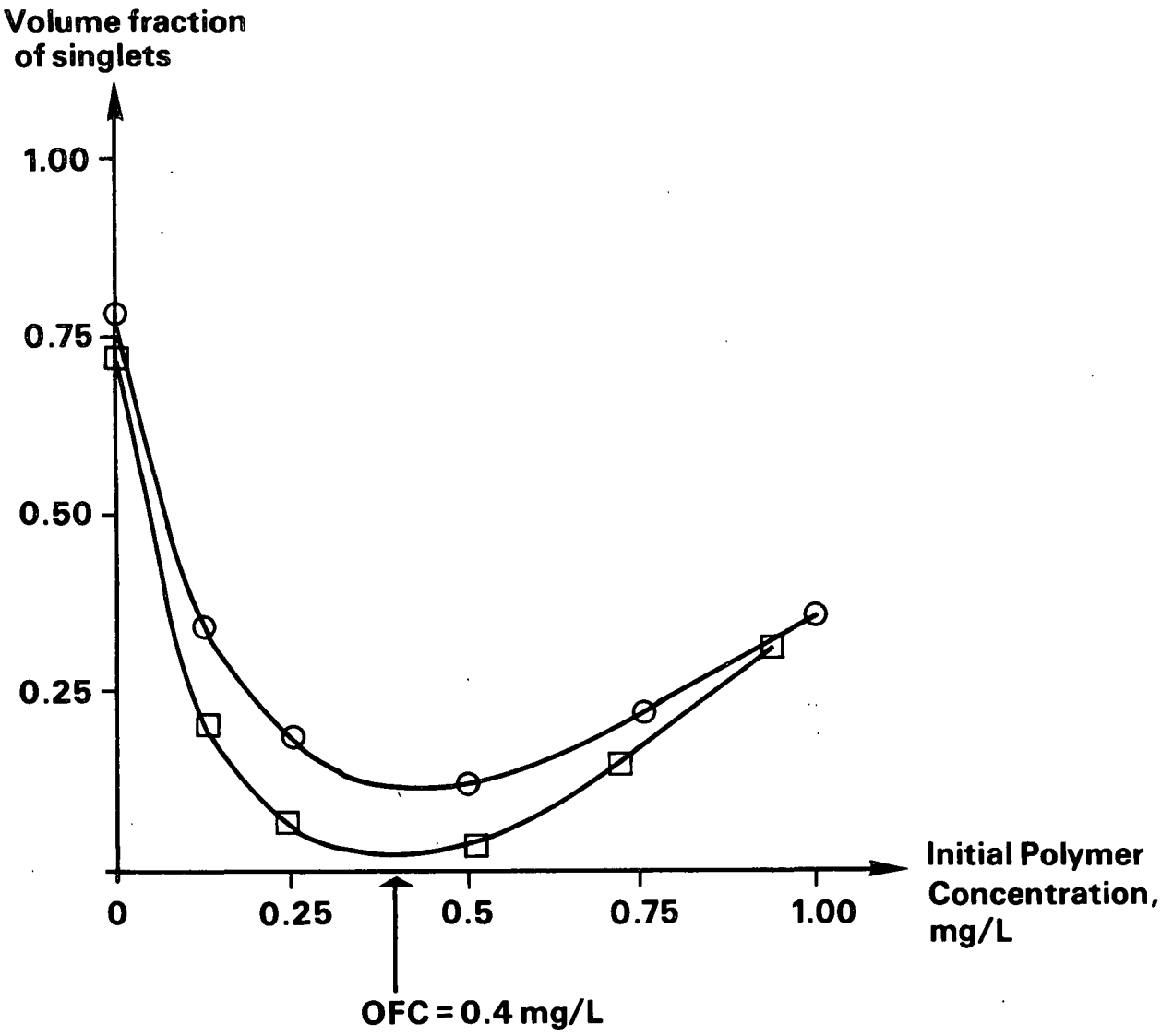

Figure 8. Determination of optimum flocculation concentration of polymer, OFC, at pH 3. Polystyrene latex concentration 1.5 g/L. High molecular weight, ○ simultaneous mixing, □ sequential mixing.

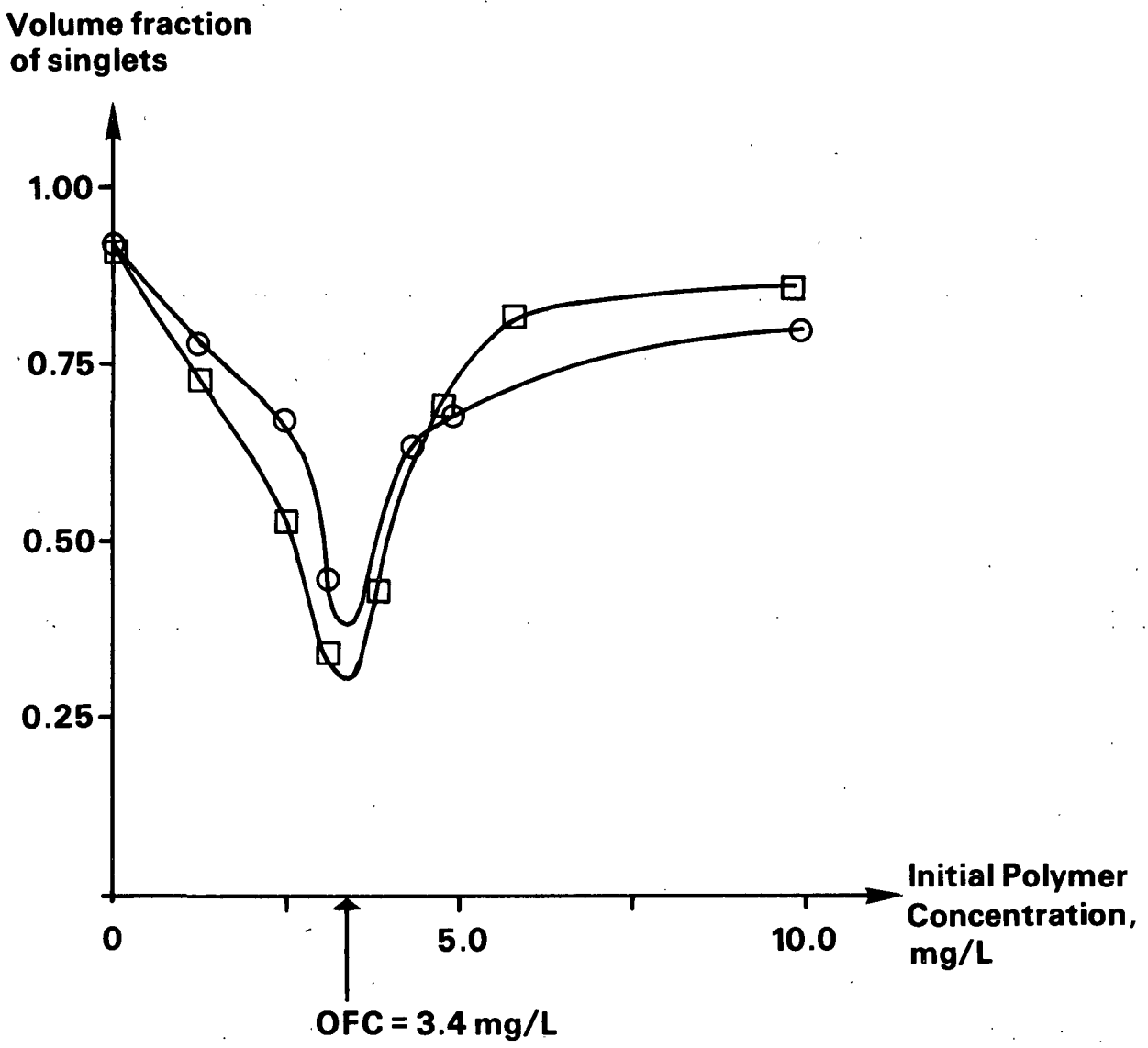

Figure 9. Determination of optimum flocculation concentration of polymer, OFC, at pH 10. Polystyrene latex concentration 1.5 g/L. ○ molecular weight $1 \cdot 10^6$, □ molecular weight $1.3 \cdot 10^5$.

Adsorption at pH 3 was complete up to twice the OFC. At pH 10 adsorption was complete up to an initial dose of about 1.5 OFC. For both molecular weights and both pH levels the zeta potential was still highly negative at polymer doses corresponding to the OFC.

COAGULATION WITH ALUMINUM CHLORIDE

Coagulation with aluminum chloride was carried out at pH 3, where the aluminum ion is not subject to hydrolysis (52). Complete destabilization occurred down to an $AlCl_3$ concentration of 0.0025M. To provide a safety margin, all rapid coagulation experiments were performed at a concentration of 0.01M $AlCl_3$.

For a sample volume of 15 mL and a latex concentration of 1.5 g/L, instantaneous quenching of the coagulation process was achieved with an equal volume of a $2 \cdot 10^{-3}$M surfactant solution. This surfactant concentration could be reduced by a factor of four without affecting the quenching efficiency. The quenched samples were stable for at least 4 days, despite the high ionic strength; stability was presumably due to steric effects. The quenching solution corresponds to a 300-fold excess compared to what is needed for charge neutralization of the latex. An estimate of the adsorption rate, using the theory presented in the Discussion section, reveals that the time required for charge neutralization for a given particle is at least two orders of magnitude shorter than the average time between collisions with other particles.

The coagulation results are presented in Fig. 10 as concentration vs. time. The concentrations have been normalized with respect to the initial total number concentration of particles, n_0, singlets plus aggregates. A singlet denotes a primary particle, a doublet consists of two primary particles, etc. The dimensionless time, τ, is the reaction time in seconds divided by a characteristic time, $t_{1/2}$, akin to the halftime in the Smoluchowski theory.

$$\tau = t/t_{1/2} \tag{16}$$

where

$t_{1/2} = 3/(16 n_o G a_1^3)$

n_o = initial total number concentration of particles (singlets + aggregates), m^{-3}

G = shear rate, s^{-1}

a_1 = radius of a singlet, m

Typical experimental values are, for example, a real coagulation time of 0.50 s and a characteristic time of 0.37 s giving a dimensionless time, τ, of 1.35 (see Appendix V, Table XI).

As pointed out in the literature section different shear rates will lead to different collision efficiencies, hence the separate coagulation curves for the two shear rate levels in Fig. 10. A detailed explanation of the modified Smoluchowski theory used to calculate the curves in Fig. 10 will be given in the Discussion section.

NONEQUILIBRIUM POLYMER ADSORPTION AND PARTICLE FLOCCULATION

The polymer flocculated samples, typically 15 mL, were also collected in an equal volume of a $2 \cdot 10^{-3}$M surfactant solution. A 30-fold decrease in the surfactant concentration still gave instantaneous quenching of the flocculation process for a latex concentration of 1.5 g/L and a polymer dose corresponding to the optimum flocculation concentration (OFC) under equilibrium conditions. It is concluded from the "slow" adsorption results presented below that rapid quenching of flocculation is also, in this case, equivalent to rapid quenching of polymer adsorption. Furthermore, the theoretical adsorption time (cf. the Discussion section) to give charge neutralization of the latex is at least two orders of magnitude shorter for the surfactant than for the polymer.

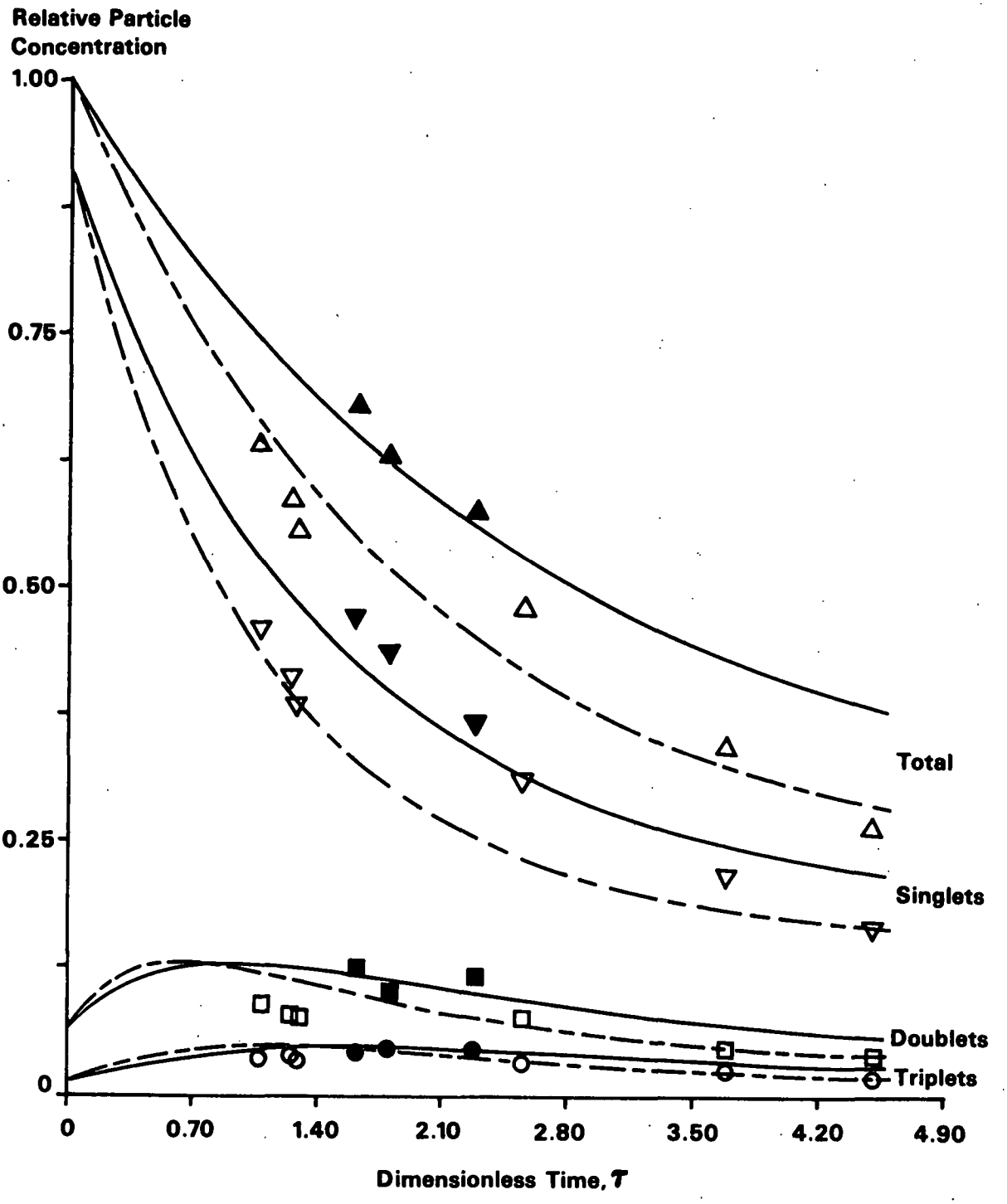

Figure 10. Coagulation with aluminum chloride at pH 3. Filled symbols and solid lines: shear rate 8000 s^{-1}. Open symbols and broken lines: shear rate 1800 s^{-1}.

Sikora (48), using polystyrene latex and polyvinylamine, also stabilized his partially flocculated suspensions with the same surfactant used in the present study (the only difference being I rather than Br as counterion). He did not find any evidence that excess polymer could displace adsorbed surfactant or vice versa.

The flocculation results are shown in Fig. 11, 12, and 13. The theoretical curves are the same as those in Fig. 10. The polymer dose has been given in OFC units. One OFC unit is equivalent to the amount of polymer required to cause maximum extent of flocculation under quiescent equilibrium conditions. The absolute value of one OFC unit, in mg/L, varies in proportion to the latex concentration. This was confirmed by an experiment where a latex concentration of 0.15 g/L gave a tenfold lower OFC than previously found for 1.5 g/L of latex. Linear relationships between the OFC and the particle concentration are also reported in the literature (57).

The flocculation rates obtained with polymer are considerably lower than those obtained with aluminum chloride. The high charge density polymer, at pH 3, is more effective as a flocculant than the low charge density polymer, at pH 10. In the pH 3 case, a dose of about 6 OFC units could produce an initial flocculation rate which was comparable to rates observed with aluminum chloride. Such a high polymer dose would, however, restabilize the suspension at longer flocculation times. Flocculation at pH 3 was about 25% faster for the high molecular weight polymer compared with the low molecular weight polymer.

Contrary to the pH 3 case, initial flocculation rates at pH 10 never approached the values of rapid coagulation, although extremely high polymer doses appeared to give restabilization. The reaction time did not have a very strong effect on the degree of flocculation. For example, the total floc concentration did not drop below 91% for a dose of one OFC unit, even for a flocculation time that was 1.6

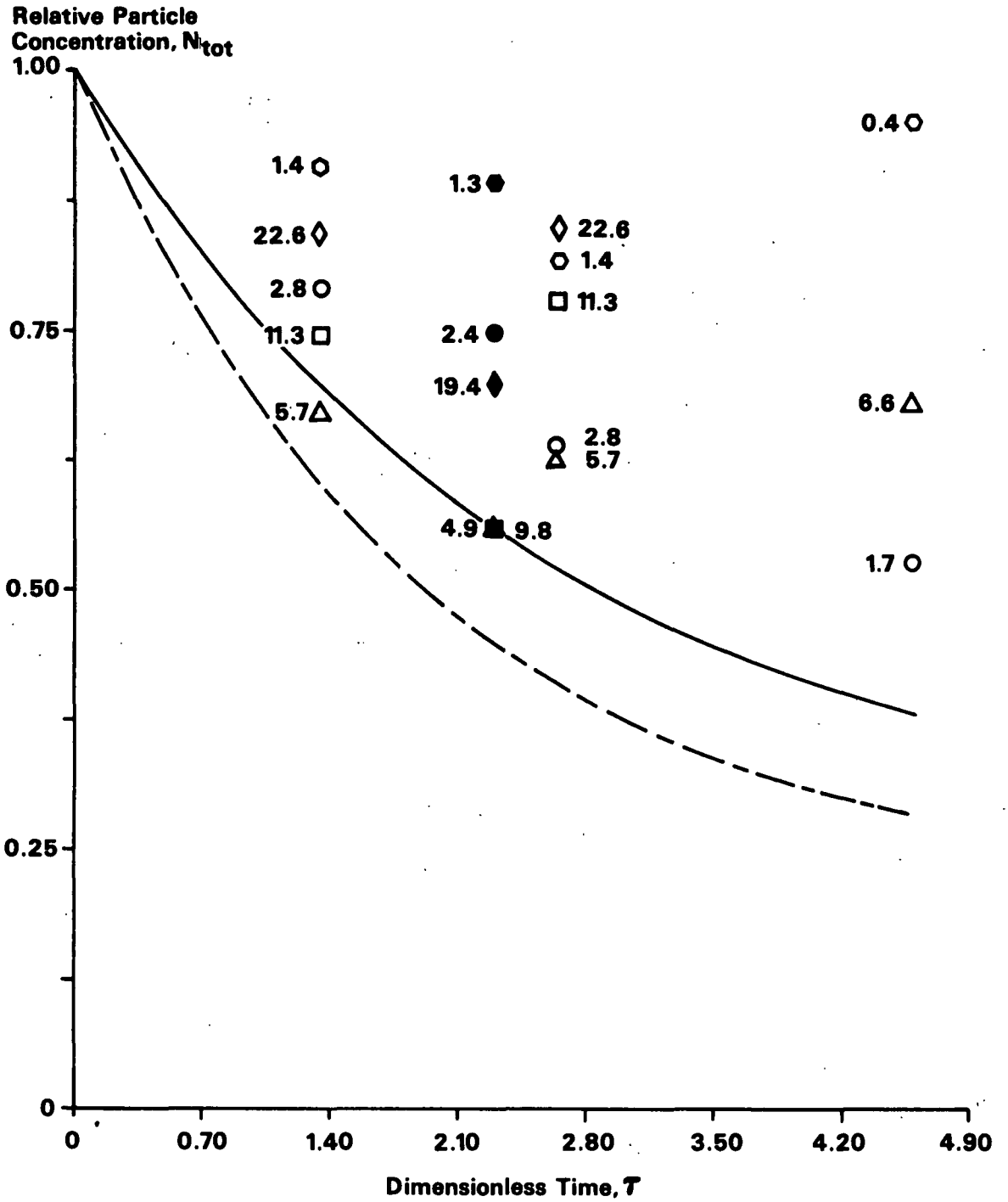

Figure 11. Flocculation at pH 3, molecular weight $1 \cdot 10^6$. Filled symbols and solid line: shear rate 8000 s^{-1}. Open symbols and broken line: shear rate 1800 s^{-1}. Numbers beside symbols indicate initial polymer concentration in OFC units.

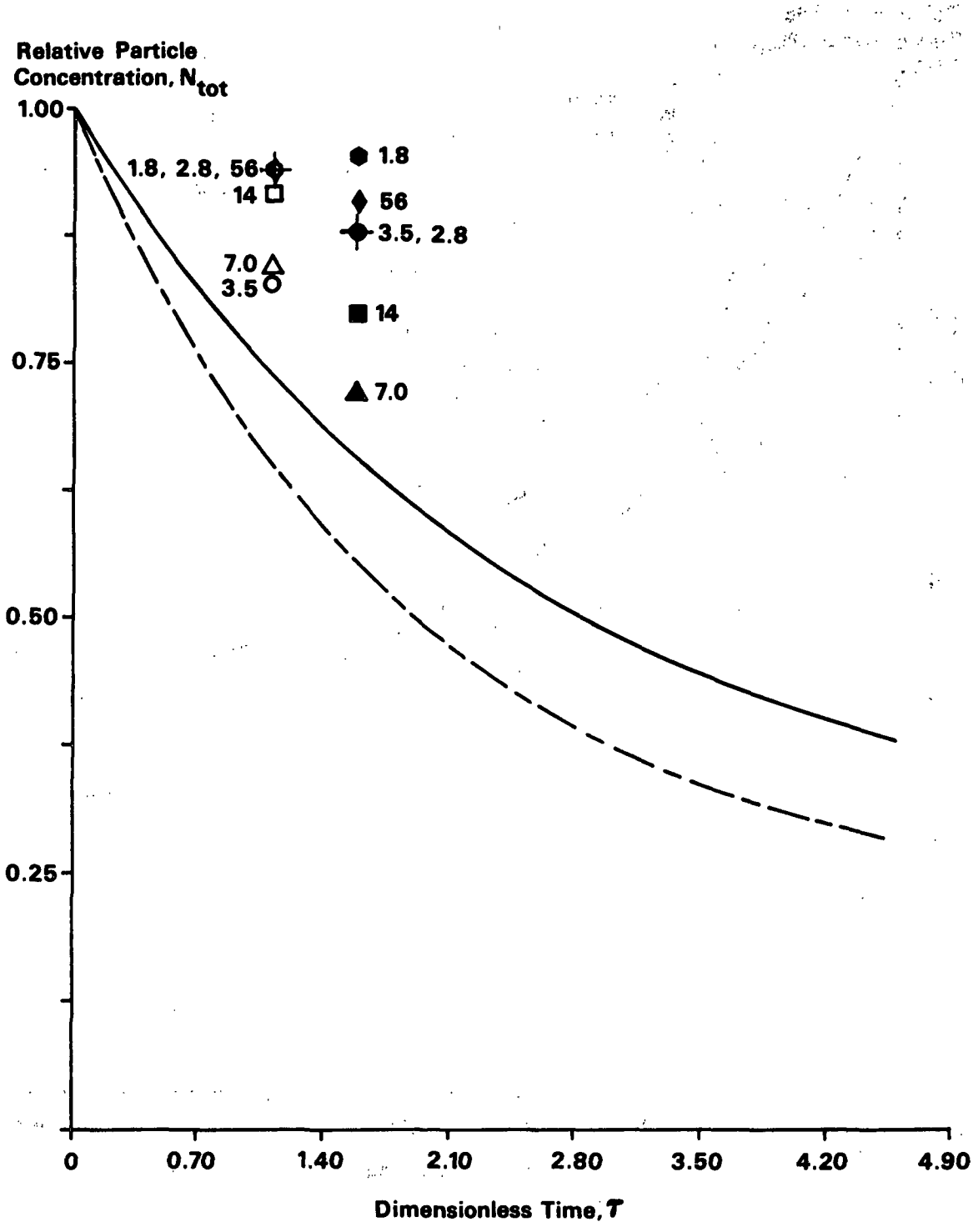

Figure 12. Flocculation at pH 3, molecular weight $1 \cdot 10^5$. Filled symbols and solid line: shear rate 8000 s^{-1}. Open symbols and broken line: shear rate 1800 s^{-1}. Numbers beside symbols indicate initial polymer concentration in OFC units.

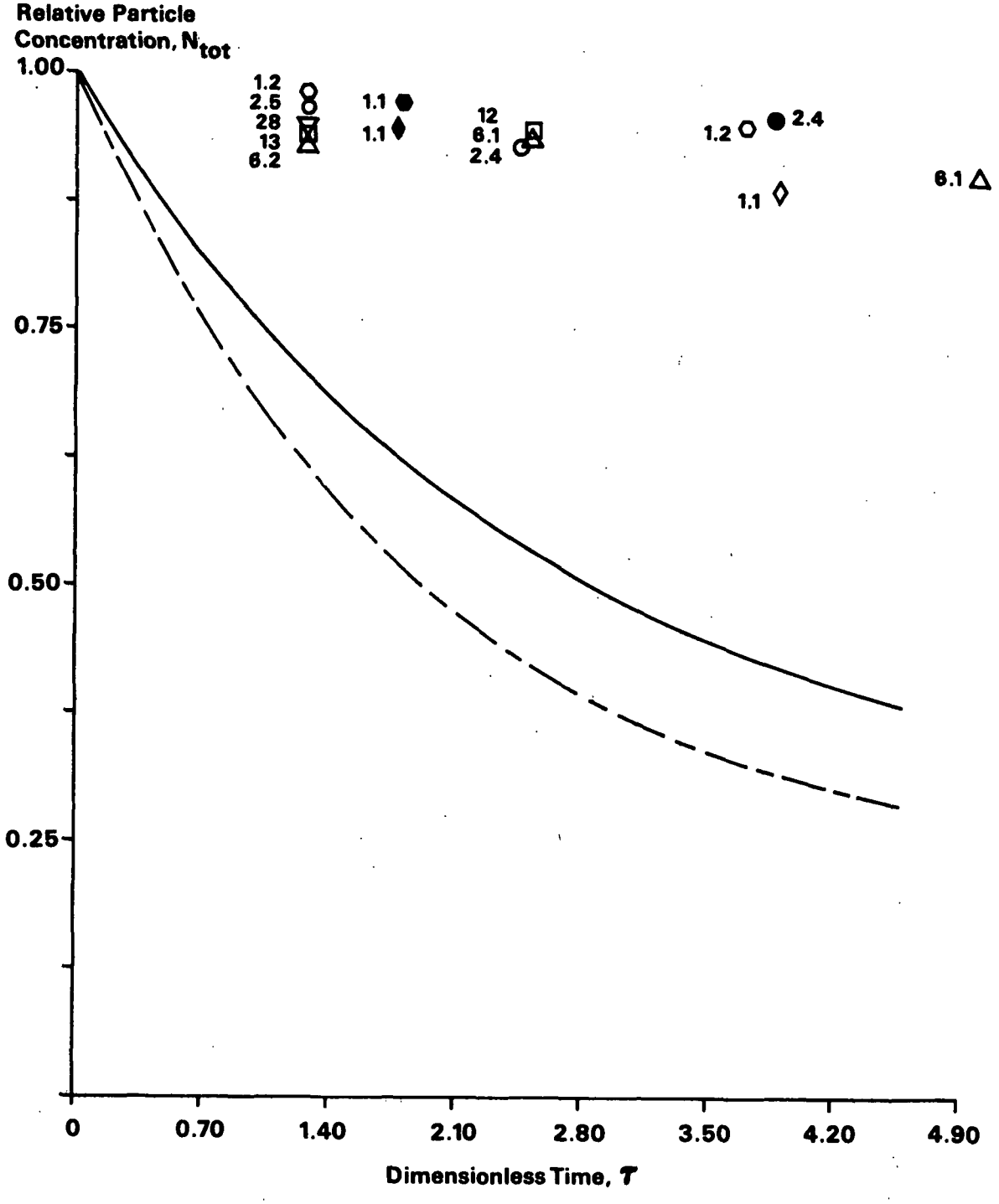

Figure 13. Flocculation at pH 10. Filled symbols and solid line: shear rate 8000 s^{-1}. Open symbols and broken line: shear rate 1800 s^{-1}. ◊ and ◆, molecular weight $1.3 \cdot 10^5$. Other symbols, molecular weight $1 \cdot 10^6$. Numbers beside symbols indicate initial polymer concentration in OFC units.

times greater than the maximum time shown in Fig. 13. Furthermore, flocculation at pH 10 was not significantly affected by either shear rate or molecular weight. These observations are attributed to floc breakup as discussed in the Discussion section.

The adsorption results corresponding to the flocculation values of Fig. 11, 12, and 13 are shown in Fig. 14 and 15. The amount adsorbed has been plotted vs. the initial dose. The polymer concentrations are again given in OFC units, and the adsorption time is identical to the flocculation time, τ. Adsorption rates were not significantly affected by molecular weight at pH 3, but at pH 10 adsorption was about 2.5 times faster for the high molecular weight polymer.

A polymer dose of one OFC unit would give complete adsorption and maximum flocculation under quiescent equilibrium conditions. However, for nonequilibrium conditions less than 25% of an initial dose of one OFC unit was adsorbed and the corresponding flocculation rates were considerably lower than the rapid coagulation rates. It is concluded that the polymer adsorption step was rate determining for the overall flocculation process for both the high and low charge density case.

Extremely high initial polymer doses produced a maximum adsorption of about one OFC unit at pH 3 and about 75% of one OFC unit at pH 10. Under equilibrium conditions one OFC unit would correspond to less than fifty per cent surface coverage. Despite these low adsorption values, restabilization occurred under nonequilibrium conditions for high polymer doses, which suggests that the effective degree of surface coverage was higher than under equilibrium conditions.

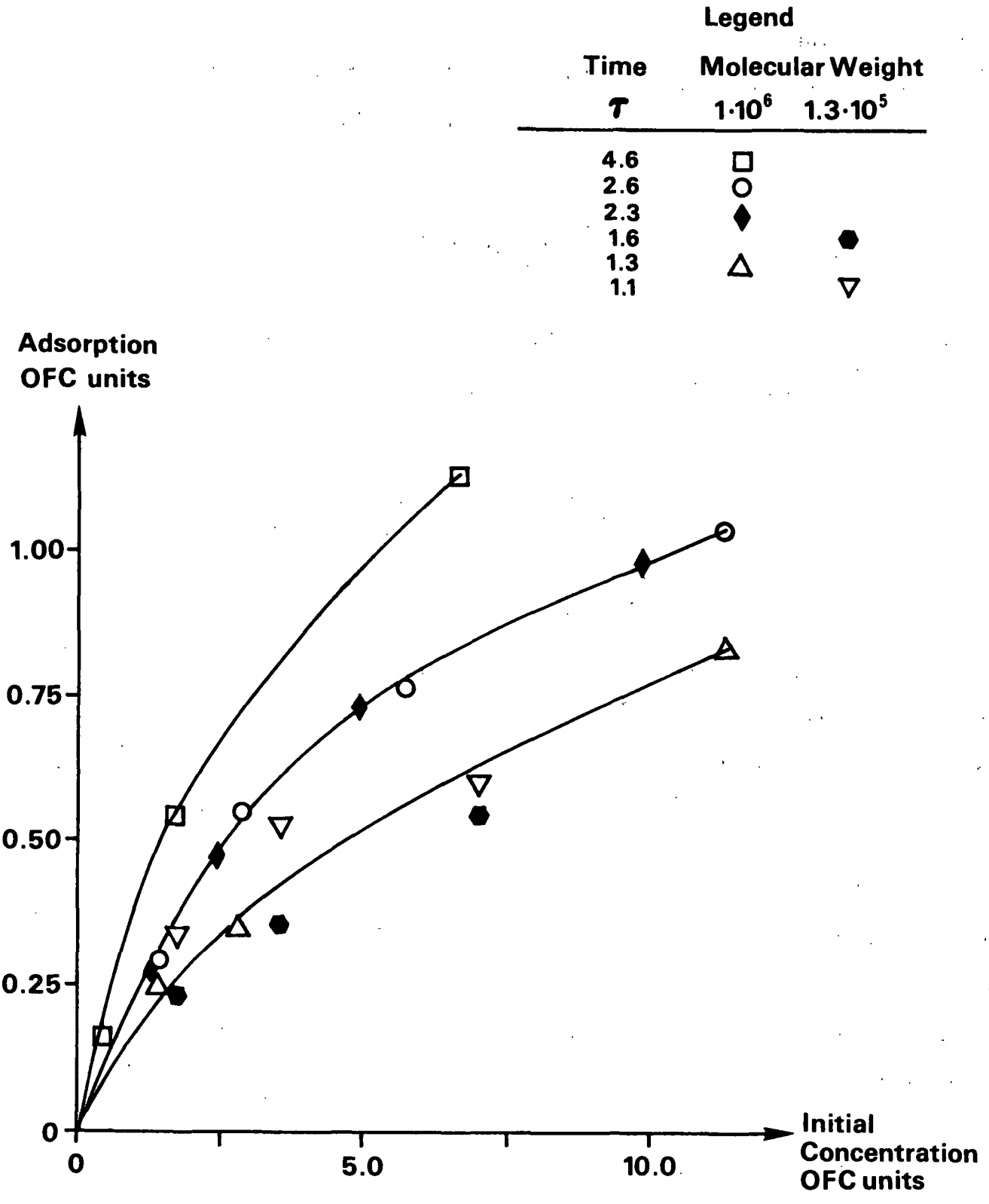

Figure 14. Nonequilibrium adsorption at pH 3. Open symbols shear rate 1800 s^{-1}, filled symbols shear rate 8000 s^{-1}.

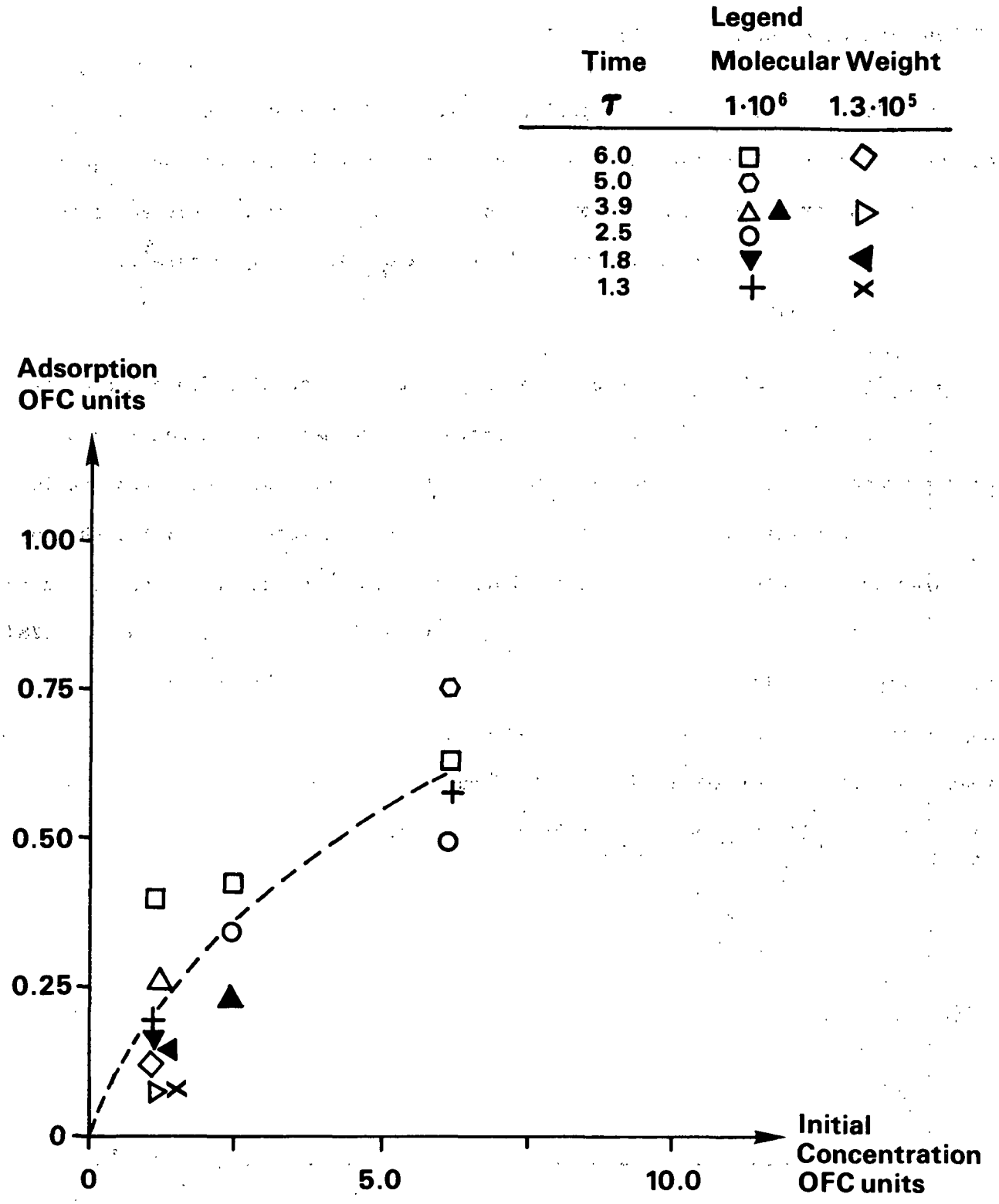

Figure 15. Nonequilibrium adsorption at pH 10. Open symbols shear rate 1800 s^{-1}, filled symbols shear rate 8000 s^{-1}.

FLOCCULATION WITH POLYMER TREATED LATEX

Flocculation experiments were performed with a mixture of equal parts of clean polystyrene latex and polymer treated latex. The treated latex had been equilibrated with an excess of polymer for six hours to ensure complete surface coverage and then washed in an ultrafiltration cell with a 0.4 μm polycarbonate filter to remove excess polymer.

As a first approximation one could assume that the resulting flocculation rate would be half of the rate for rapid coagulation, since half of the collisions would occur between particles of equal charge. The observed flocculation rates are in fact higher than this assumption would suggest. The increase was 49% for the low molecular weight polymer at pH 3 (high charge density), 56% for the high molecular weight polymer at pH 3 and for the low molecular weight polymer at pH 10, and 128% for the high molecular weight polymer at pH 10. These observations lend further support to the conclusion that polymer adsorption was the rate limiting step in the experiments with simultaneous flocculation and polymer adsorption. More detailed considerations will be given in the Discussion section.

DISCUSSION

THE COAGULATION MODEL

Mathematical models for the coagulation, adsorption and flocculation processes were developed to aid the interpretation of the experimental results.

The rate equations of von Smoluchowski, (1) and (2), were taken as a starting point. Several assumptions were then made to simplify the analysis: 1) mixing at the tee is instantaneous, 2) an average shear rate can be calculated as $G = (\varepsilon/\nu)^{1/2}$, 3) an irregular aggregate (floc) can be assigned a radius of an equivalent sphere, 4) collision efficiencies calculated for spheres can be applied to irregular aggregates (flocs). In view of the complexity of a rigorous model and the lack of proven theory, it was felt that these assumptions were justified for a comparison of coagulation and flocculation rates.

The Smoluchowski Eq. (2) for orthokinetic coagulation, including a collision efficiency α, was then made dimensionless to simplify computations and presenting of results.

$$dN_k/d\tau = \sum_{\substack{i=1 \\ j=k-i}}^{i=k-1} \alpha\sigma_{ij} N_i N_j - 2 \sum_{i=1}^{\infty} \alpha\sigma_{ik} N_i N_k \qquad (17)$$

where

$N_k = n_k/n_o$

$\tau = t/t_{1/2}$

$t_{1/2} = 3/(16 n_o G a_1^3)$

$\sigma_{ij} = (i^m + j^m)^3/8$

i, j, k = number of singlets in a floc

$k = i + j$

m = exponent determining effective floc radius

In the present study the perikinetic coagulation rate was less than 1% of the orthokinetic coagulation rate and could therefore be neglected.

The effective radius of a floc containing i singlets was calculated as

$$a_i = i^m a_1 \tag{18}$$

If m = 1/3 it is assumed that the flocs will coalesce upon collision, like oil drops in water, and the radius formula can be derived from the volume relation $V_i = iV_1$. But if the particles are solid and do not coalesce, a porous floc structure must be assumed. Several investigations (58,59,60), both theoretical and experimental, have concluded that an average radius for a porous floc can be calculated with a formula of the type $a_i = ki^m a_1$, with $m > 1/3$. For example, using computer simulations, Goodarz-Nia (59) found the relation $a_i = 1.057i^{0.450} a_1$, and Tambo and Watanabe (60) obtained the expression $a_i = i^{0.476} a_1$. The former expression was based on the enclosed floc volume and the latter, which was chosen for this study, was based on the radius of gyration of a floc.

The hydrodynamic collision efficiency, α, for rapid coagulation was calculated from literature data on solid spheres (13,14,17,20). The Hamaker constant for polystyrene latex was taken to be $5 \cdot 10^{-21}$ J (15). The collision efficiency in the present study for singlet particles and Brownian coagulation could then be calculated as (14)

$$\alpha_{11} = 0.5 \tag{19}$$

For orthokinetic coagulation an expression from (17), see Eq. (8), was used to calculate the singlet collision efficiency.

$$\alpha_{11} = 0.788G^{-0.18} \tag{20}$$

Values for typical shear rates used in this study were

$$\alpha_{11} = 0.204 \quad \text{for} \quad G = 1800\ s^{-1} \tag{21}$$

$$\alpha_{11} = 0.156 \quad \text{for} \quad G = 8000\ s^{-1} \tag{22}$$

The results of Higashitani et al. (20) were employed to account for the effect of particle size on the collision efficiency. The following approximation for equal sized particles was derived from their Fig. 5 and 6, Fig. 3 in the present study.

$$\alpha_{ii} = i^{-0.294}\ \alpha_{11} \tag{23}$$

i = no of singlets in floc ?

An approximate expression for particles of different sizes was also derived from Fig. 3

$$\alpha_{ij} = 0.95 N_s^{-(0.04\lambda + 0.16)} = 0.95(1.168G((i^m + j^m)/2)^3)^{-(0.04\lambda + 0.16)} \tag{24}$$

where

$$N_s = 6\pi\mu\ a_{ij}\ G/A$$

$$a_{ij} = (a_i + a_j)/2$$

$$\lambda = a_i/a_j$$

Equation (24) appears to be reasonable for $N_s < 10^3$ and $\lambda < 5$. For larger values of these parameters the approximation overestimates the collision efficiency, which will be discussed below in comparison with experimental results. No explicit values of the collision efficiency, α_{ij}, for dissimilar particles have been published for the perikinetic case. Spielman (13) has, however, given expressions which permit the determination of α_{ij} for Brownian motion through rather lengthy numerical calculations. As in the orthokinetic case the collision efficiency will decrease as the size ratio increases.

The effective average shear rate, $G = (\varepsilon/\nu)^{1/2}$, is not easily calculated in turbulent pipe flow. An upper bound is given by the energy dissipation calculated from the total pressure drop.

$$\varepsilon = \Delta PQ/(V\rho) = fU^3/2D = f^{-0.5}\ 11.3u_f/D \tag{25}$$

where

ΔP = pressure drop N/m^2

Q = volume flow rate, m^3/s

ρ = density, kg/m^3

V = pipe volume, m^3

f = friction factor, dimensionless

U = average velocity, m/s

D = pipe diameter, m

$u_f = U(f/8)^{1/2}$, friction velocity, m/s

Laufer (61) measured the energy dissipation as a function of radial position in fully developed turbulent pipe flow, Fig. 16, [see also Hinze (62)]. His data are useful if only the core of the pipe is considered. Rotta (63) gave an expression for the energy dissipation in turbulent flow past a wall

$$\varepsilon = u_f^3/(\kappa y) \tag{26}$$

where

$\kappa = 0.4$, von Karman constant

y = distance from the wall, m

Assuming that Eq. (26) is valid for pipe flow an average energy dissipation can be calculated for a fraction of the pipe cross section according to Eq. (27).

$$\bar{\varepsilon}_{x_1} = (2u_f^3/(\kappa D)) \int_0^{x_1} [2\pi x/(1-x)]dx / \int_0^{x_1} 2\pi x dx \qquad (27)$$

where x = 1-2y/D, dimensionless radius

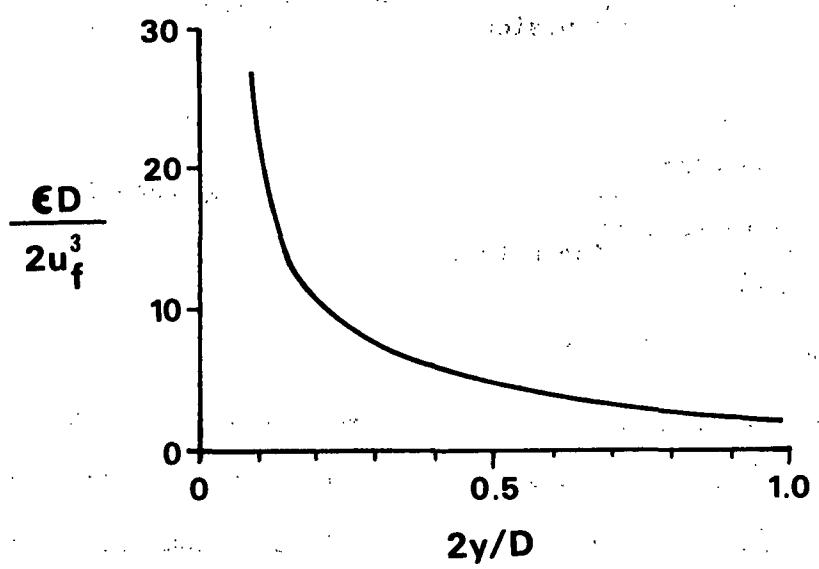

Figure 16. Energy dissipation in turbulent pipe flow. Adapted from (61) by permission of the copyright owner.

Equation (27) agrees with Laufer's experimental values within 10% for an average dissipation over 90% of the pipe diameter. The dissipation increases rapidly close to the wall, cf. Fig. 16, and $\bar{\varepsilon}_{x_1}$, according to Eq. (27), begins to exceed the upper bound, (based on the pressure drop) given by Eq. (25), for a dimensionless radius of 0.997.

It is argued below that floc breakup, which always occurs to some extent, may have been insignificant in the present coagulation study. However, a floc breakup term, from (64), was given some consideration.

$$dn_k/dt = -bGk^{m2}n_k \qquad (28)$$

It is assumed that the breakup mechanism consists of the subsequent stripping of singlets from larger aggregates. The breakup rate is proportional to the shear rate, the floc surface area and the floc concentration. No other form of the breakup term was evaluated, since floc breakup per se was not a part of this study. See Spielman (65) for a short discussion on floc breakup mechanisms.

The coagulation model, Eq. (17), results in rate equations for each particle size. This system of differential equations was solved by numerical integration on a Burroughs B6900 computer; see Appendix VI.

Comparison with Experimental Results

Delichatsios and Probstein (11) implicitly assumed a collision efficiency of unity in their investigation of coagulation in turbulent pipe flow. This assumption is not justified in light of more recent work on interactions of particles in shear flow (15,44,66). The good agreement between theory and experiments obtained by Delichatsios and Probstein may have been fortuitous because they based their theoretical coagulation rates on the energy dissipation in the center of the pipe, which is considerably lower than the average dissipation for the whole pipe width, cf. Eq. (25) and (26).

The possibility of error cancellation by choosing a high collision efficiency and a low shear rate is shown in Fig. 17, which is based on experiments and theory of the present study. In Fig. 17 the shear rate is calculated from the energy dissipation in the center of the pipe. Curves 1 (coalescence) and 2 (porous flocs) are based on a collision efficiency of unity and curves 3 and 4 (porous flocs) are calculated using a collision efficiency according to Eq. (20), $\alpha_{11} = 0.788G^{-0.18}$.

It is clearly seen in Fig. 17 that the choice of a high collision efficiency (unity) and a low shear rate (based on the dissipation in the center of the pipe)

may give an apparent agreement between theory and experiments. However, it is argued that a physically sound coagulation model cannot rely on a collision efficiency of unity in light of recent theoretical (16,18,20,66) and experimental (15,44,66) results. Neither does a shear rate based on the energy dissipation in the center of the pipe appear to be justified. A reasonable agreement between the coagulation model and the experimental results is obtained for a shear rate based on the total energy dissipation, Eq. (25), and collision efficiencies that are slightly higher than the theoretical predictions according to Eq. (20) and (24), see Fig. 18.

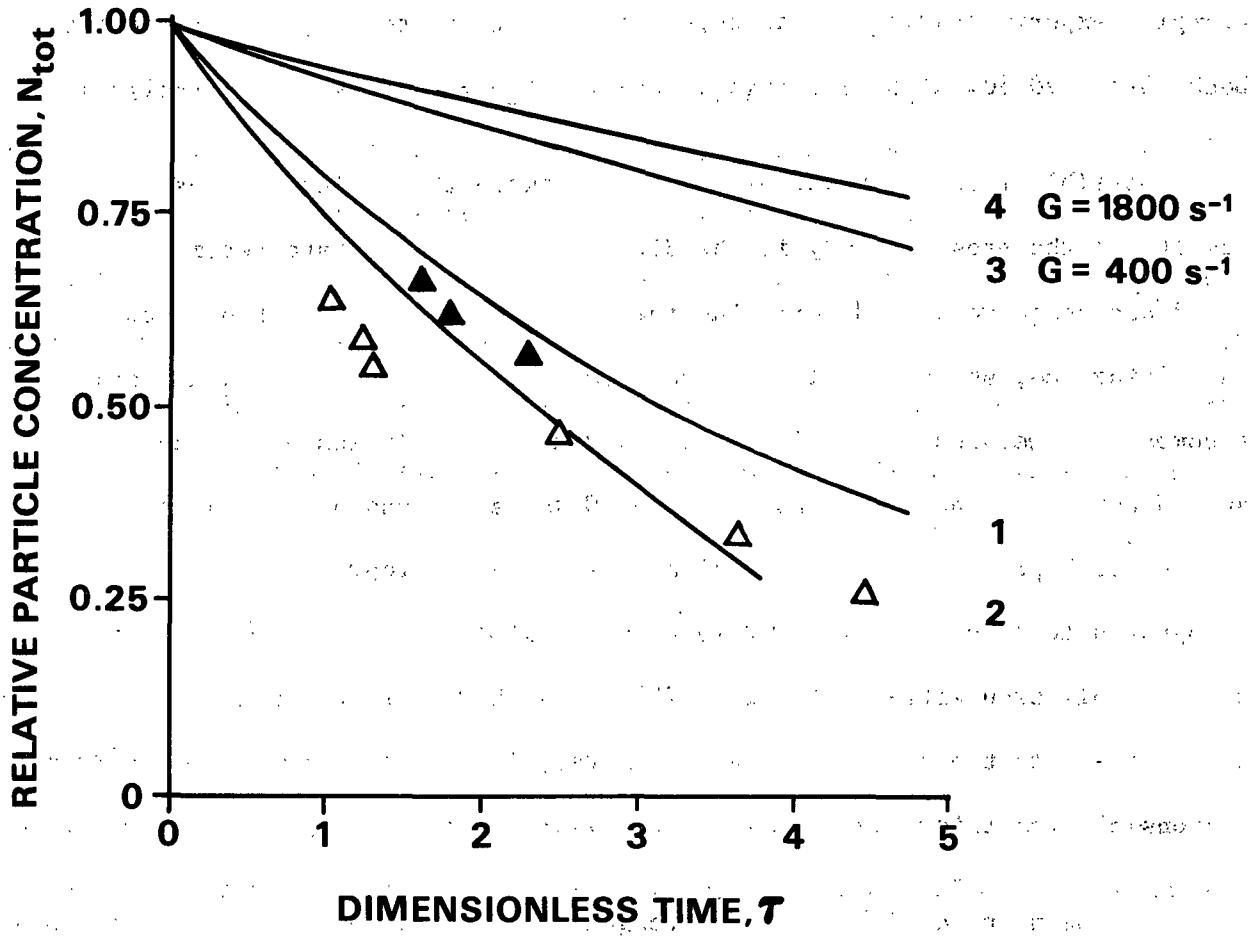

Figure 17. Rapid coagulation. Model calculations. 1. Coalescence, $\alpha_{11} = 1.0$. 2. Porous flocs, $\alpha_{11} = 1.0$. 3. and 4. Porous flocs, $\alpha_{11} = 0.788\ G^{-0.18}$. Experimental: G = 400 s^{-1}, Δ; G = 1800 s^{-1}, Δ. Shear rates calculated from energy dissipation in the center of the pipe.

For initial flocculation rates the effect of different floc sizes can be neglected and the collision efficiency can be taken to be equal to the singlet collision efficiency, curves 5 and 7 in Fig. 18. The experimentally determined collision efficiencies for singlets are higher than the theoretical values, Eq. (20), by a factor of 1.60 and a factor of 1.25 for shear rates of 1800 s^{-1} and 8000 s^{-1}, respectively. However, the experimental collision efficiency at 1800 s^{-1} is still only 0.327, which is reasonable compared with published experimental results (15,44, 66). Furthermore, at the present time perfect agreement between theoretical and experimental collision efficiencies have not been reported in the literature. For example, experiments in laminar tube flow have given collision efficiencies that are both lower, 20-30%, (15) and higher, 10-110% (66) than the theoretical predictions.

A possible reason for the discrepancy between theoretical and experimental results in the present study is the difficulty in fully characterizing the flow field and unequivocally determining the shear rates, because of disturbances from the mixing tee, short tube lengths and comparatively low Reynolds numbers. However, a comparison between theoretical and experimental collision efficiencies should give an indication of whether or not a chosen G-value is reasonable. A shear rate based on the total pressure drop, Eq. (3) and (25), should represent an upper bound. But it appears that the actual shear rates were even higher, since the experimental singlet collision efficiencies were 25% to 60% higher than the theoretical values. It is likely that nonideal mixing at the tee, causing locally high shear rates, is responsible for this result.

It is seen in Eq. (17) that the coagulation rate is dependent on the product of G and α. For initial coagulation rates α can be taken to be equal to the singlet collision efficiency, and the product $G\alpha$ can then be determined by fitting the

experimental results to the model, even if the absolute value of the shear rates is unknown. It will be apparent from the continued discussion that, in this case, the absolute values of the shear rates and the collision efficiencies do not have to enter into a relative comparison of coagulation, flocculation and adsorption rates in the orthokinetic regime; cf. Eq. (42). (The absolute value of G will, of course, determine whether or not the process is orthokinetic or perikinetic.)

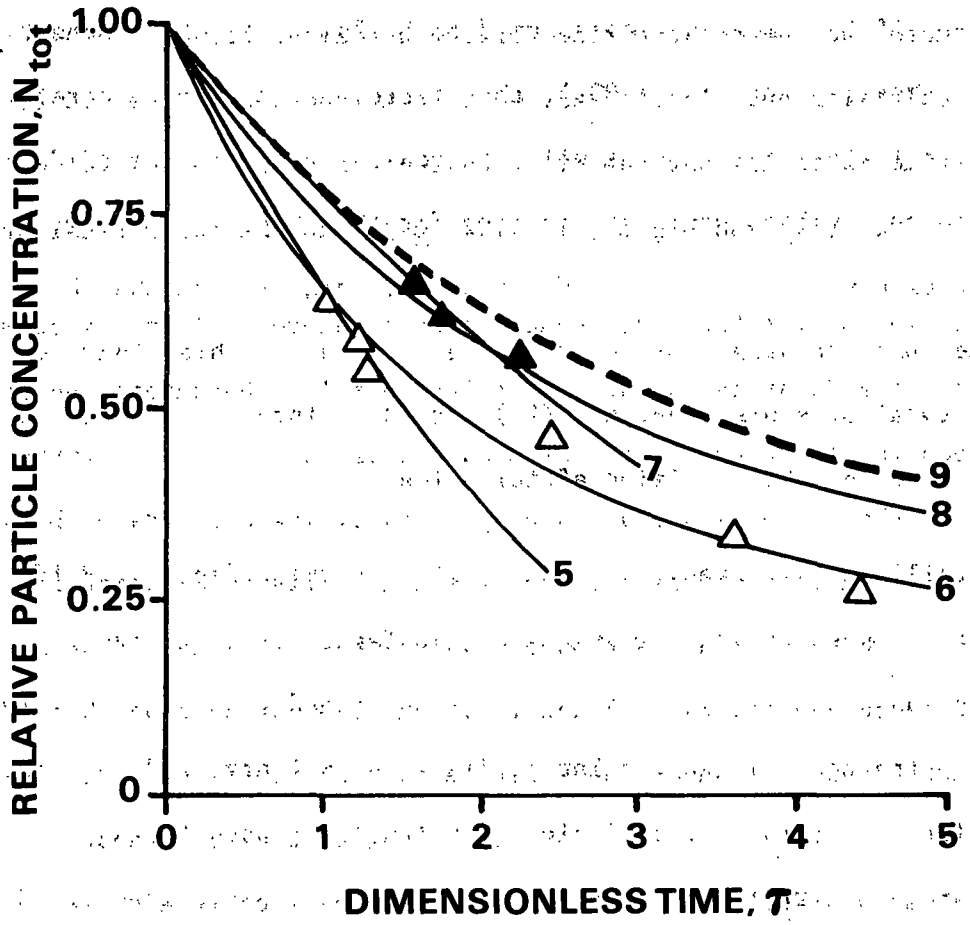

Figure 18. Rapid coagulation. Model calculations: 5. $G = 1800\ s^{-1}$, $\alpha = 1.60\ \alpha_{11}$. 6. $G = 1800\ s^{-1}$, $\alpha = 1.85\ \alpha_{ij}$. 7. $G = 8000\ s^{-1}$, $\alpha = 1.25\ \alpha_{11}$. 8. $G = 8000\ s^{-1}$, $\alpha = 1.85\ \alpha_{ij}$. 9. $G = 1800\ s^{-1}$, $\alpha = \alpha_{ij}$. Experimental: $G = 1800\ s^{-1}$, Δ; $G = 8000\ s^{-1}$, Δ. $\alpha_{11} = 0.788G^{-0.18}$, $\alpha_{ij} = 0.95(1.168G((i^m + j^m)/2)^3)^{-(0.04\lambda + 0.16)}$

Some concern was given the possibility of relaminarization of the flow at the lowest Reynolds number (3,300) in this study. However, the average shear rate, if the flow is assumed to be laminar, is only 53% of the shear rate based on the actual pressure drop. The lower laminar shear rate results in a larger discrepancy between experiment and theory, with an experimental singlet collision efficiency which is 2.7 times the theoretical value. This should be compared with an experimental α-value of 1.60 times the theoretical collision efficiency for a shear rate based on the pressure drop. If the flow is also assumed to be laminar at the highest flow rate in this study (Reynolds number 12,000), the discrepancy between theoretical and experimental collision efficiencies will be even higher, a factor of 3.0. The shear rate based on the total pressure drop gives, for this Reynolds number, a singlet collision efficiency that is only a factor of 1.25 higher than the theoretical prediction. The absolute values of the shear rates given in this study were therefore based on the total pressure drop, Eq. (25) and (3), since this method gave the most reasonable values for the collision efficiencies.

Using a collision efficiency which accounts for the effects of different floc sizes results in experimental values that are a factor of 1.85 higher than the theoretical prediction of Eq. (24); see curves 6, 8 and 9 in Fig. 18. This factor is higher than the one for the singlet collision efficiency, and the discrepancy between singlet and "complete" collision efficiencies arises because the initial suspensions are not perfectly monodisperse (typically 91% singlets, 6% doublets, and 3% triplets and larger flocs). The experimental conditions and the estimated collision efficiencies are summarized in Table I.

Floc breakup is always of concern in coagulation and flocculation studies, and a breakup function, Eq. (28), was used to calculate curves 6 and 8 in Fig. 18, improving

the agreement with experimental results. This breakup function is, however, rather weak, and a clear effect is seen only at longer flocculation times, i.e., for larger floc sizes. The "complete" collision efficiency, Eq. (24), overestimates α_{ij} for larger floc sizes compared with the solution shown in Fig. 3, and a better approximation of α_{ij} may well prove floc breakup to be negligible in this system.

TABLE I

THE COAGULATION MODEL - TESTED PARAMETERS

Case Number	Flow Velocity, m/s	Shear Rate, s^{-1}	Collision Efficiency	Comments
1	0.8		1.00	1, 2
2	0.8		1.00	2
3	0.8	400	1.00 α_{11}	3
4	2.6	1800	1.00 α_{11}	3
5	0.8	1800	1.60 α_{11}	4
6	0.8	1800	1.85 α_{ij}	4, 5
7	2.6	8000	1.25 α_{11}	4
8	2.6	8000	1.85 α_{ij}	4, 5
9	0.8	1800	1.00 α_{ij}	4, 5

$\alpha_{11} = 0.788\ G$

$\alpha_{11} = 0.204$ for $G = 1800\ s^{-1}$

$\alpha_{11} = 0.156$ for $G = 8000\ s^{-1}$

$\alpha_{ij} = 0.95(1.168G((i^{0.476} + j^{0.476})/2)^3) - (0.04\lambda + 0.16)$

Comments

1. Case No. 1: coalescence. Case No. 2-9: porous flocs.
2. Collision efficiency independent of shear rate.
3. Shear rate based on energy dissipation in the center of the tube.
4. Shear rate based on total energy dissipation.
5. Limited floc breakup assumed, Eq. (28).

In summary, reasonable agreement between theory and experiments was obtained, provided the shear rate was based on the total energy dissipation and the theoretical collision efficiency, including floc size effects, was increased by a factor of 1.85. To the author's knowledge, this is the first attempt for turbulent pipe flow

to include both the concept of porous flocs and collision efficiencies which vary with floc size and shear rate. More research is needed to firmly establish this approach, but it is believed that this model is sufficient for the present purpose of comparing coagulation and flocculation under similar conditions of shear rate, particle concentration and reaction time.

THE POLYMER ADSORPTON AND PARTICLE FLOCCULATION MODEL

The same assumptions used in developing the coagulation model were also employed in the adsorption and flocculation model. In addition, it was assumed that polymer molecules could be treated as solid spheres with a radius equal to the radius of gyration of the polymer molecule, see Table II.

TABLE II

RADIUS OF GYRATION OF THE POLYMER

Molecular Weight	pH	Radius of Gyration, nm
$1 \cdot 10^6$	3	200
$1.3 \cdot 10^5$	3	53
$1 \cdot 10^6$	10	38
$1.3 \cdot 10^5$	10	14

The dimensionless equation for the adsorption rate under orthokinetic conditions is given by (see Appendix VII)

$$dP/d\tau = -2 \sum_{i=1}^{\infty} \alpha(1-\theta_i)\, \sigma_{ip}\, N_i\, P \qquad (29)$$

where

$P = p/p_o$ = dimensionless polymer concentration

θ_i = effective fractional surface coverage of polymer on a floc containing i singlets

$$\sigma_{ip} = (i^{0.476} + r)^3/8$$

$$r = a_p/a_1$$

a_p = hydrodynamic radius of polymer molecule

In addition to a collision efficiency, α, arising from hydrodynamic effects, it is also assumed that the probability of a successful particle-polymer collision is proportional to the effective free surface area, $(1-\theta_i)$.

The effective polymer coverage is not to be confused with the equilibrium surface coverage. Instead, the concept of an effective fractional surface coverage is an approximation of the interaction energy between flocs and polymer molecules. With $\theta_i = 0$, corresponding to a polymer free floc, the probability of adsorption is maximum. When $\theta_i = 1.0$, the floc has such a high degree of polymer coverage that the probability of further adsorption is assumed to be zero.

The orthokinetic flocculation rate equation is the same as the one for rapid coagulation, with one exception. A successful collision can only occur if a polymer-covered area on one floc hits a polymer-free area on another floc or vice versa. This is expressed mathematically in Eq. (30), which gives the dimensionless flocculation rate.

$$\begin{aligned} dN_k/d\tau = & \sum_{\substack{i=1 \\ j=k-i}}^{i=k-1} \alpha\,[(1-\theta_i)\theta_j + \theta_i\,(1-\theta_j)]\,\sigma_{ij}\,N_i N_j \\ & - 2\sum_{i=1}^{\infty} \alpha[(1-\theta_i)\theta_k + \theta_k\,(1-\theta_i)]\,\sigma_{ik}\,N_i\,N_k \\ & = (dN_k/d\tau)_f - (dN_k/d\tau)_d \end{aligned} \qquad (30)$$

where

$(dN_k/d\tau)_f$ = formation rate of k-flocs

$(dN_k/d\tau)_d$ = disappearance rate of k-flocs

It is assumed that the total surface area of a floc is proportional to the number of singlets in that floc, a reasonable assumption for small flocs and open floc structures. Furthermore, an average surface coverage is assigned to every floc size. The rate of change of surface coverage in shear flow can then be written as (see Appendix VII for derivation)

$$d\theta_k/d\tau = (2s\ \theta_e/k)\ \alpha(1-\theta_k)\ \sigma_{kp}\ P + (1/N_k)(dN_k/d\tau)_f\ (\theta_k^f-\theta_k) \qquad (31)$$

where

s = total initial number concentration of particles if all aggregates are broken down to singlets, divided by n_o

θ_e = initial polymer dose divided by dose required to give 100% effective surface coverage

θ_k^f = average effective surface coverage of k-flocs formed by collisions between i- and j-flocs during the time interval $d\tau$.

The first term on the right hand side of Eq. (31) is the rate of change in effective surface coverage due to polymer adsorption, and the second term is the rate of change of effective surface coverage due to flocculation.

The collision frequency of particles due to Brownian motion is negligible compared with the collision frequency due to shear. However, for the smallest polymer size, radius of gyration 14 nm, the frequency of polymer molecules colliding with particles is of the same order of magnitude in both Brownian motion and shear flow. According to van de Ven (16), when Brownian motion is dominating, the additional collision frequency due to shear is proportional to $\alpha_p G^{0.5}$ if

$$Pe = rGa_1^2/D_1 \ll 1 \qquad (32)$$

where

Pe = modified Peclet number, ratio between convection and diffusion rates

α_p = perikinetic collision efficiency

For Pe >> 1 the collision frequency will be proportional to $\alpha_o G$, where α_o is the orthokinetic collision efficiency. For the smallest polymer molecule, the Peclet number according to Eq. (32) is Pe = 32. This is in a transition region and, although not fundamentally justified, additivity of perikinetic and orthokinetic effects can be used as an interpolating technique. This was shown by Guzy et al. (67) for the deposition of colloidal particles onto cylindrical collectors. In the present study additivity is assumed and the perikinetic adsorption rate is calculated according to Eq. (33) below (see Appendix VII for a derivation).

$$dP/d\tau = -K_{Ga} \sum_{i=1}^{\infty} \alpha(1-\theta_1)\, \beta_{ip}\, N_i\, P \qquad (33)$$

where

$$K_{Ga} = k_B T/(8\mu G a_1^3)$$

$$\beta_{ip} = (i^m+r)^2/(i^m r)$$

The factor K_{Ga} represents the ratio of the time scales for orthokinetic and perikinetic adsorption. The collision radius factor, β_{ip}, is derived from the relationship between radii and relative diffusion coefficients shown in Eq. (34) [adapted from (1)].

$$D_{ip}(a_i + a_p) = D_p a_p (a_i+a_p)^2/(a_i a_p) \qquad (34)$$

Analogous equations were also derived for perikinetic flocculation and perikinetic rate of change of surface coverage. They differ from the corresponding orthokinetic equations only by the addition of the factor K_{Ga} and the substitution of β for σ.

Comparison with Experimental Results

The hydrodynamic collision efficiency, α, and the effective fractional surface coverage, θ_i, were used as adjustable parameters to fit the adsorption-flocculation model to the experimental results.

The floc size effect on α was neglected, since flocculation generally did not proceed very far, see Fig. 11-13, and the theoretical singlet collision efficiency, α_{11}, was used as a starting point in the calculations. Very little is known about the hydrodynamic interactions between polymer molecules and solid particles. The starting values for the adsorption collision efficiencies in Eq. (29) and (33) were therefore also taken to be equal to the singlet particle collision efficiencies for orthokinetic and perikinetic encounters, respectively. The collision efficiencies for orthokinetic and perikinetic collisions were then varied in the same proportion with respect to their starting values, when the model was fitted to the experimental results.

The fact that restabilization occurred despite adsorbed amounts of less than one OFC unit led to the conclusion that the maximum amount of polymer adsorbed per unit area was much smaller under nonequilibrium conditions than at equilibrium. The effective fractional surface coverage, θ_i, for a given amount of adsorbed polymer was therefore also taken to be an adjustable parameter.

Experiments at pH 3

The results of the model calculations for the pH 3 conditions are shown in Fig. 19-21 and Table III. A "pseudo" optimum flocculation concentration of about 6 OFC units was found experimentally for short flocculation times. Higher polymer concentrations gave restabilization. The mathematical model did not predict restabilization to occur within the range of experimental conditions if it was

assumed that the fractional surface coverage for a given amount of adsorbed polymer was equal under equilibrium and nonequilibrium conditions. However, assuming higher θ_i values for the dynamic experiments greatly improved the model. The best fit between the model and the experimental results was obtained for a θ_i function, Eq. (31), that predicted 100% effective surface coverage for an amount of adsorbed polymer corresponding to about 1 OFC unit. It is interesting to note in Fig. 14 (nonequilibrium adsorption) that the system had to be highly overdosed to approach an adsorbed amount of one OFC unit. A comparison with Fig. 6 shows that maximum adsorption at equilibrium was 3.5 times higher than maximum adsorption under dynamic conditions, although the effective surface coverage was 100% in both cases.

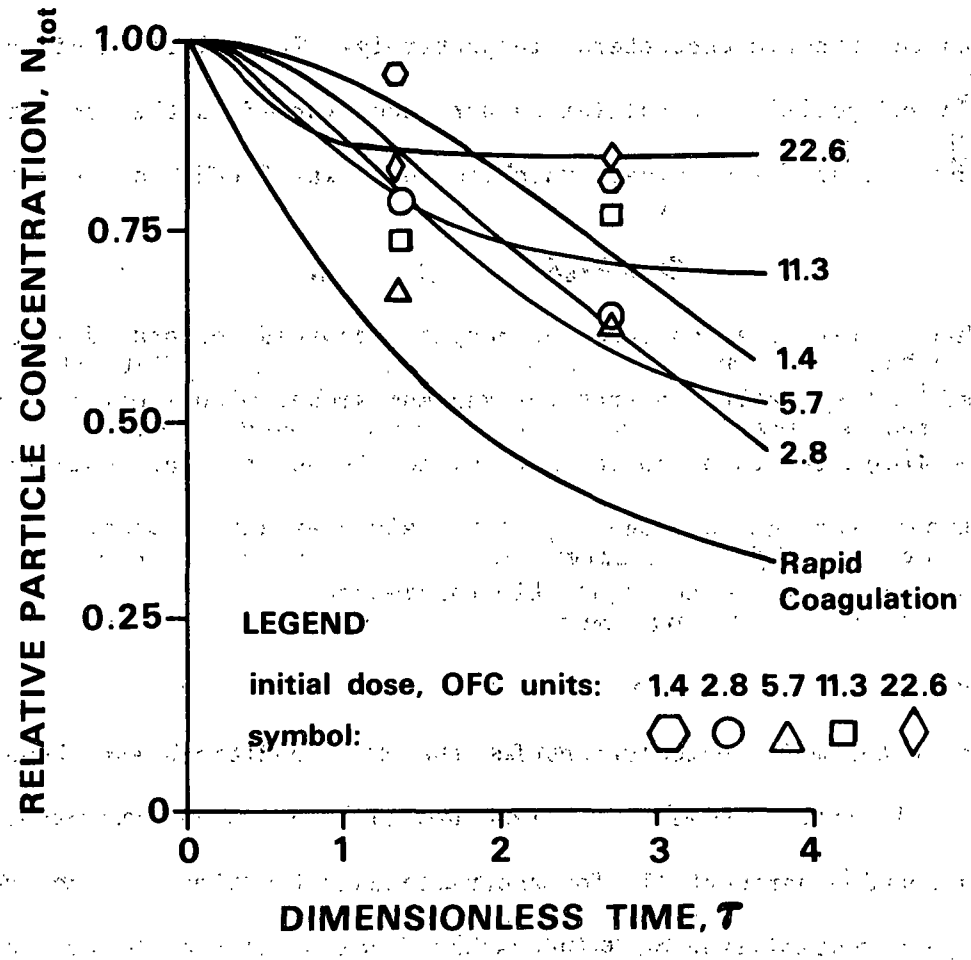

Figure 19. Theoretical and experimental flocculation rates. Molecular weight $1 \cdot 10^6$, pH 3, G = 1800 s^{-1}. Initial polymer dose in OFC units beside curves.

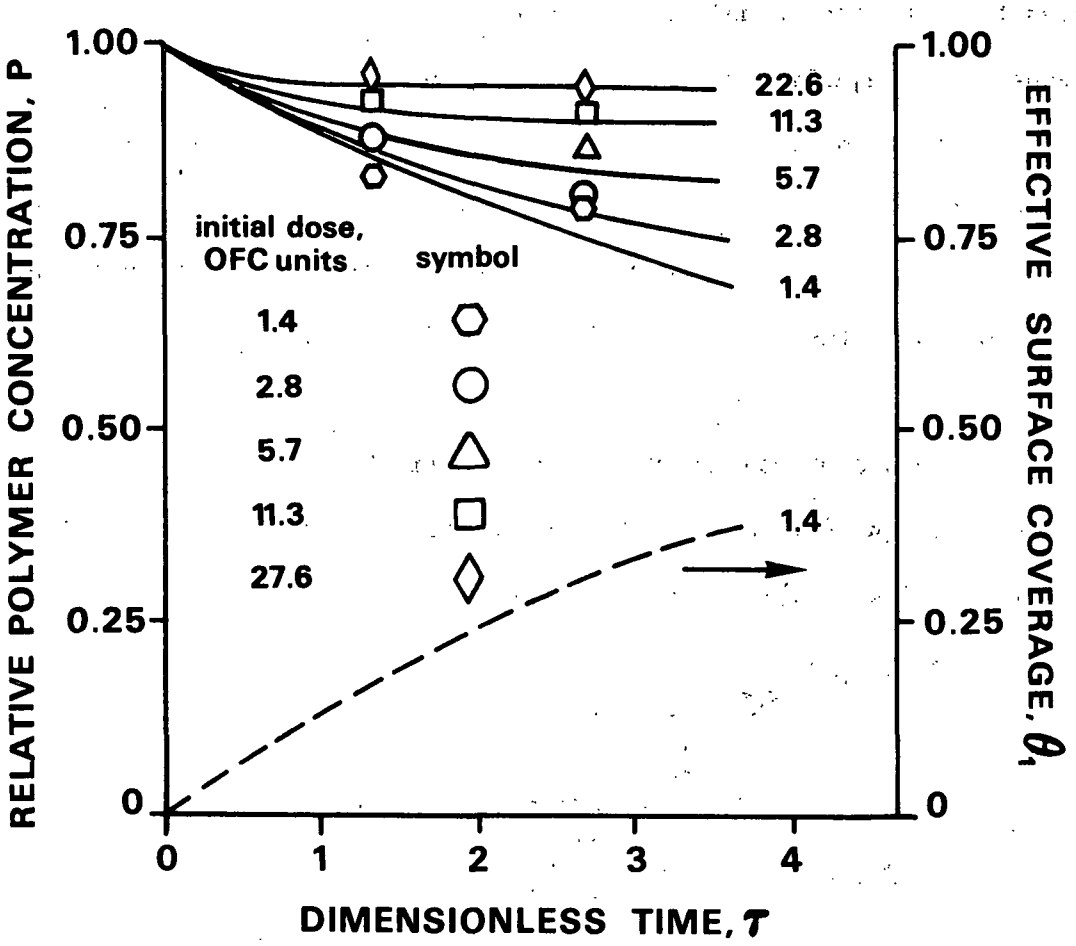

Figure 20. Theoretical and experimental adsorption rates. Molecular weight $1 \cdot 10^6$, pH 3, G = 1800 s^{-1}. Initial polymer dose in OFC units beside curves. Dashed line: effective surface coverage of singlets, θ_1.

The reason for this higher effective surface coverage is presumably that a polymer molecule first adsorbs with only a few segments and the rest of the chain dangles out into solution, sweeping across an area which becomes inaccessible to other polymer molecules. This phenomenon is another manifestation of Gregory and Sheiham's (30) "nonequilibrium flocculation" observed under Brownian conditions. Further improvement of the model could have been obtained if the reconformation rate of the polymer were known; in the present study it was assumed that this rate was negligible compared to the time scale of the experiments, 0.16 to 2.4 seconds. Gregory and Sheiham (30) found experimental evidence of a reconformation time on the

order of 1-4 seconds. However, very little information is available about this process, and the reconformation time could be considerably longer. Computer simulations indicate that, in some cases, a true equilibrium may never be achieved (22).

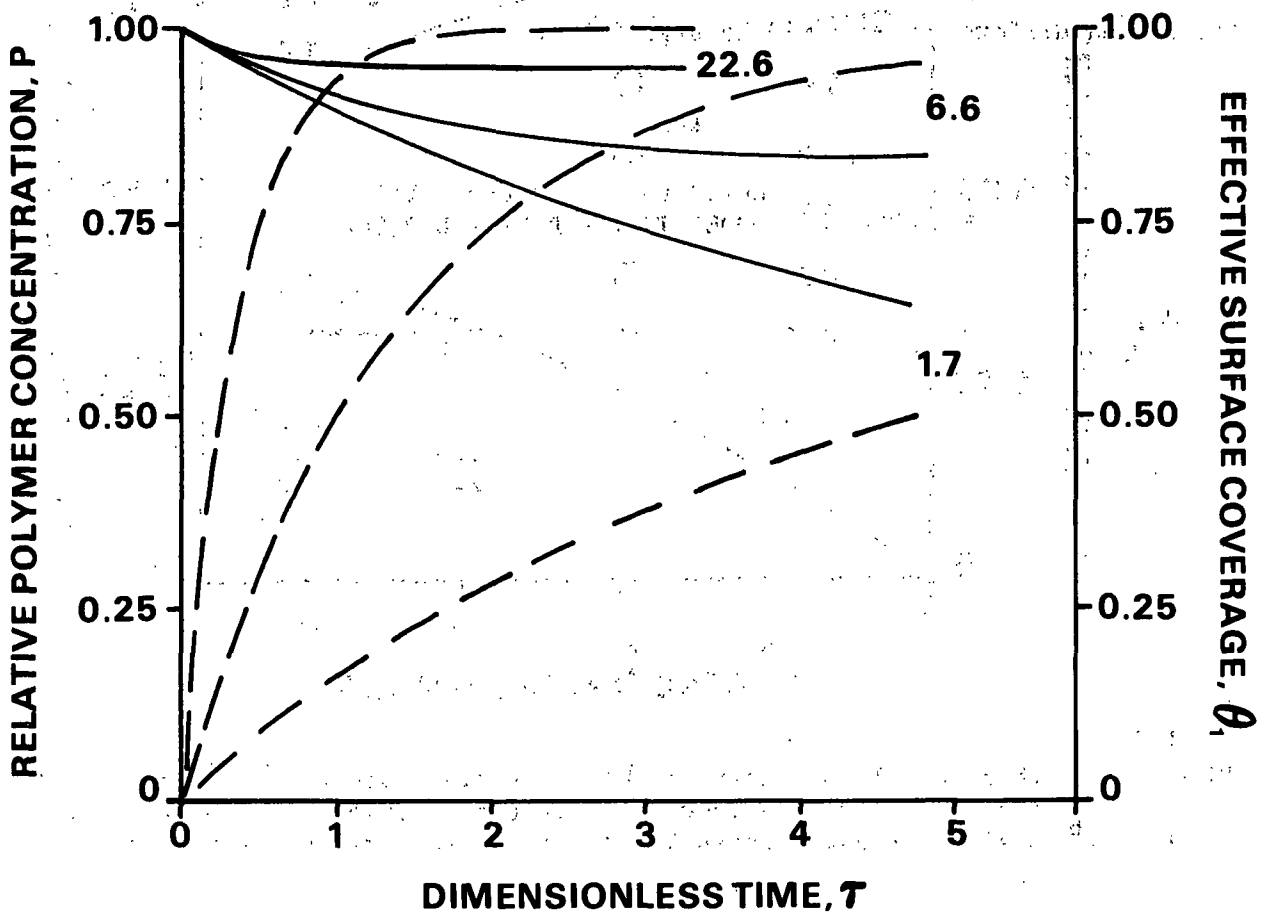

Figure 21. Theoretical curves of polymer concentration, P, solid lines —— and effective surface coverage of singlets, θ_1, dashed lines - - -. molecular weight $1 \cdot 10^6$, pH 3, G = 1800 s^{-1}. Initial dose in OFC units.

Despite the simplifying assumptions prescribed to the adsorption-flocculation model the calculated hydrodynamic collision efficiencies appear to be reasonable, Table III. The flocculation efficiencies are close to, or slightly higher than, the values obtained for rapid coagulation, and the hydrodynamic adsorption efficiencies are slightly lower. The higher hydrodynamic adsorption efficiency for the lower

molecular weight polymer is unexpected. It may be due to differences in the reconformation rate or effects of Brownian motion not properly accounted for in the model. Higher shear rates appear to increase the hydrodynamic flocculation efficiencies, not in absolute terms but relative to α_{11}. This is plausible (68, 69), but the calculated differences may not be significant.

TABLE III

COLLISION EFFICIENCIES ESTIMATED FROM FITTING THE MATHEMATICAL MODEL TO EXPERIMENTAL RESULTS

Molecular Weight	pH	G, s^{-1}	F/A[a]	α/α_{11}[b] o[c]	α/α_{11}[b] p[d]	θ_e/θ_∞[e]
$1.3 \cdot 10^5$	3	1800	F	1.5	0.75	
			A	1.5	0.75	3.9
		8000	F	2.0	1.0	
			A	1.5	0.75	3.5
$1 \cdot 10^6$	3	1800	F	1.75	0.88	
			A	0.8	0.4	3.5
		8000	F	2.7	1.35	
			A	0.8	0.4	3.1
$1.3 \cdot 10^5$	10	--[f]	F	1.0	0.5	
			A	0.3	0.15	1.0
$1 \cdot 10^6$	10	--[f]	F	1.0	0.5	
			A	0.5	0.25	1.0
Rapid coagulation		1800		1.60[g]	0.5[h]	
		8000		1.25[g]	0.5[h]	

[a] F = flocculation, A = adsorption.
[b] $\alpha_{11} = 0.788\ G^{-0.18}$ for shear flow, $\alpha_{11} = 0.5$ for Brownian motion.
[c] o = orthokinetic.
[d] p = perikinetic.
[e] Ratio between effective surface coverage under turbulent non-equilibrium and quiescent equilibrium conditions for a given amount of adsorbed polymer
[f] No shear rate dependence.
[g] Estimated from experiments and model calculations.
[h] Estimated from literature data.

The decrease in polymer concentration and the development of surface coverage for singlets with time, as predicted by the model for the higher molecular weight polymer, are shown in Fig. 21. It is seen that the adsorption of an initial dose of 1 OFC unit is far from complete at the end of the experimental time interval. This clearly illustrates why polymer adsorption is rate limiting for the overall flocculation process. Only total polymer concentration could be measured and no experimental data exist to verify the surface coverage curves.

Experiments at pH 10

There is no strong effect on flocculation of either time or polymer dose at pH 10. Nor is restabilization as clearly evident as at pH 3. The theoretical predictions of flocculation and adsorption of the high molecular weight polymer at pH 10 are presented in Fig. 22 and 23, respectively.

The theoretical model overestimates the extent of flocculation at longer times. An attempt to get better agreement between predicted and experimental flocculation results would probably require the inclusion of a floc breakup term in the model, since there is no reason to believe that the flocculation efficiencies would be much smaller than already assumed (see Table III, p. 65). On the contrary, it appears that the effective polymer surface coverage at pH 10 may also be higher under nonequilibrium conditions than at equilibrium, which would increase the flocculation rate for a given amount of adsorbed polymer. However, this assumption was not used in the model calculations. Predicted maximum adsorption values, assuming equilibrium polymer conformation, are about 1.4 OFC units for the highest polymer doses and the longest adsorption times used in the experiments. The actually measured adsorption values never exceeded 75% of one OFC unit, which would indicate the existence of a higher nonequilibrium degree of effective surface coverage at pH 10. Another indication of

this is the apparent occurrence of restabilization at higher polymer doses despite adsorption values below one OFC unit; see Appendix V, Table XVIII.

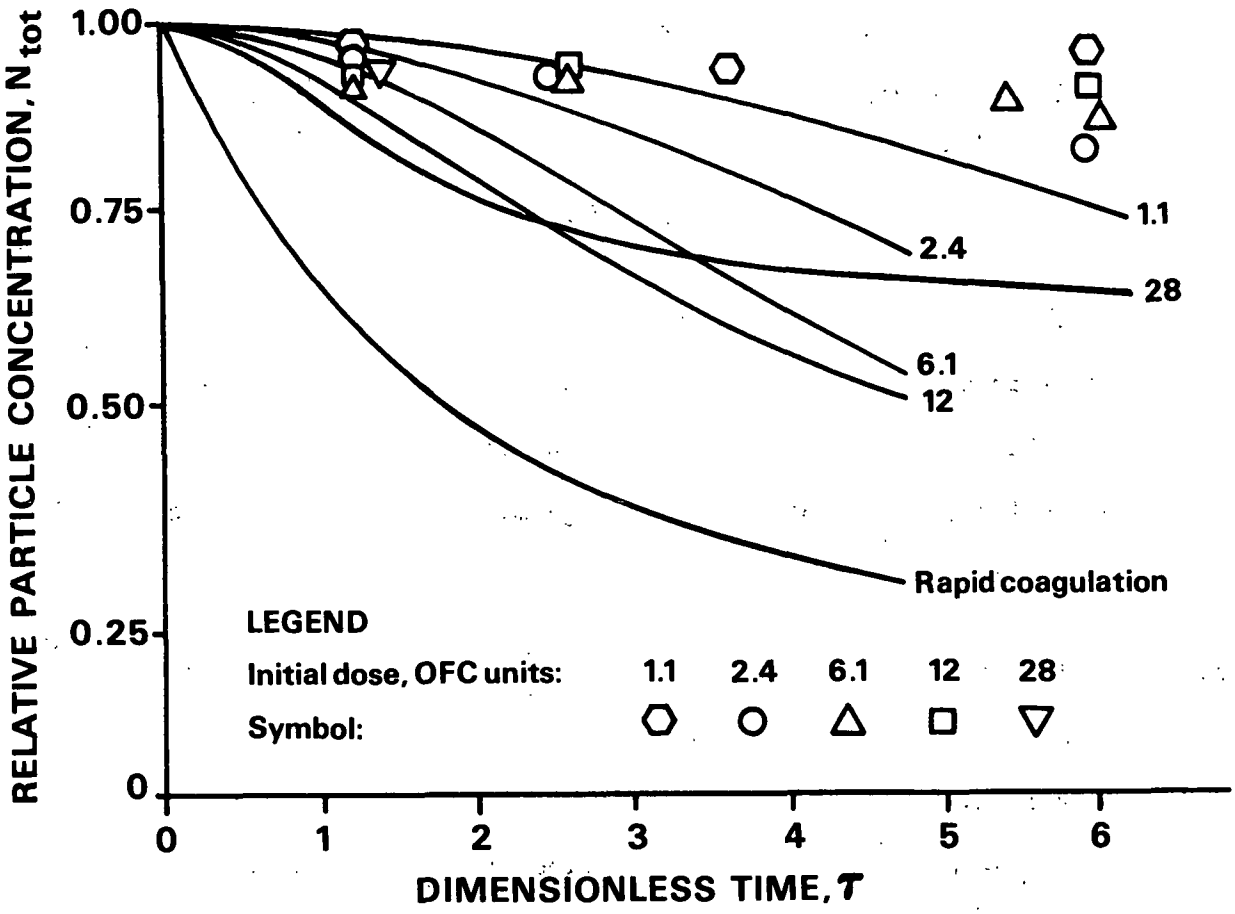

Figure 22. Theoretical and experimental flocculation rates. Molecular weight $1 \cdot 10^6$, pH 10, G = 1800 s^{-1}. Initial polymer dose in OFC units beside curves.

The collision efficiencies for adsorption and flocculation, estimated for both polymer molecular weights, are listed in Table III, p. 65. The values are lower than at pH 3. This result is expected, since the hydrodynamic size of the polymer is smaller and the effect of electrostatic attraction is less at pH 10.

Theoretical concentration and surface coverage curves for the high molecular weight polymer at pH 10 are given in Fig. 24. A comparison with Fig. 21, at pH 3,

shows that the adsorption rate is lower at pH 10, in part explaining the observed lower flocculation rates at this pH.

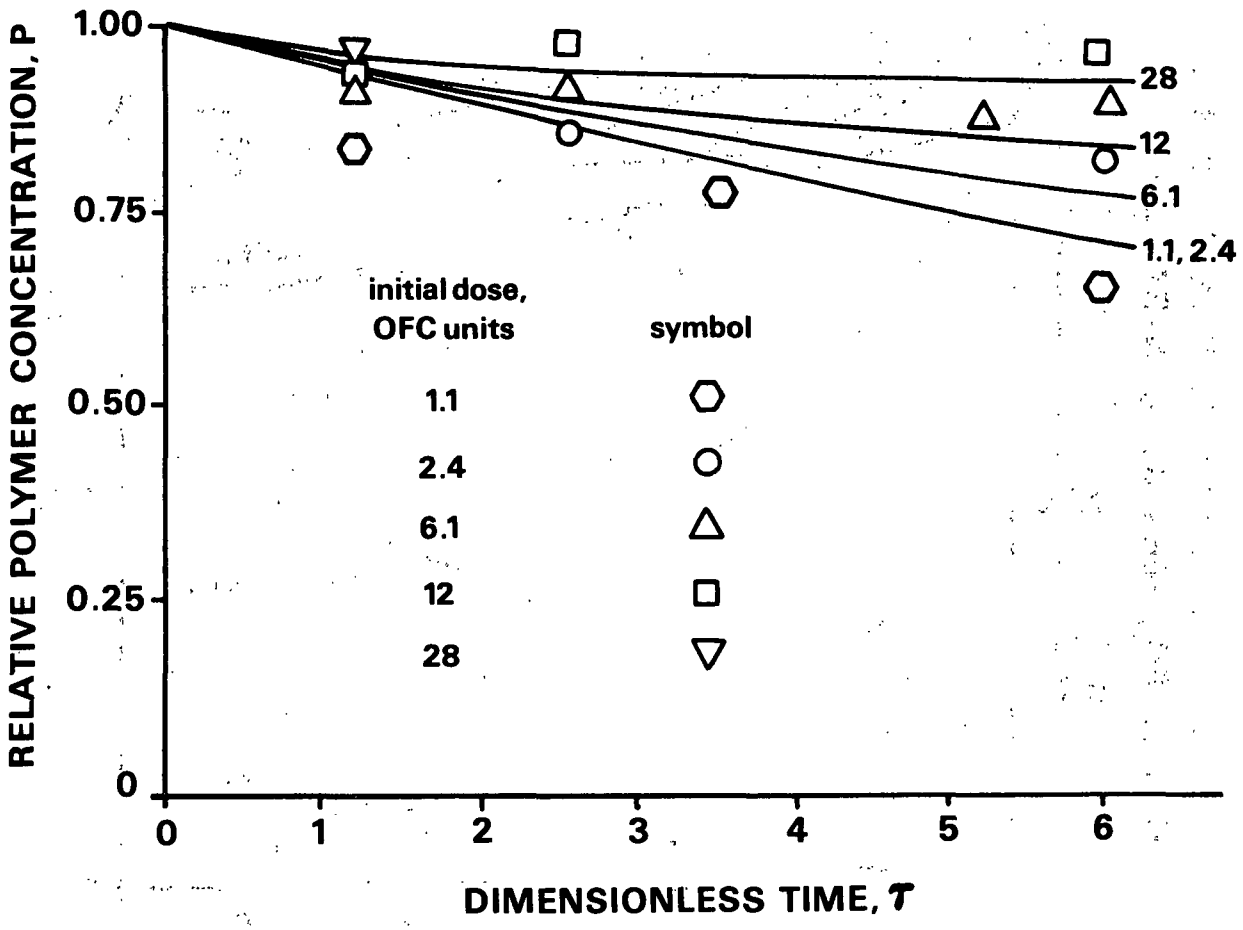

Figure 23. Theoretical and experimental adsorption rates. Molecular weight $1 \cdot 10^6$, pH 10, G = 1800 s^{-1}. Initial dose in OFC units beside curves.

FLOCCULATION WITH POLYMER TREATED LATEX

Collisions between clean particles as well as between polymer covered particles were assumed to be elastic in the model calculations. The hydrodynamic collision efficiency was further assumed to be equal to the experimentally found value for rapid coagulation and a shear rate of 1800 s^{-1}, i.e., 1.60 α_{11} = 0.327. Flocculation rates for partially covered flocs were also taken to be proportional to the

degree of surface coverage according to the factor $[(1-\theta_i)\theta_j + \theta_i(1-\theta_j)]$. The computer program could accommodate two initial floc size distributions, i.e., one distribution for clean particles and one distribution for polymer covered particles.

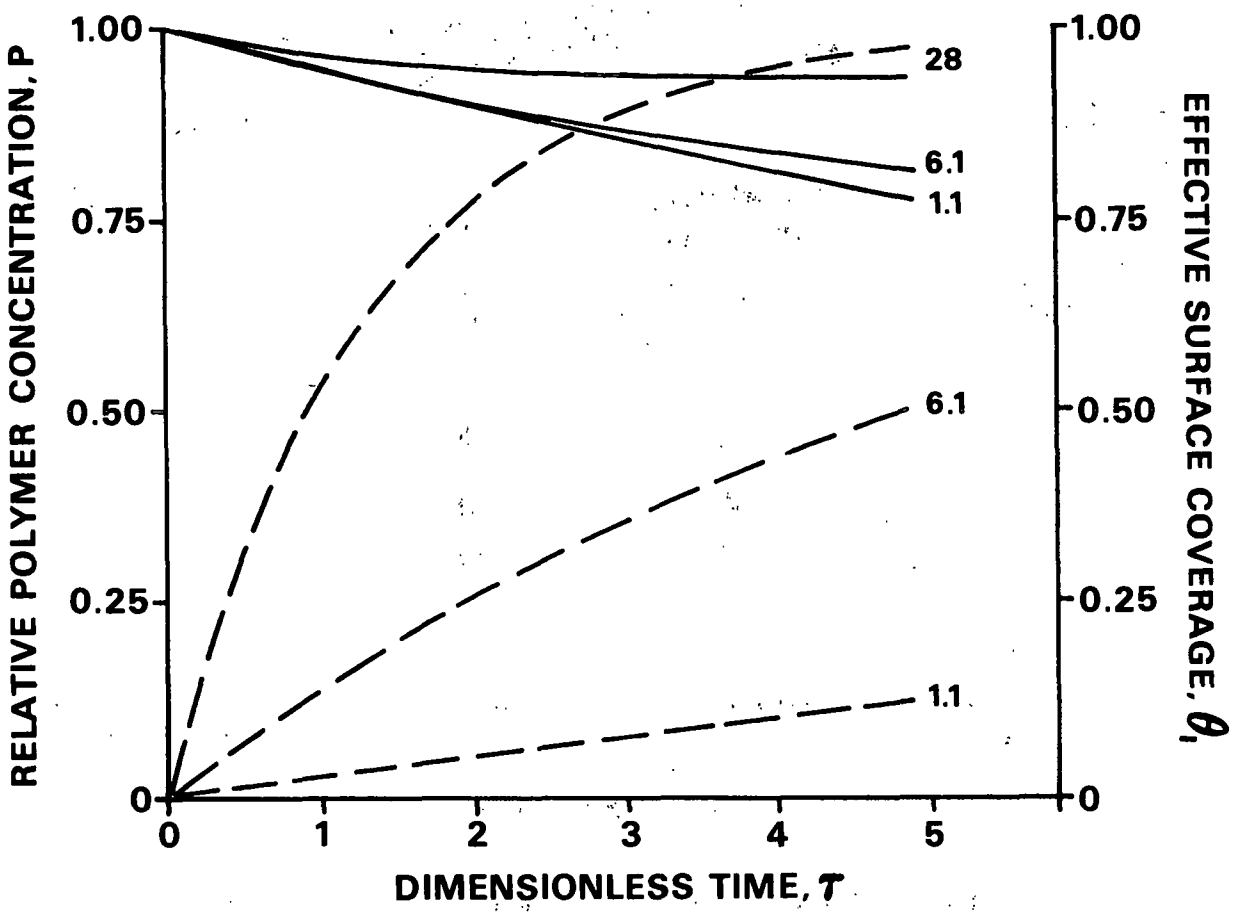

Figure 24. Theoretical curves of polymer concentration, P, solid lines ——, and effective surface coverage of singlets, θ_1, dashed lines - - -. Molecular weight $1 \cdot 10^6$, pH 10, G = 1800 s^{-1}. Initial dose in OFC units beside curves.

The predicted flocculation rates were compared with the experimental results using a concentration vs. time diagram, Fig. 25. The experimental rates were higher than the theoretical predictions. This increase can be expressed in terms of a higher collision efficiency compared with the initial assumption. When the collision

efficiency, as in this case, is taken to be independent of floc size it can be incorporated in the dimensionless time, giving

$$\tau_\alpha = \alpha\tau \qquad (35)$$

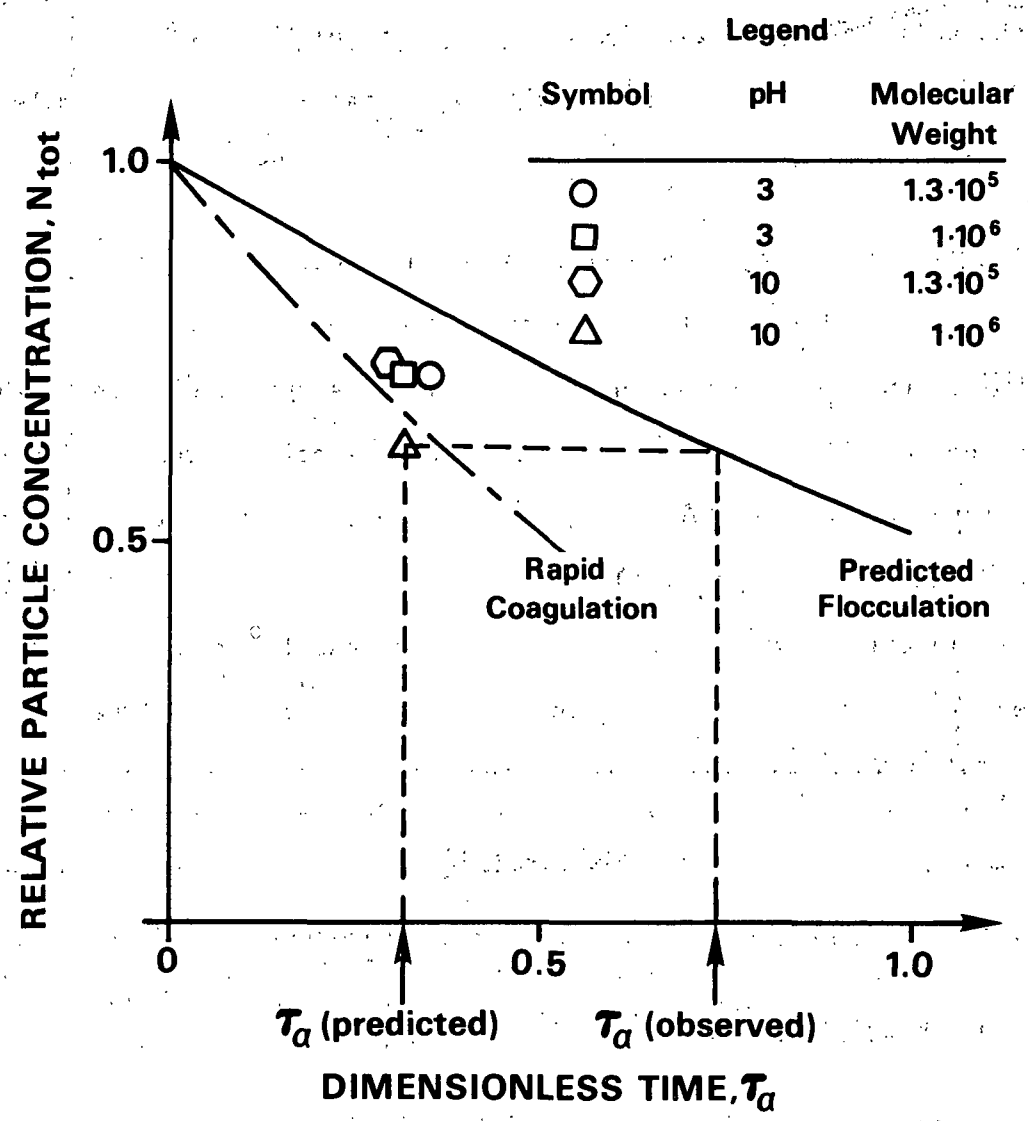

Figure 25. Flocculation with 50% polymer pretreated latex. Solid line: predicted flocculation. Broken line: rapid coagulation. G = 1800 s^{-1}.

The experimentally observed floc concentrations can be assigned corresponding flocculation times, see Fig. 25. The ratio between the observed flocculation time

and the predicted time is equivalent to an increase in collision efficiency above the initially assumed value, that is

$$\tau_\alpha(\text{observed})/\tau_\alpha(\text{predicted}) = \alpha(\text{observed})/\alpha(\text{predicted}) \quad (36)$$

The increase was 49% for the low molecular weight polymer at pH 3. The high molecular weight polymer at pH 3 and the low molecular weight polymer at pH 10 gave an increase of 56%. The highest increase, 128% was obtained by the high molecular weight polymer at pH 10.

It was a little unexpected to note that the high molecular weight polymer at pH 10 had the fastest flocculation rate, considering the poor flocculation results obtained in the adsorption-flocculation case. If the adsorption of this polymer would increase the particle diameter by 76 nm, twice the polymer radius of gyration, a flocculation rate increase of 23% could then be expected (neglecting any changes in collision efficiency). Gregory (15), using laminar tube flow, noted a more than twofold increase in collision efficiency for a polystyrene latex, half of which had been pretreated with a high molecular weight, high charge density polymer.

The rapid flocculation rates obtained with pretreated latex confirm the conclusion that polymer adsorption was indeed the rate limiting step in the simultaneous adsorption and flocculation process.

COMPARISON OF ADSORPTION AND FLOCCULATION RATES

The ratio of adsorption halftime to coagulation halftime is a convenient measure of whether adsorption will be rate limiting or not. The adsorption halftime, t_A, is the time required to reduce the polymer concentration to half of its initial value. Similarly, the coagulation halftime, t_C, is defined as the time required to halve

the total particle concentration (singlets + aggregates) in rapid coagulation. The coagulation halftime, t_C, can also be regarded as the average time between collisions for a given particle. Adsorption will be fast compared with the particle-particle collision frequency, and the adsorption step will not be rate limiting for the overall flocculation process if

$$t_A \ll t_C \tag{37}$$

An analysis of how the halftimes for adsorption and coagulation and the ratios between them vary with shear rate and polymer-particle size ratio, r, is given below. The rate equations for monodisperse systems at time zero can be integrated to give approximate expressions of the halftimes. The initial orthokinetic adsorption rate is

$$dp/dt = -\alpha_{Ao}(4G/3)(a_1 + a_p)^3 n_o p = -\alpha_{Ao}(4G/3)a_1^3(1+r)^3 n_o p \tag{38}$$

where α_{Ao} = collision efficiency for adsorption

r - ratio polymer radius / singlet radius

$$\ln(p/p_o) = -\alpha_{Ao}(4G/3)a_1^3(1+r)^3 n_o t$$

no polymer molecules at time t
no of polymer molecules to start

By definition $t = t_{Ao}$ for $p/p_o = 1/2$

$$\ln 2 = \alpha_{Ao}(4G/3)a_1^3(1+r)^3 n_o t_A$$

$$t_{Ao} = 3\ln 2/(\alpha_{Ao} 4G a_1^3(1+r)^3 n_o) \tag{39}$$

The initial orthokinetic coagulation rate gives

$$dn/dt = -\alpha_{Co}(4G/3)(a_1+a_1)^3 n^2 \tag{40}$$

where α_{Co} = collision efficiency for coagulation

$$t_{Co} = 3/(\alpha_{Co} 32 G a_1^3 n_o) \tag{41}$$

The ratio of orthokinetic adsorption time to orthokinetic coagulation time can then be written:

$$t_{Ao}/t_{Co} = (\alpha_{Co}/\alpha_{Ao})8\ln 2/(1+r)^3 \tag{42}$$

$$t_{Ao} < t_{Co} \text{ if } r > 0.8 \quad \text{and } \alpha_{Ao} = \alpha_{Co} \tag{43}$$

If the collision efficiencies are equal, then the polymer diameter has to be larger than 80% of the particle diameter to produce an adsorption time which is shorter than the coagulation time.

Under perikinetic conditions the halftime ratio is

$$t_{Ap}/t_{Cp} = (\alpha_{Cp}/\alpha_{Ap})4r\ln 2/(1+r)^2 \tag{44}$$

$$t_{Ap} \leq 0.7t_{Cp} \text{ if } \alpha_{Ap} = \alpha_{Cp} \tag{45}$$

This ratio, Eq. (44), will have a maximum of 0.7 for $r = 1.0$ and $\alpha_{Ap} = \alpha_{Cp}$. Consequently, if the collision efficiencies are equal, the adsorption time will always be shorter than the coagulation time.

The sizes of the particles and polymer molecules and the shear rate will determine whether the adsorption and coagulation processes will be orthokinetic or perikinetic. The halftime ratio for orthokinetic adsorption to perikinetic adsorption at 25°C in water can be written:

$$t_{Ao}/t_{Ap} = (\alpha_{Ap}/\alpha_{Ao})\ 2.06 \cdot 10^{-18}/(Ga_1{}^3(1+r)r)$$
$$t_{Ao}/t_{Ap} = 22(\alpha_{Ap}/\alpha_{Ao}), \quad G = 1\ s^{-1} \quad a_1 = 0.5\ \mu m \quad r = 0.5 \tag{46}$$

The halftime ratio for orthokinetic coagulation to perikinetic coagulation is:

$$t_{Co}/t_{Cp} = (\alpha_{Cp}/\alpha_{Co})1.03 \cdot 10^{-18}/(Ga_1^3)$$
$$t_{Co}/t_{Cp} = 8(\alpha_{Cp}/\alpha_{Co}), \qquad G = 1\ s^{-18} \quad a_1 = 0.5\ \mu m \tag{47}$$

If adsorption is mainly due to Brownian motion and coagulation is due to shear motion, then the halftime ratio of perikinetic adsorption to orthokinetic coagulation should be considered:

$$t_{Ap}/t_{Co} = (\alpha_{Co}/\alpha_{Ap})2.70 \cdot 10^{18} Ga_1^3 r/(1+r)^2$$
$$t_{Ap}/t_{Co} = 7.5 \cdot 10^{-2}\ (\alpha_{Co}/\alpha_{Ap}), \qquad G = 1\ s^{-1} \quad a_1 = 0.5\ \mu m \quad r = 0.5 \tag{48}$$

The reverse situation, viz. orthokinetic adsorption and perikinetic coagulation may also be of interest:

$$t_{Ao}/t_{Cp} = (\alpha_{Cp}/\alpha_{Ao})\ 5.70 \cdot 10^{-18}/(Ga_1^3(1+r)^3)$$
$$t_{Ao}/t_{Cp} = 13.5\ (\alpha_{Cp}/\alpha_{Ao}), \qquad G = 1\ s^{-1} \quad a_1 = 0.5\ \mu m \quad r = 0.5 \tag{49}$$

Experimental halftimes obtained by extrapolation to 50% of initial concentration, cf. Fig. 18-23, are listed in Table IV. The adsorption halftime, t_A, is considerably larger than the coagulation time, t_C, and the flocculation halftime is closer to t_A than to t_C. Equations (39) and (41) were also used to calculate halftimes assuming monodisperse initial conditions and $\alpha_A = \alpha_C = 0.204$, $G = 1800\ s^{-1}$. The results are listed within parentheses in Table IV. It is seen that the analytical halftimes, from Eq. (39) and (41) are good qualitative approximations of the numerical results.

TABLE IV

HALFTIMES FOR COAGULATION, t_C, FLOCCULATION, t_F, AND ADSORPTION, t_A

Values without parentheses are based on model calculations, cf. Fig. 18-23, and values within parenthesis are calculated with Eq. (39) and (41) assuming monodisperse initial conditions and $\alpha_A = \alpha_C = 0.204$. $G = 1800\ s^{-1}$, $n_o = 2 \cdot 10^{15}\ m^{-3}$, (91% singlets, 6% doublets, 3% triplets and larger flocs), molecular weight = $1 \cdot 10^6$, initial polymer dose = OFC.

HALFTIMES IN SECONDS

	t_C	t_F	t_A	t_A/t_C
pH 3	0.6(0.7)	1.4	2.0(1.6)	3.3(2.1)
pH 10	0.6(0.7)	3.1	3.2(3.4)	5.3(4.5)

Interpretation of Literature Data

Polymer adsorption may or may not be rate limiting for the flocculation process depending on particle and polymer size, collision efficiency and shear rate. If the flocculation process is perikinetic, the adsorption halftime will always be shorter than the flocculation halftime, assuming equal collision efficiencies. In this case adsorption is very likely not to be rate limiting. This is in agreement with observations in the literature. Generally a flocculation rate enhancement is seen compared with the coagulation rate. This is often explained in terms of a higher collision efficiency for particles with a fractional surface coverage of polymer, the very likely reasons being electrostatic attraction and/or reduced viscous interactions. The diffusion coefficient of a spherical particle is inversely proportional to its diameter, so an increase in effective particle diameter due to polymer adsorption will not be beneficial.

If the flocculation process is orthokinetic, the polymer must either be larger or very much smaller than the particles to avoid adsorption limitation. This is in

agreement with the predictions of Gregory (15,22) and the experimental results of Birkner and Morgan (41), although the latter did not subscribe to this explanation. How then, can reported rate enhancements compared with orthokinetic coagulation be explained? Three mechanisms, similar to the perikinetic case, appear likely: 1) The adsorbed polymer increases the collision radius of the particle. 2) The flow field around the particle is disturbed by the adsorbed polymer, thereby increasing the collision efficiency. 3) Electrostatic attraction due to patch-type adsorption increases the collision efficiency.

In Franco's work (43) the particle diameter was about 75 nm and the high molecular weight, low charge density polymer giving the highest flocculation rate increase compared with coagulation was estimated to have a radius of gyration of 178 nm (70). This gives an r-value, a_p/a_1, of 2.4, and the adsorption halftime is therefore expected to be shorter than the coagulation halftime according to Eq. (43). Furthermore, a low charge density polymer is assumed to adsorb in a bulky state similar to its solution conformation, which would in this case result in a substantial increase in the effective particle radius (maximum, a factor of 5.7). Thus, it is clear that the theoretical treatment in the present study is consistent with the experimental results of Franco.

The results of Graham (44) are seemingly in conflict with the present study. A rate increase of 30 times was observed for flocculation with a high molecular weight polymer compared with rapid coagulation at a shear rate of 100 s^{-1}. The reported collision efficiency for rapid orthokinetic coagulation, $\alpha_{11} = 0.017$ is surprisingly low. An estimation using Fig. 3 gives $\alpha_{11} = 0.10$ for spherical particles with a radius of 3.8 μm, as used by Graham, and a Hamaker constant of $1.3 \cdot 10^{-20}$ J [glass (71)]. However, a low collision efficiency explains why adsorption may not be rate

limiting. Applying Eq. (42) and using the following values $\alpha_C = 0.017$, $\alpha_A = 1.0$, and $r = 0.1$, gives $t_A/t_C = 0.07$, implying that the adsorption rate is not a problem. In interrupted flocculation experiments, like the work of Graham and the present study, adsorption limitation may be circumvented by overdosing the system. Graham appears to have determined his OFC values under dynamic conditions. These considerations do not, however, explain the tremendous rate increases observed in polymer-aided flocculation. Explanations 2) and 3), reduced hydrodynamic interactions and increased electrostatic attraction, seem plausible. Graham also noted a fifteen-fold rate increase going from the lowest to the highest molecular weight. "Nonequilibrium flocculation" according to Gregory and Sheiham (30) is not a likely explanation, since the particle concentration was very low ($2.6 \cdot 10^5$ particles/mL) and the flocculation time long (10 minutes). The silica particles were extremely porous, and pore adsorption is perhaps a possibility for the low molecular weight polymers. Assuming that the particle surfaces have a "microroughness" it is also quite possible that the high molecular weight polymers would be better flocculants because they would not conform as well to the surface, increasing the microroughness and increasing the effectiveness of the cationic polymer patches.

As already discussed in the literature review, Black, Birkner and Morgan (40) concluded that the adsorption step was not rate limiting in their orthokinetic flocculation experiments. But their flocculation rates were not quantitative and no comparison with coagulation rates was made. In the following study by Birkner and Morgan (41), the authors measured orthokinetic coagulation rates that were actually faster than the corresponding polymer-aided flocculation rates. They argued, by referring to the previous study (40), that adsorption limitation could not be the reason for this observation. They concluded that floc breakup occurred at higher shear rates when the polymer was used for destabilization. However, at low shear

rates they assumed that steric effects were responsible for the lower flocculation rates. In light of the present study it is quite likely that adsorption rate limitation may have been the reason, at least partially, for the lower flocculation rates.

It is obvious that flocculation studies can produce results that are seemingly in conflict. Interpretation of these results is often subject to some degree of speculation because of missing pieces of information. It is hoped that the approach and analysis presented in this study will prove useful in the interpretation of adsorption and flocculation phenomena in dilute systems.

CONCLUSIONS

Polymer adsorption halftimes were significantly longer than coagulation halftimes in this study. This led to adsorption rate-limited orthokinetic flocculation, which was considerably slower than coagulation. It was also concluded that the effective surface coverage for a given amount of adsorbed polymer was higher under nonequilibrium conditions than at equilibrium. This finding was interpreted as a result of finite polymer reconformation rates. A flocculation experiment where half of the particles had been pretreated with polymer led to the conclusion that collisions between polymer-covered and polymer-free particles were more efficient than particle collisions in rapid coagulation.

The experimental results could, at least qualitatively, be predicted with a mathematical model based on modified coagulation rate theory. It was shown that the ratio of adsorption halftime to coagulation halftime is an indicator of whether the flocculation process will be adsorption rate-limited or not.

For perikinetic flocculation the adsorption halftime is always shorter than the coagulation halftime and the adsorption step is not likely to be rate-limiting. This conclusion is confirmed by experimental data in the literature.

Orthokinetic flocculation, on the other hand, is likely to be adsorption rate-limited if the hydrodynamic size of the polymer is smaller than the particles. However, the adsorption step may not be rate-limiting if the polymer is so small that the adsorption process is perikinetic or if the polymer is larger than the particles. In some cases where the adsorption step is rate-limiting, flocculation may still be faster than coagulation, because optimum polymer coverage can improve particle collision efficiencies.

The results of this study also explained seemingly conflicting literature reports, where orthokinetic flocculation rates were either slower or faster than coagulation rates.

SUGGESTIONS FOR FUTURE RESEARCH

The reconformation rate of a high molecular weight, linear polymer could be measured using a radioactively tagged surfactant to stop the polymer adsorption reaction. The amount of adsorbed surfactant, corresponding to the surface area not occupied by polymer, should be measured directly on the particles after the solution has been filtered through a polycarbonate filter and the filter cake resuspended in clean water.

Floc breakup could be studied by running the surfactant stabilized suspension several times through the same pipe, measuring floc size distributions before and after each run. This experiment should give useful information on floc strength as a function of type of flocculant as well as information on the breakup mechanism.

From a papermaker's view the present study has been geared toward adsorption onto and flocculation of fillers and fines. A natural extension would be to study the kinetics of polymer adsorption onto fibers in turbulent pipe flow. The kinetics of heteroflocculation of fibers and fine material could also be investigated in turbulent pipe flow comparing the results of 1) flocculation with simultaneous polymer adsorption, 2) flocculation with polymer pretreated surfaces, and 3) coagulation with a simple electrolyte.

NOMENCLATURE

a_i radius of floc of size i, m

a_{ij} $(a_i + a_j)/2$

a_p radius of polymer molecule, m

A Hamaker constant, J

b breakup coefficient, dimensionless

D_i diffusion coefficient, m^2/s

D_{ij} $D_i + D_j$, relative diffusion coefficient, m^2/s

f Blasius friction factor, dimensionless

k_B Boltzmann's constant, $1.38 \cdot 10^{-23}$ J/K

K_{Ga} $k_B T/(8 Ga_1^3)$, dimensionless

m floc size exponent, dimensionless

n_o total initial number concentration of particles, singlets plus aggregates, m^{-3}

n_i number concentration of flocs containing i singlets at time t, m^{-3}

N_i n_i/n_o, dimensionless floc concentration

p initial number concentration of polymer molecules, m^{-3}

P p/p_o, dimensionless polymer concentration

Pe Peclet number

PSL polystyrene latex

PVAm polyvinylamine

r a_p/a_1, ratio of polymer radius to singlet radius

s total initial number concentration of particles if all aggregates are broken down to singlets, divided by n_o

t time, s

$t_{1/2}$ $3/(16 n_o Ga_1^3)$, characteristic time for coagulation and flocculation, s

t_A halftime for polymer adsorption, s

t_C halftime for rapid coagulation, s

t_F halftime for flocculation, s

T absolute temperature, K

u_f $U(f/8)^{1/2}$, friction velocity, m/s

U average velocity, m/s

V volume, m^3

y distance from wall of pipe, m

Greek Letters

α collision efficiency, dimensionless

α_{ij} collision efficiency for binary encounters between flocs containing i and j singlets

β_{ij} $(i^m + j^m)^2/(ij)^m$

β_{ip} $(i^m + r)^2/(i^m r)$

ε energy dissipation, W/kg

κ von Karman constant, dimensionless

λ a_i/a_j, $i > j$

λ_L London wave length, nm

μ viscosity, kg/ms

ν kinematic viscosity, m^2/s

ρ density, kg/m^3

τ $t/t_{1/2}$, dimensionless time

σ_{ij} $(i^m + j^m)^3/8$

σ_{ip} $(i^m + r)^3/8$

θ_e initial polymer dose divided by dose required to give 100% effective surface coverage, dimensionless

θ_i effective fractional surface coverage of a floc containing i singlets, dimensionless

θ_k^f average effective fractional surface coverage of k-flocs formed by collisions between i- and j-flocs, dimensionless

Subscripts

A adsorption

C coagulation

F flocculation

d disappearance rate

f formation rate

i,j,k floc size, number of singlets in a floc

k i+j

o orthokinetic or initial

p perikinetic or polymer

ACKNOWLEDGMENTS

I should like to express my appreciation to my thesis advisory committee, Dr. R. A. Stratton, Chairman, Dr. E. J. Bonano and Dr. M. R. Doshi. Dr. J. W. Swanson and Dr. G. J. Howard are also thanked for their support during the early stages of this study.

I am grateful to Mr. Gunnar Nicholson, New York, and The Institute of Paper Chemistry for giving me the opportunity to undertake this research. Special thanks go to the staff and students of the Institute for providing a pleasant atmosphere to work and live in.

My sincere thanks go to my parents, who always supported and encouraged me in this endeavor, despite the great separation in distance between us.

Most of all, my gratitude is extended to my wife, Barbara, without whose sacrifice and support this work could not have been done.

LITERATURE CITED

1. Kruyt, H. R. Colloid Science. Vol. 1. Elsevier Publ. Co., New York, 1949. 389 p.

2. Vincent, B., Adv. Colloid Interface Sci. 4:193(1974).

3. Vincent, B. and Whittington, S. G., Adv. Colloid Interface Sci. 12:1(1982).

4. Tadros, Th. F. The effect of polymers on dispersion properties. Academic Press, New York, 1982. 423 p.

5. Adv. Colloid Interface Sci., Vol. 16 and 17, 1982.

6. La Mer, V. and Healy, T. W., Rev. Pure Appl. Chem. 13:112-33(1963).

7. von Smoluchowski, M., Physik. Zeitschr. XVII:557, 585(1916).

8. von Smoluchowski, M., Zeitschrift f. physik. Chemie XCII:129(1917).

9. Camp, T. R. and Stein, P. C., J. Boston Soc. Civ. Eng. 30:219(1943).

10. Saffman, P. G. and Turner, J. S., J. Fluid Mech. 1:16(1956).

11. Delichatsios, M. A. and Probstein, R. F., J. Colloid Interface Sci. 51:394 (1975).

12. Levich, V. G. Physicochemical hydrodynamics. Prentice-Hall, Inc., Englewood Cliffs, New Jersey, 1962. 700 p.

13. Spielman, L. A., J. Colloid Interface Sci. 33:562(1970).

14. Honig, E. P., Roebersen, G. J. and Wiersema, P. H., J. Colloid Interface Sci. 36:97(1971).

15. Gregory, J. Polymer flocculation in flowing dispersions. In Tadros' the effect of polymers on dispersion properties. p. 301. Academic Press, New York, 1982.

16. van de Ven, T. G. M., Adv. Colloid Interface Sci. 17:105(1982).

17. van de Ven, T. G. M. and Mason, S. G., Colloid Polymer Sci. 256:468(1977).

18. Schowalter, W. R., Adv. Colloid Interface Sci. 17:129(1982).

19. Adler, P. M., J. Colloid Interface Sci. 83:106(1981).

20. Higashitani, K., Ogawa, R., and Hosokawa, G., J. Chem. Eng. Japan 15:299(1982).

21. Kasper, D. R. Theoretical and experimental investigations of the flocculation of charged particles in aqueous solutions by polyelectrolytes of opposite charge. Doctor's Dissertation. Pasadena, California, California Institute of Technology, 1971. 201 p.

22. Gregory, J. Effects of polymers on colloid stability. In Ives' the scientific basis of flocculation. p. 101. Sijthoff and Noordhoff, Alphen aan den Rijn, The Netherlands, 1978.

23. Morawetz, H. Macromolecules in solutions. 2nd Ed., High Polymers. Vol. XXI. Wiley-Interscience, New York, 1975. 549 p.

24. Noda, I., Tsuge, T., and Nagasaura, M., J. Phys. Chem. 74:710(1970).

25. Tan, J. S. and Gasper, S. P., J. Polymer Sci. (Polymer Phys. Ed.) 13:1705(1975).

26. Soumpasis, D. M. and Benneman, K. H., Macromols. 14:50(1981).

27. Stigter D., Macromols. 15:635(1982).

28. Petersen, C. and Kwei, T. K., J. Phys. Chem. 65:1330(1961).

29. Sato, T. and Ruch, R. Stabilization of colloidal dispersions by polymer adsorption. Surfactant Science Series Vol. 9. Marcel Dekker, Inc., New York, 1980. 155 p.

30. Gregory, J. and Sheiham, J., Br. Polymer J. 6:47(1974).

31. Hesselink, F. Th., J. Colloid Interface Sci. 60:448(1977).

32. Smellie, R. H., Jr. and La Mer, V. K., J. Colloid Sci. 13:589(1958).

33. Gregory, J., J. Colloid Interface Sci. 42:448(1973).

34. Uriarte, F. A. Kinetics of colloid aggregation. I. Coagulation rate constants by turbidimetry. II. Kinetics of colloid flocculation using polyelectrolytes. Doctor's Dissertation. Pittsburgh, Pennsylvania, Carnegie-Mellon University, 1971. 351 p.

35. Singer, J. M., Vekemans, F. C. A., Lichtenbelt, J. W. Th., Hesselink, F. Th., and Wiersema, P. H., J. Colloid Interface Sci. 45:608(1973).

36. Gregory, J., J. Colloid Interface Sci. 55:35(1976).

37. Fleer, G. J. Polymer adsorption and its effect on colloidal stability. A theoretical and experimental study on the polyvinyl alcohol-silver iodide system. Mededelingen Landbouwhogeschool Wageningen, The Netherlands, 71-20 (1971). 144 p.

38. van der Scheer, A., Tanke, M. A., and Smolders, C. A., Faraday Discuss. Chem. Soc. 65:264(1978).

39. Walles, W. E., J. Colloid Interface Sci. 27:4(1968).

40. Black, A. P., Birkner, F. B. and Morgan, J. J., J. AWWA 57:1547(1965).

41. Birkner, F. B. and Morgan, J. J., J. AWWA 60:175(1968).

42. Klute, R. and Hahn, H. H., Vom Wasser 43:215(1974).

43. Franco, R. P., Unpublished work. The Institute of Paper Chemistry, Appleton, Wisconsin, 1978.

44. Graham, N. J. D., Colloids Surfaces 3:61(1981).

45. Stratton, R. A., Tappi 66(3):141(1983).

46. Glasgow, L. A. and Hsu, J. P., AIChE J. 28:779(1982).

47. Lipatov, Yu. S. and Sergeeva, L. M. Adsorption of polymers. Halsted Press, New York, 1974. 177 p.

48. Sikora, M. D. The role of polyelectrolyte charge density in the mechanism of hydrodynamic shear-induced restabilization of a flocculated colloidal dispersion. Doctor's Dissertation. Appleton, Wisconsin, The Institute of Paper Chemistry, 1978. 170 p. Sikora, M. D. and Stratton, R. A., Tappi 64(11):97(1981).

49. Hearn, J., Wilkinson, M. C., and Goodall, A. R. Polymer latices as model colloids. Adv. Colloid Interface Sci. 14:173(1981)

50. Vanderhoff, J. W., van den Hul, H. Y., Tansk, R. J. M., and Overbeck, J. Th. G. The preparation of monodisperse latexes with well-characterized surfaces. In Goldfinger's Clean Surfaces: Their preparation and characterization for interfacial studies. p. 15. Marcel Dekker, Inc., New York, 1970.

51. Ahmed, S. M., El-Aasser, M. S., Pauli, G. H., Poehlein, G. W., and Vanderhoff, J. W., J. Colloid Interface Sci. 73:388(1980).

52. Arnson, T. R. The adsorption of complex aluminum species by cellulosic fibers from dilute solutions of aluminum chloride and aluminum sulfate. Doctor's Dissertation, Appleton, Wisconsin, The Institute of Paper Chemistry, 1980. 143 p.

53. Connor, P. and Ottewill, R. H., J. Colloid Interface Sci. 37:642(1971).

54. Horn, D., Progr. Colloid Polymer Sci. 65:251(1978).

55. Eggert, A. R. The role of particle size and molecular weight on the adsorption and flocculation of polystyrene latex with poly (1,2-dimethyl-5-vinyl pyridinum bromide). Doctor's Dissertation. Appleton, Wisconsin, The Institute of Paper Chemistry, 1976. 190 p.

56. Ho, C. H. and Howard, G. J. The destabilization of anionic polystyrene latices by vinyl pyridine/acrylamide copolymers and homopolymers. In Tadros' the effect of polymers on dispersion properties. p. 343. Academic Press, New York, 1982.

57. Casson, D. and Rembaum, A., Polymer Letters 8:773(1970)

58. Medalia, A. I. Computer simulation of colloidal systems. In Matijevic's Surface and Colloid Science. Vol. 4. p. 1. Wiley-Interscience, New York, 1971.

59. Goodarz-Nia, I., J. Colloid Interface Sci. 62:131(1977).

60. Tambo, N. and Watanabe, Y., Water Res. 13:409(1979).

61. Laufer, J. U.S. Natl. Advisory Comm. Aeronautics Rept. No. 1174 (1954).

62. Hinze, J. O. Turbulence. 2nd ed. McGraw-Hill, Inc., New York, 1975. 790 p.

63. Rotta, J. C. Turbulente Stromungen. p. 157. B. G. Teubner, Stuttgart, 1972. 265 p.

64. Argaman, Y. and Kaufman, W. J., J. San. Eng. Div., Proc. Amer. Soc. Civ. Engrs. 96(SA2):223(1970).

65. Spielman, L. A. Hydrodynamic aspects of flocculation. In Ives' the scientific basis of flocculation. p. 63. Sijthoff and Noordhoff, Alpen aan den Rijn, The Netherlands, 1978.

66. Higashitani, K., Miyafusa, S., Matsuda, T., and Matsuno, Y., J. Colloid Interface Sci. 77:21(1980).

67. Guzy, C. J., Bonano, E. J. and Davis, E. J., J. Colloid Interface Sci., to be published.

68. Warren, L. J., J. Colloid Interface Sci. 50:307(1975).

69. Warren, L. J., Colloids Surfaces 5:301(1982).

70. Stratton, R. A., Personal Communication, 1983.

71. Rabinovich, Ya. I., Derjaguin B. V., and Churaev, N. V., Adv. Colloid Interface Sci. 16:63(1982).

72. Brandrup, J., Immergut, E. H., and McDowell, W. Polymer handbook. 2nd ed. Wiley-Interscience, New York, 1975.

73. Takahashi, A., Kato, T., and Nagasawa, M., J. Phys. Chem. 71:2001(1967).

74. Wu, W. C., El-Aasser, M. S., Micale, F. J., and Vanderhoff, J. W. Surface charge density and electrophoretic mobility of monodisperse polystyrene latexes. In Becher and Yudenfreund's emulsions, latices and dispersions. p. 71. Marcel Dekker, Inc., New York, 1978.

75. Matthews, B. A. and Rhodes, C. T., J. Colloid Interface Sci.32:339(1970).

76. Ives, K. J. and Al Dibouni, M., Chem. Eng. Sci. 34:983 (1979).

77. Few, A. V. and Ottewill, R. H., J. Colloid Sci. 11:34(1956).

APPENDIX I

RADIUS OF GYRATION OF A POLYELECTROLYTE

Random flight statistics (23) give an expression for the mean square end-to-end distance, $\langle r^2 \rangle$, of a linear nonionic polymer in solution

$$\langle r^2 \rangle = nl^2 f(\theta) g(\phi) \tag{50}$$

where

n = number of bonds in the polymer backbone

l = bond length, m

$f(\theta)$ = expansion factor due to fixed bond angles

$g(\phi)$ = expansion factor due to restricted rotation about the backbone

For a vinyl polymer with a carbon backbone, the value of $f(\theta) = 2$ and the bond length is 1.53 Å

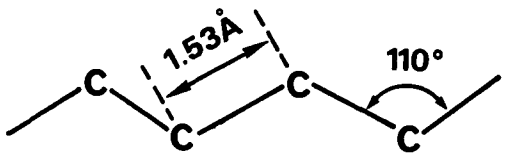

Taking the average for polyethylene and polystyrene (72) should give a fair approximation of $g(\theta)$ for polyvinylamine, $g(\theta) = 4$.

The number of bonds, n, is equal to two times the degree of polymerization, DP. The DP value is the molecular weight divided by the monomer weight, giving for PVAm

Low molecular weight: $DP = 1.3 \cdot 10^5/43 = 3.02 \cdot 10^3$

High molecular weight: $DP = 1 \cdot 10^6/43 = 2.3 \cdot 10^4$

A charged polymer, a polyelectrolyte, is more expanded in solution than Eq. (50) would suggest. This expansion arises because of electrostatic repulsion between charges of like sign along the polymer chain. An expansion factor is often defined as

$$\phi = \langle s^2 \rangle^{1/2} / \langle s_o^2 \rangle^{1/2} \qquad (51)$$

where $\langle s_o^2 \rangle^{1/2} = (\langle r_o^2 \rangle / 6)^{1/2}$, radius of gyration of the uncharged polymer.

The expansion factor can be estimated qualitatively on theoretical grounds (23, 26,27), but experimental data are needed for quantitative results. The expansion factors for PVAm at pH 3 were estimated from literature data on high charge density vinyl polymers, Table V:

TABLE V

EXPANSION FACTORS OF POLYELECTROLYTES

Polymer 100% charged	Expansion Factor, ϕ		Reference
	DP = $3.02 \cdot 10^3$	DP = $2.3 \cdot 10^4$	
NaPSS	4.2	6.1	73
NaPAA	3.6	5.0	24
NaPMOS	3.5	4.9	25
Average	3.8	5.3	

Applying the values of Table V to PVAm and using Eq. (50) and (51) gives the following sizes for PVAm in solution, Table VI:

TABLE VI

SIZES OF PVAM IN SOLUTION

Dimension	Size, nm	
	DP = $3.02 \cdot 10^3$	DP = $2.3 \cdot 10^4$
Contour length	800	5800
$\langle s^2 \rangle^{1/2}$ at pH 3	53	200
$\langle s^2 \rangle^{1/2}$ at PH 10[a]	14	38

[a]No electrostatic expansion is assumed. These values are lower bounds, since excluded volume and polymer-solvent effects will increase the chain dimensions. However, this will only change the calculated adsorption rates by, at the most, 10%, since the polymer radius appears as a small ratio, $r=a_p/a_l$, in the collision factor $(1+r)^3$.

APPENDIX II

POLYSTYRENE LATEX CHARACTERIZATION

The purchased polystyrene latex (Dow Diagnostics) was stabilized by emulsifier remaining from the polymerization step. To remove the emulsifier and inorganic electrolytes the latex was cleaned using ion exchange (50) and serum replacement (51). The former method is well established and has been described elsewhere (50,55). The serum replacement method, which is a more recent development, was used because of its relative speed and simplicity to clean up the last batches of polystyrene latex. The water employed in the cleaning and characterization procedures was triply distilled, the second distillation from alkaline potassium permanganate to remove organic impurities. A short description of the serum replacement method is given below.

A 350 mL Amicon Ultrafiltration cell, diameter 75 mm, was used with a Nuclepore polycarbonate filter, pore size 0.4 μm. The latex was kept at 3-4% concentration and the volume was 150-200 mL. The nitrogen pressure was 2.5 psi and the elution rate was 6 mL/minute under constant stirring. The latex was first rinsed with a fivefold excess of triply distilled water, which reduced the conductivity of the serum to nearly that of water. Then the latex was eluted with a fivefold turnover of $5 \cdot 10^{-4}$M HCl to replace Na^+ counter ions with H^+ ions. Finally the latex was washed with a fifteenfold excess of triply distilled water.

The charge density of the latex was determined using conductrometric titration (74). The sample, 70 mL at approximately 4% PSL concentration, was contained in a glass beaker placed on an air-driven magnetic stirrer in a constant temperature water bath. A glass cell with newly platinized electrodes and a nominal cell constant of 0.1 cm^{-1} was used together with a Digital Electromark Analyzer (Markson Science Inc.). Nitrogen was bubbled through the sample until a constant reading was obtained (approximately 1 hour). The nitrogen tube was then raised to just above the sample

surface to provide a blanket of N_2. 0.01M NaOH was then delivered in increments of 0.05 to 0.07 mL (toward the end 0.10 mL) from a burette graduated in hundredths of a mL. Each data point took one minute to complete and forty-five points were taken without interruptions to obtain a titration curve. The NaOH was prepared from boiled-out, triply distilled water and Dilut-it Analytical Concentrate (carbonate-free) from J.T. Baker Chemical Co. The dilution was done in a glove bag filled with nitrogen.

It is important to work at as high a latex and NaOH concentration as possible. Preliminary trials with 1% latex and 0.002M NaOH gave considerable scatter due to adsorption of CO_2 despite blanketing with N_2. An example of a titration curve is given in Fig. 26. The descending leg results from neutralization of H^+ ions associated with the sulfate groups on the latex surface. The ascending leg is due to excess NaOH. The average of four titrations gave a charge density of 0.53 ± 0.02 charges/$Å^2$ or 8.5 ± 0.3 $\mu C/cm^2$.

Two different sizes of polystyrene latex were purchased, here called PSL 1 and PSL 2 (see Table VII). The Coulter Counter gave a diameter difference of about 4%, whereas the values given by Dow differed by less than 1%. Photographs of the particles were taken with the Institute's transmission electron microscope, a model JEM-100CX made by JEOL LTD. The magnification was 18,620 times. The negatives were then measured on an optical device (Institute design by K. Hardacker) with a magnification of 42.5 times.

The number of particles measured were 25 for PSL 1 and 20 for PSL 2. The difference between the two particle sizes, 4.5%, agrees with the Coulter Counter findings. The latex called PSL 1 was only used for preliminary studies and the PSL 2, with the measured diameter of 1.070 μm, was used for the final experiments.

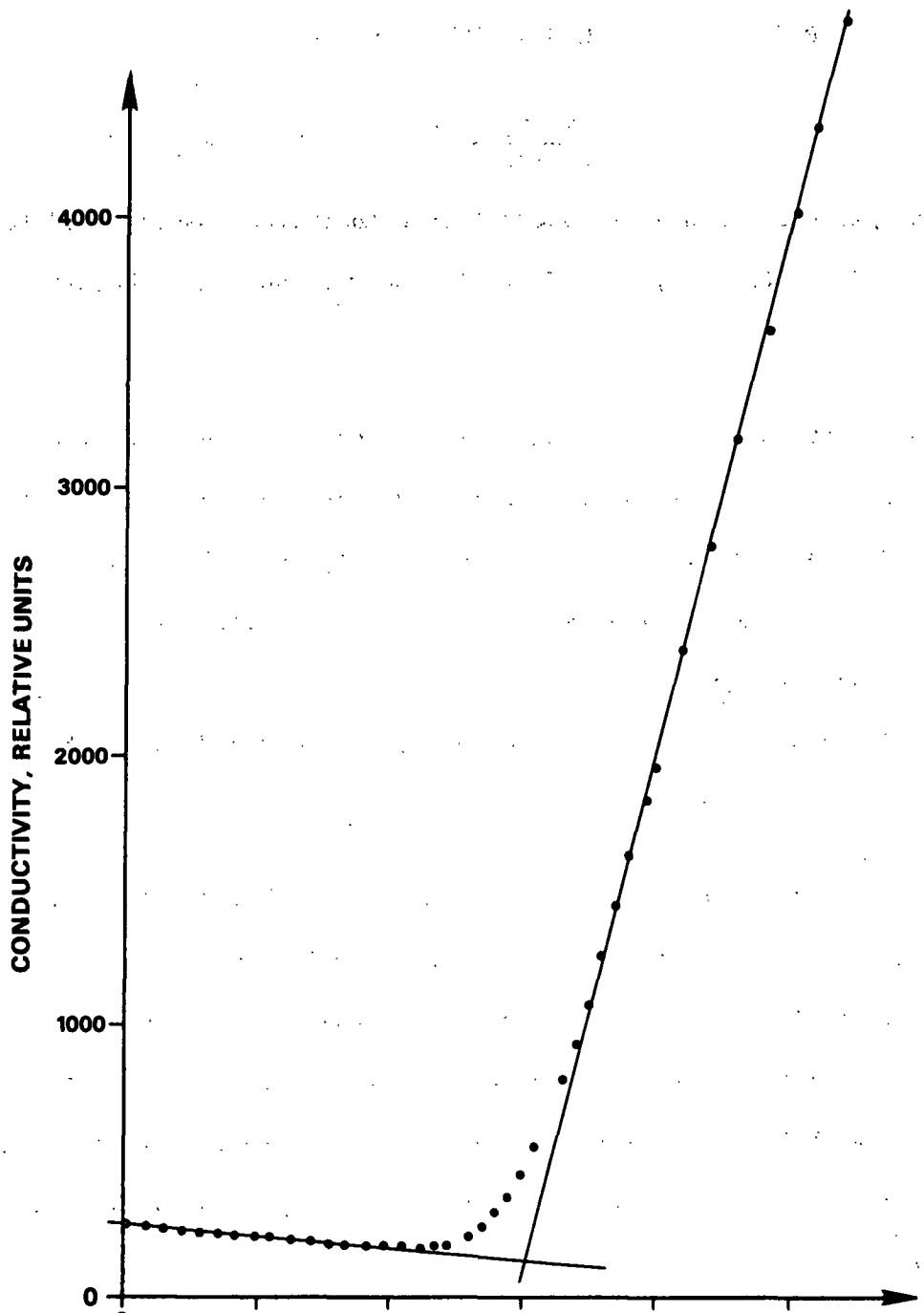

Figure 26. Titration of PSL. Conductivity vs. NaOH volume.

TABLE VII

PARTICLE SIZE DETERMINATION WITH ELECTRON MICROSCOPE

	Particle Diameter (Standard Deviation), μm	
	PSL 1	PSL 2
Dow's value	1.101 (0.0055)	1.091 (0.0082)
Measured	1.119 (0.020)	1.070 (0.021)

APPENDIX III

COULTER COUNTER. OPERATION AND EVALUATION OF DATA

Floc size distributions were determined using a Coulter Counter Model TA II (Coulter Electronics). The sensing part of the instrument is two electrodes immersed on opposite sides of a small aperture in a conductive fluid (in this case 2% NaCl in water). A particle passing through the aperture changes the resistance between the electrodes. A current pulse is produced, which has a magnitude proportional to the particle volume. The particles are counted and grouped in 16 channels. The lower threshold of each channel corresponds to twice the particle volume of the lower threshold of the preceding channel. For a 30 μm aperture used in this study, the lower limit of channel five may correspond to a volume of 0.5236 μm^3 or an equivalent spherical particle having a diameter of 1.00 μm. By means of calibration a particle size can be moved up or down one channel. The instrument has to be calibrated with a particle of known size. The latex used in the adsorption-flocculation study, diameter 1.070 μm, was also used for this purpose.

The electrolyte was filtered through a 0.22 μm Millipore filter. One filtration was usually enough, but the electrolyte had to be used within one day. The background count in channel 5 (singlets) was typically less than 0.2%. Coincidence, i.e., two or more particles simultaneously passing through the aperture, and coagulation in the electrolyte are potential problems. It was determined that the dilution of an unflocculated suspension to 0.05 mg/L or less gave a constant count, i.e., no coincidence and no coagulation. Floc breakup in the aperture is also a concern. However, studies (75,76) have shown that this might not be a serious problem. Even if a floc breaks apart in the aperture it may not create a problem, because it is the total volume of displaced electrolyte that is counted (76).

The particles can be counted in three different modes: constant electrolyte volume, constant number of particles or constant time. In this study 100,000 particles were counted to obtain a floc size distribution. The data are presented as differential or cumulative population and differential or cumulative volume percentage. The data can be plotted, whereby the population data are normalized to 100%. The instument is also equipped with an oscilloscope, a numerical read-out and a printer.

As mentioned above, the lower threshold of each channel corresponds to twice the particle volume of the lower threshold of the preceding channel. This means that a discrete particle size distribution is not directly obtained. However, the so-called step gain can be changed in three steps, increasing the resolution four times. Each step moves the channel thresholds down one quarter of a channel width. This feature is illustrated in Fig. 27.

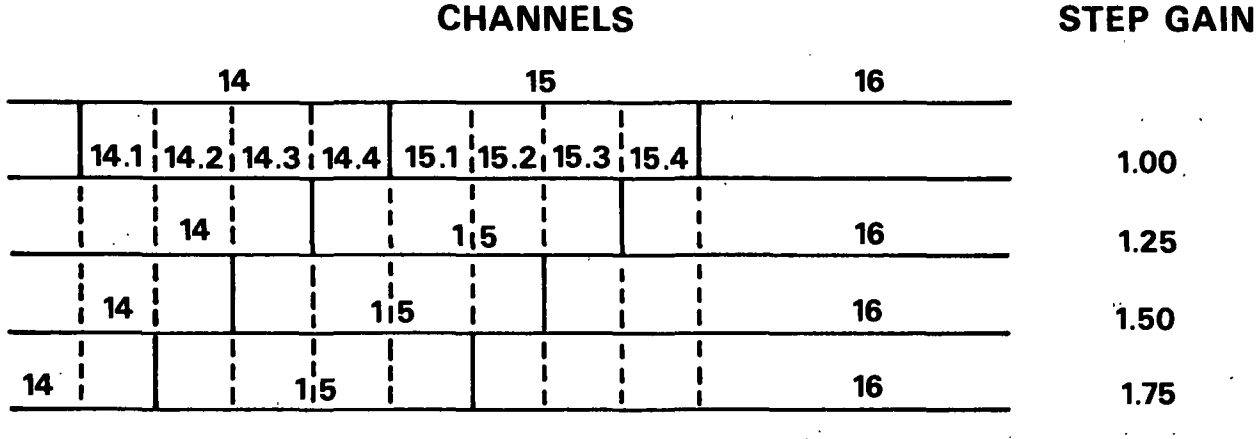

Figure 27. Schematic representation of the channels in the Coulter Counter.

The rectangles in Fig. 27 represent channels in the Coulter Counter. Each channel is divided into four quarters by dashed lines. Each row of channels

corresponds to one setting of the step gain. Note that channel 16 is open ended toward larger particles.

A fourfold increase in resolution of the cumulative distribution is directly obtained by counting the sample four times, using the four different step gain settings; the instrument adds the particles from right to left, from large particles to small. However, to obtain a fourfold increase in resolution of the differential distribution the cumulative values have to be subtracted, one after the other, in the following pattern. The differential value of channel 15.4 (see Fig. 27) is the difference between the cumulative values of channel 16 at a step gain of 1.25 and channel 16 at a step gain of 1.00. In the same way the differential value for 15.3 is the difference between the cumulative values of 16 at a step gain of 1.50 and 16 at a step gain of 1.25, etc.

The channel volumes can be translated to particle sizes, which are multiples, k, of a singlet particle. It is thus possible to obtain discrete distributions for particles up to a size of k = 8. At this point the channels become wide enough to contain more than one particle size.

A computer program was developed to convert the raw data from the Coulter Counter to floc size distributions. The program first reads the electrolyte background count and then the differential population data from the four step gain settings. Cumulative distributions are calculated for each step gain, and by successive subtractions according to Fig. 27 a differential distribution is obtained, which has a fourfold increase in resolution compared to a single count at one step gain setting. The program also substitutes floc sizes for the corresponding Coulter Coulter channel numbers and prints and plots the differential and cumulative floc size distributions. Finally, the total number concentration and the number concentration of

singlets through quartets, all divided by the initial total number concentration, are calculated and printed.

The total number concentration in the flocculated suspension is expressed as a fraction of the initial total number concentration in the unflocculated suspension and can be calculated as

$$N_{tot} = V_o/V_f \tag{52}$$

where

$V_o = 1n_{o1} + 2n_{o2} + 3n_{o3} + \ldots\ldots$; initial total floc volume

$V_f = 1n_{f1} + 2n_{f2} + 3n_{f3} + \ldots\ldots$; final total floc volume

n = number concentration of flocs

Equation (52) stems from the fact that a constant number of particles (100,000) are counted for both the initial and the final (flocculated) suspension, but the initial total floc volume is only a fraction of the final total floc volume, as expressed by Eq. (52).

An example of an original plot from the Coulter Counter is shown in Fig. 28 followed by computer drawn floc size distribution curves, Fig. 29 and 30. Table VIII is a listing of channel numbers and corresponding floc sizes. The computer program for calculation of floc size distributions is available at the Computer Center of The Institute of Paper Chemistry.

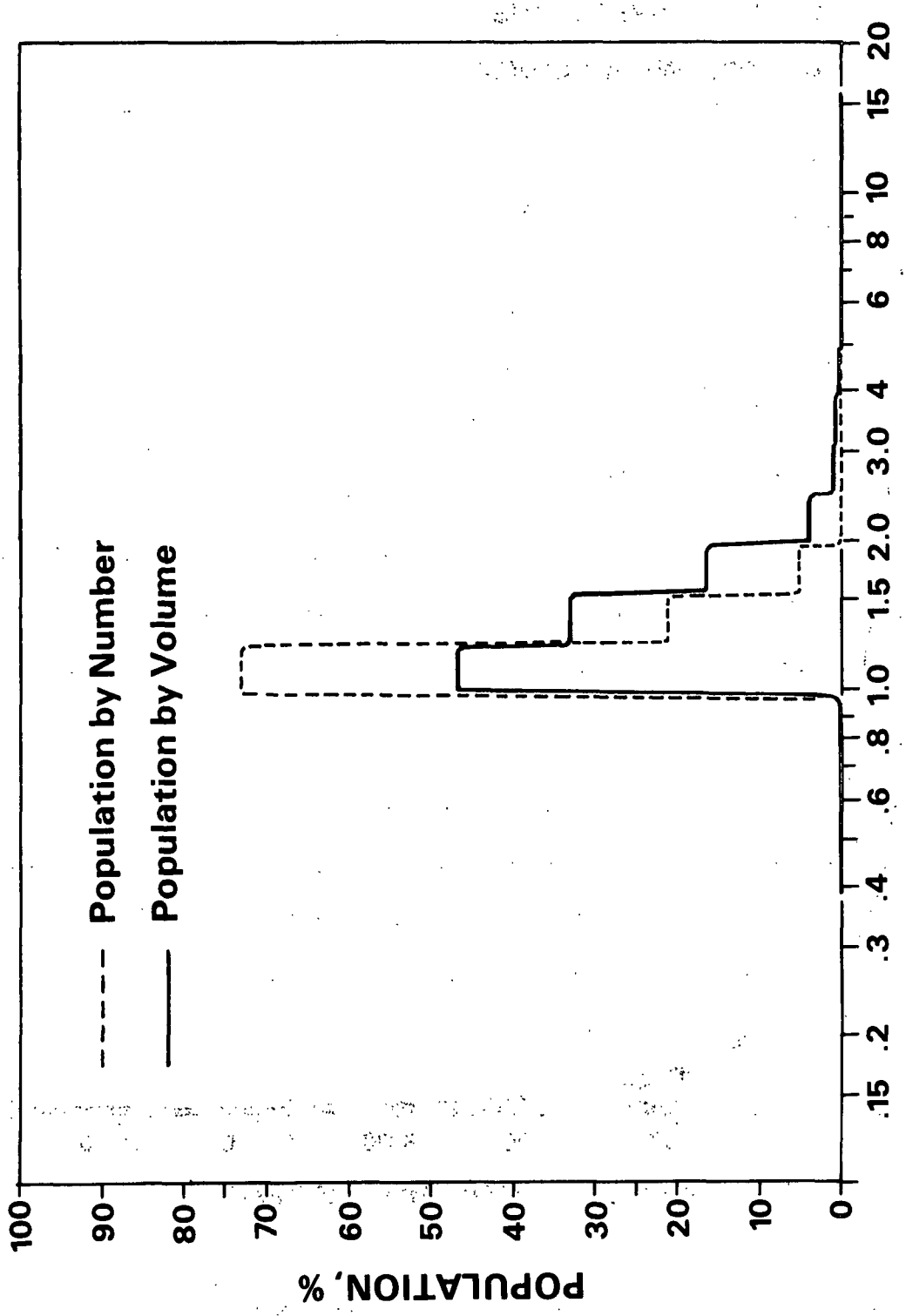

Figure 28. Raw Coulter Counter data. Step gain 1.0.

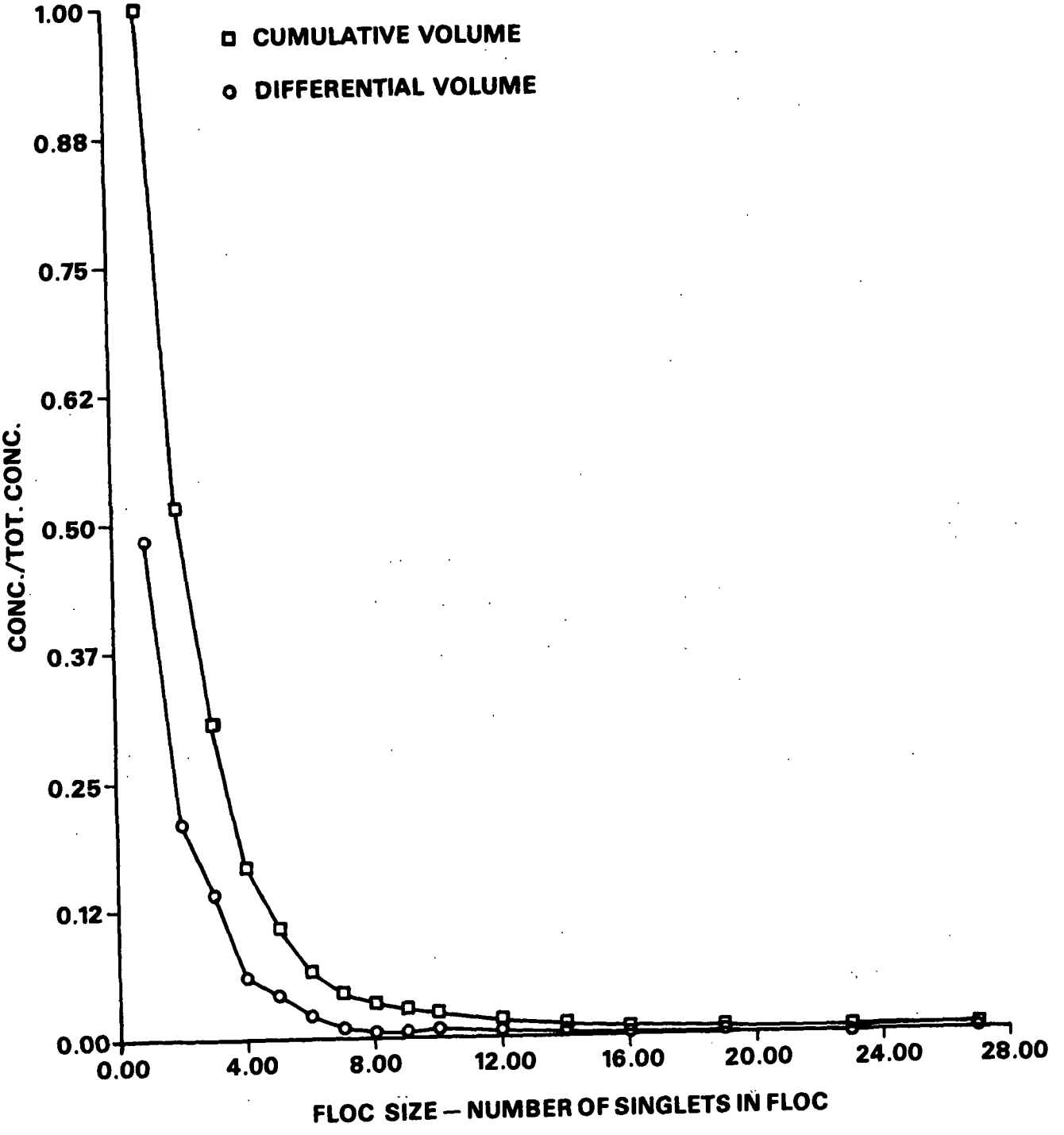

Figure 29. Computer drawn floc size distribution.

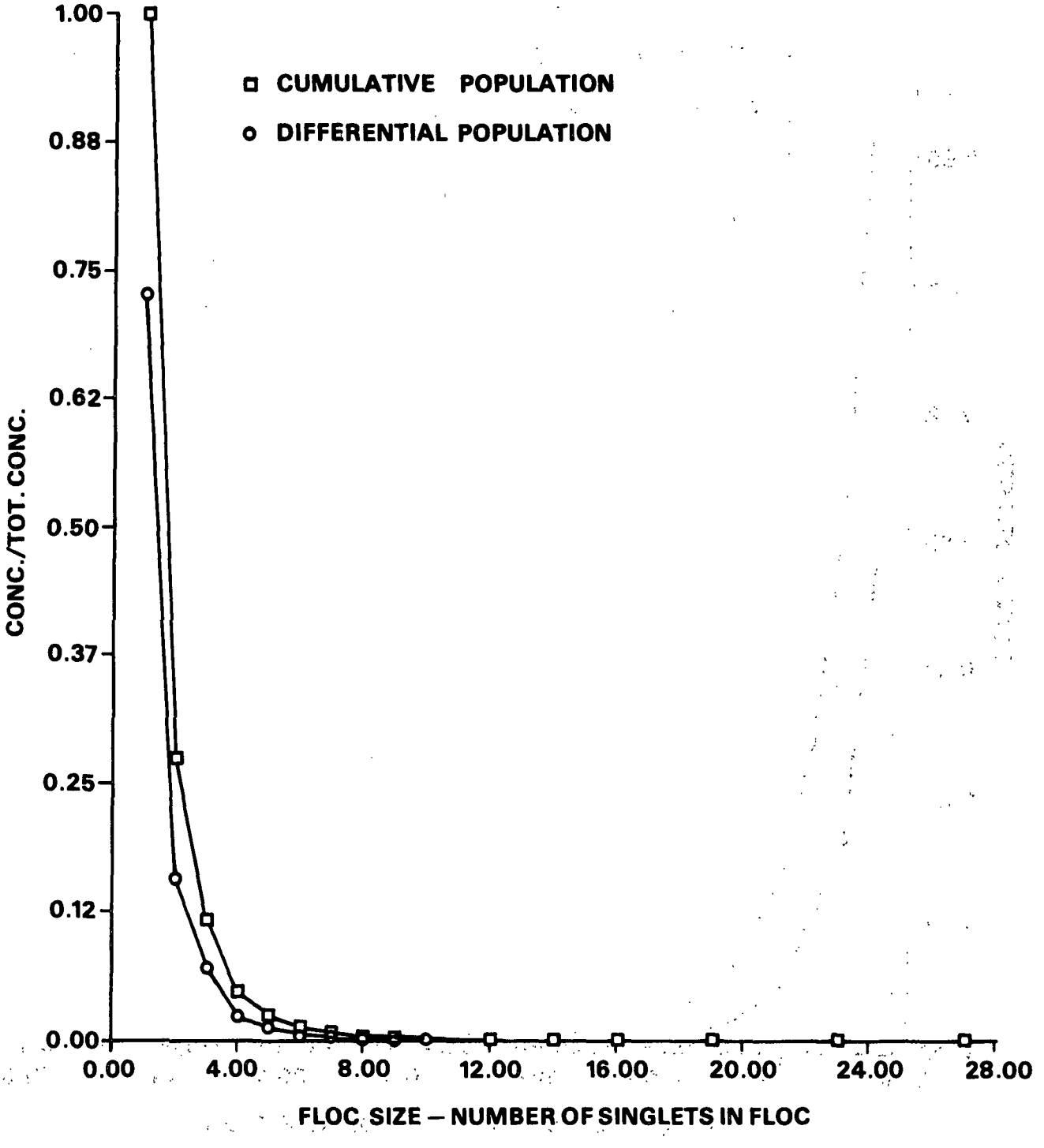

Figure 30. Computer drawn floc size distribution.

TABLE VIII

COULTER COUNTER CHANNELS AND CORRESPONDING FLOC SIZES

Channel number 5.1 denotes the first quarter of channel 5, 5.2 the second quarter etc. Floc size is given by the number of singlets, i, in a floc.

Channel No.	Floc Size, i	Channel No.	Floc Size, i
5.1-5.4	1	9.2	16- 18
6.1-6.3	2	9.3	19- 22
6.3-7.1	3	9.4	23- 26
7.2	4	10.1	27- 31
7.3	5	10.2-10.4	32- 52
7.4	6	11	53- 104
8.1	7	12	105- 209
8.2	8, 9	13	210- 418
8.3	10, 11	14	419- 836
8.4	12, 13	15	837-1671
9.1	14, 15	16	1672-

APPENDIX IV

POLYMER AND SURFACTANT ANALYSIS

POLYMER ANALYSIS

This procedure is a modification of the so-called colloid titration method (54). The reagents are an anionic polymer, the potassium salt of polyvinylsulfuric acid or PVSK, and a cationic dye, o-toluidine blue or OTB, (Nalco Chemical Co). The following procedure was used:

1. Add a 40 mL sample at pH 3 with a polymer concentration of less than 0.1 mg/L to a 60 mL polypropylene bottle
2. Add 5 mL of PVSK, concentration 2 mg/L
3. Add 5 mL of OTB, concentration 11 mg/L
4. Measure absorbance at 625 nm using a 10 cm cuvette
5. Subtract the absorbance of a blank sample (H_2O + reagents) and divide by 4.55 L/mg (the slope in Fig. 31) to get the polymer concentration in mg/L

The PVSK solution is stable but the OTB slowly adsorbs onto the walls of the storage container, resulting in a different blank absorbance value each time the procedure is used. The slope is, however, constant as long as there is excess dye in the system.

The success of this method is dependent on extreme cleanliness. The sample bottles were soaked in 2M NaOH at 90°C for 12 hours, then rinsed with acetone and finally with distilled water.

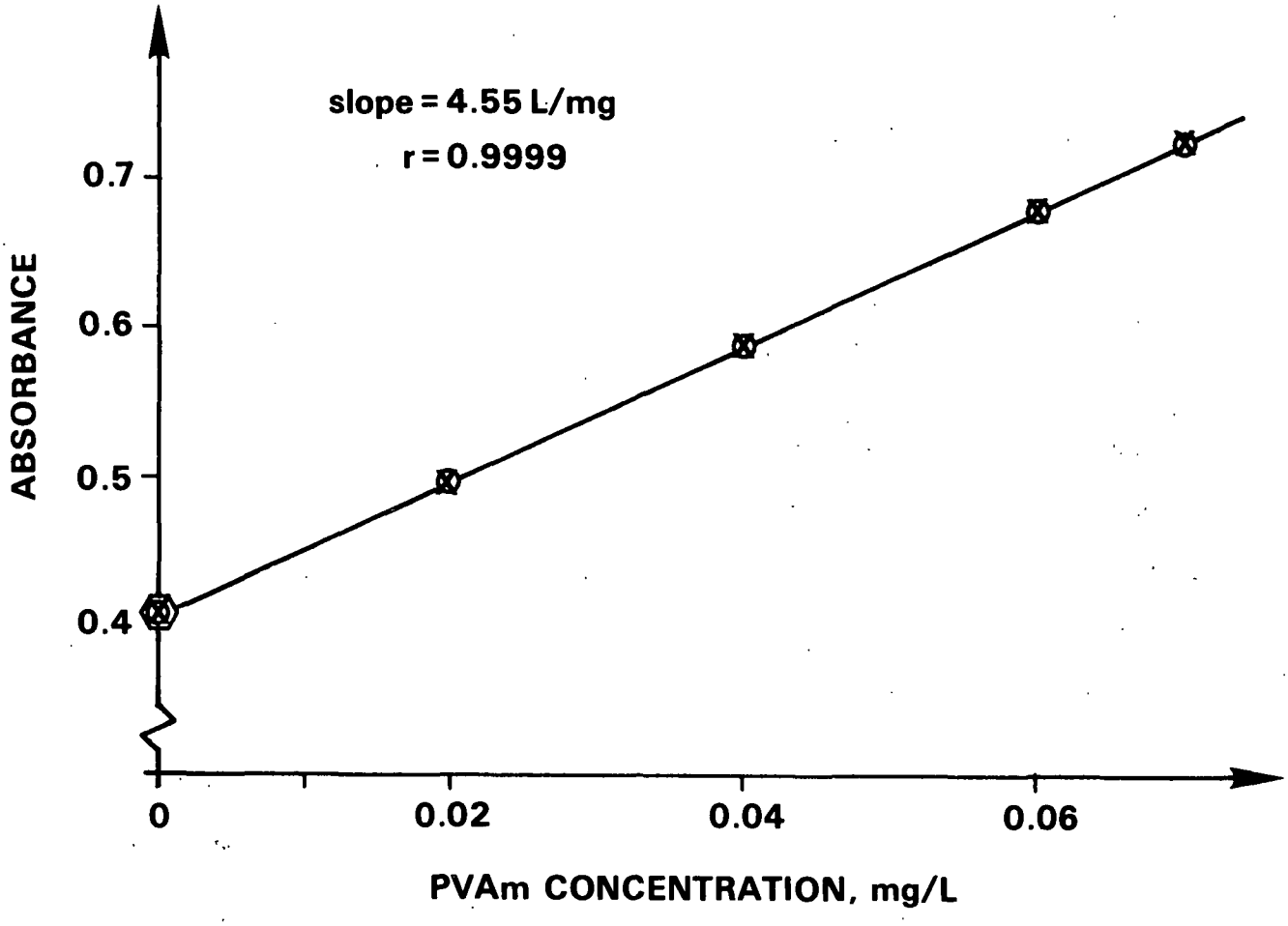

Figure 31. Absorbance at 625 nm vs. PVAm concentration.

SURFACTANT ANALYSIS

A very sensitive method was developed to determine the concentration of the surfactant dodecyltrimethylammonium bromide or DTABr (Sigma). The procedure given below is a modification of a method originally proposed by Few and Ottewill (77).

1. Mix 25 mL sample + 5 mL 5% Na_2CO_3 + 1 mL dye + 5 mL $CHCl_3$.
2. Shake for 3 minutes.
3. Centrifuge for 5 minutes.
4. Measure absorbance at 486 nm.

Dye: 40 mg Orange II + 0.2 g NaCl + 50 mL H_2O

Figure 32 shows a calibration curve for surfactant analysis.

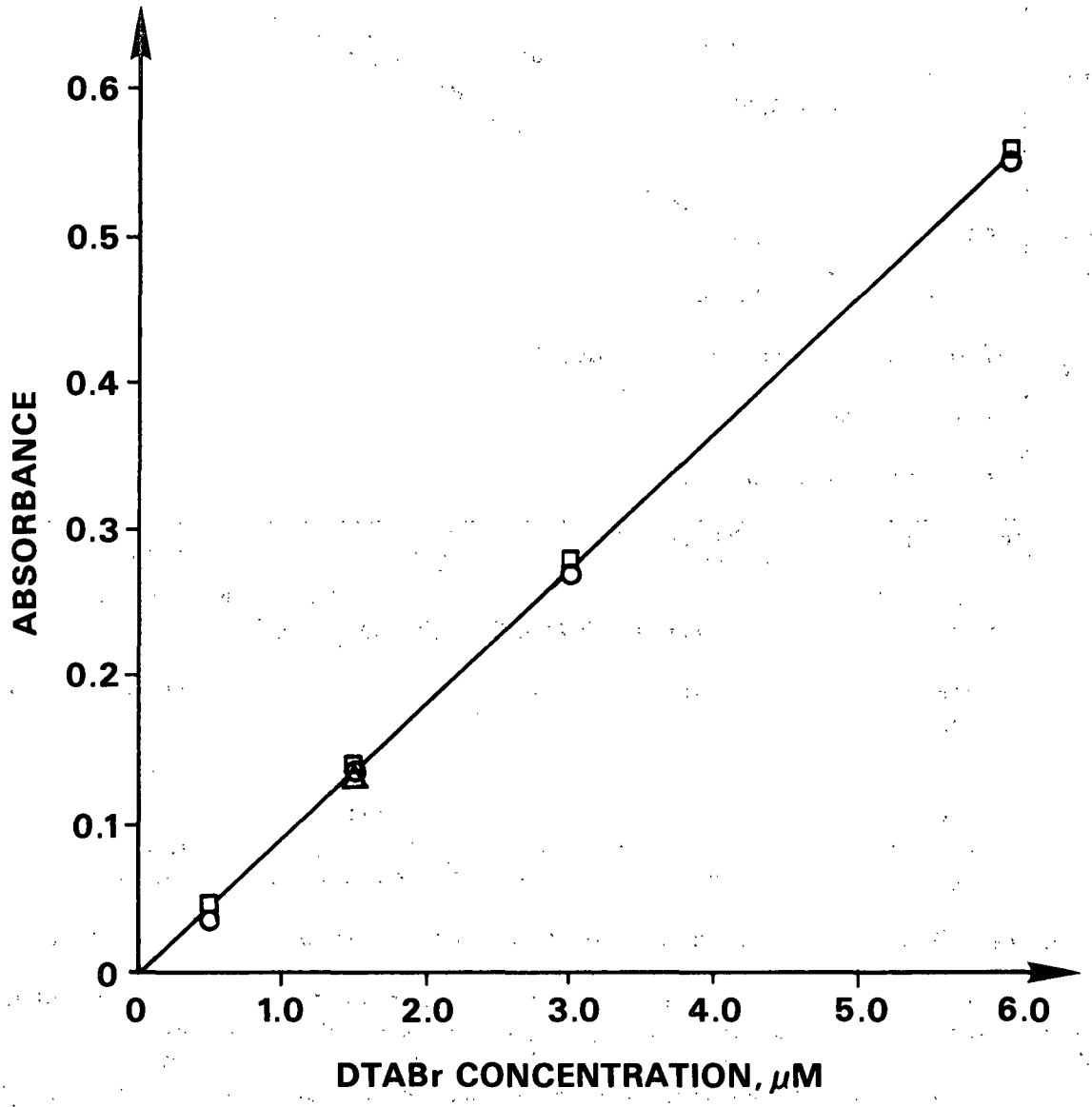

Figure 32. Absorbance at 486 nm vs. DTABr concentration.

INFLUENCE OF SURFACTANT ON POLYMER ANALYSIS

The cationic surfactant competes with the cationic polymer in the concentration analysis method. The contribution of the surfactant to a measured absorbance value is a function of both the surfactant and the polymer concentrations. Within a surfactant concentration range of 10 $\mu\underline{M} < D < 100\ \mu\underline{M}$ and a polymer concentration range of 0.02 mg/L < P < 0.10 mg/L the following empirical equation is valid:

$$A = B + k_p P + k_D D + I_D - k_{Dp} P$$

$$A = B + 4.55P + 3.45 \cdot 10^{-4} D + 0.0243 - 0.30P \qquad (53)$$

where

A = total absorbance

B = absorbance of blank sample

k_p = polymer absorbance coefficient, L/mg

P = polymer concentration mg/L

k_D = surfactant absorbance coefficient, $\mu\underline{M}^{-1}$

D = surfactant concentration, $\mu\underline{M}$

I_D = apparent intercept (or "increase in blank reading") due to presence of surfactant

k_{Dp} = interaction coefficient, reducing the surfactant contribution due to presence of polymer, L/mg.

The influence of the surfactant on the polymer analysis is shown qualitatively in Fig. 33 and quantitatively in Table IX. The largest effect is seen at low polymer concentrations, but the influence is almost negligible at high polymer concentrations. This method was used in the adsorption rate measurements at pH 10, where the high polymer concentrations required sufficiently large dilutions that the surfactant concentration was reduced to below 100 $\mu\underline{M}$. The contribution of the surfactant to the measured absorbance values was 5-7%.

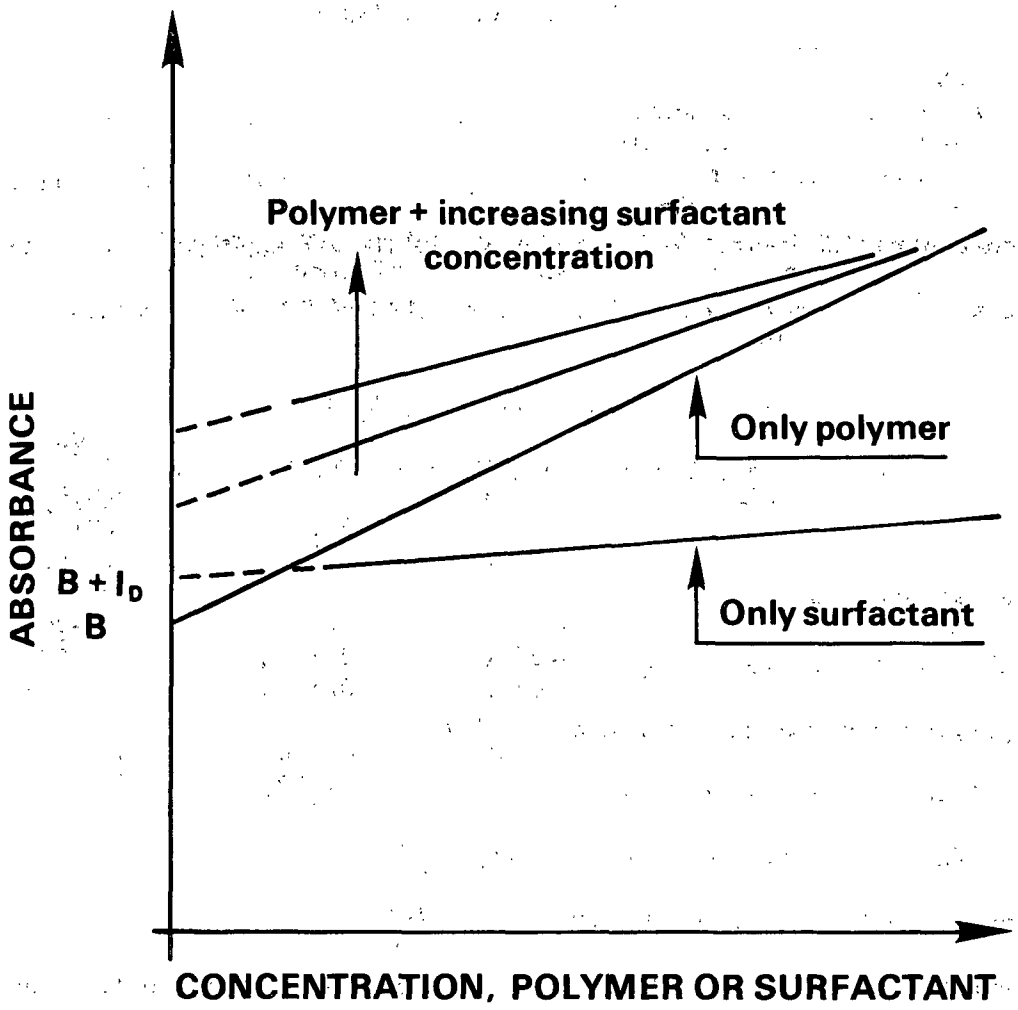

Figure 33. Qualitative depiction of the influence of surfactant on the polymer analysis.

This method of correcting the polymer concentration for the presence of surfactant could not be used for the experiments at pH 3. The lower polymer doses employed at pH 3 required less dilution of the samples before polymer analysis, resulting in too high surfactant concentrations. The surfactant had to be removed by ultrafiltration before the polymer concentration could be measured.

TABLE IX

EFFECT OF SURFACTANT ON POLYMER ANALYSIS

LEGEND:
D = surfactant concentration
P = polymer concentration
A = total absorbance
B = absorbance of blank sample
ΔA_D = absorbance due to surfactant - no polymer present
ΔA_p = absorbance due to polymer - no surfactant present
ΔA_{Dp} = increase in absorbance of a polymer sample due to presence of surfactant

D, μM	ΔA_D	P, mg/L	ΔA_p	ΔA_{Dp}
10	0.0256	0.0204	0.0928	0.0196
		0.0511	0.2326	0.0138
		0.0801	0.3644	0.0059
50	0.0455	0.0201	0.0916	0.0400
		0.0511	0.2326	0.0258
		0.0821	0.3735	0.0173
100	0.0571	0.0506	0.2302	0.0404
		0.1000	0.4550	0.0010

The following relationships were found

$\Delta A_D = k_D D + I_D$; coefficient of correlation = 0.977

$A = B + k_p P + k_D D + I_D - k_{Dp} P$

$A = B + 4.55P + 3.45 \cdot 10^{-4} D + 0.0243 - 0.300P$

$P = [(A-B) - 3.45 \cdot 10^{-4} D - 0.0243]/4.25$

SOURCES OF SCATTER IN THE POLYMER CONCENTRATION ANALYSIS

The polymer analysis is extremely sensitive with a lower detection limit of less than 0.005 mg/L. However, there are several sources of scatter that have to be carefully controlled.

1. Sample bottles. The bottles have to be carefully cleaned to remove any traces of polymer and reagents (see procedure above). The

adsorption of polymer onto clean bottle surfaces caused a loss of 2.0% for a concentration of 0.06 mg/L and an adsorption time of 10 hours. This loss dropped to 0.8 and 0.6% for polymer concentrations of 0.5 and 2.0 mg/L, respectively.

2. Latex separation. The latex was removed from the sample by filtration through a 0.4 μm polycarbonate filter (Nuclepore) before the polymer concentration was determined. The adsorption losses were negligible as long as the filter was pretreated with polymer.
3. Ultrafiltration. The polymer loss during ultrafiltration, using a standardized procedure, was determined to be 5.2% with a standard deviation of 2.6%. Several different types of ultrafiltration membranes were tested, but the YM-10 membrane (Amicon) used in this study gave by far the lowest polymer loss. This polymer loss was mainly due to adsorption, but for extremely high concentrations of the lower molecular weight PVAm some polymer could also be detected in the filtrate. This was unexpected, since the nominal molecular weight cut-off was 10^4 for the membrane and the polymer had a molecular weight of $1.3 \cdot 10^5$.
4. Sample dilution and absorbance measurement. The samples were diluted in two steps and 5 mL of each reagent was then added. A maximum pipetting error of 1 drop or 0.05 mL in each step would typically result in an error of 0.026 absorbance units. This should be compared to actually experienced deviations. A stock solution of known concentration was diluted to give 26 samples with a concentration of 0.0766 mg/L. The average absorbance was 0.348 with a standard deviation of 0.006 (1.7%). The difference between the highest and the lowest value was 0.028 (8.0%).

The actual polymer analysis was carried out with five blank samples and triplicate dilutions of the polymer containing samples. For high polymer concentrations (at pH 10) this procedure was performed twice. The measured polymer concentration was corrected for ultrafiltration losses (at pH 3) or surfactant effects (at pH 10). Adsorption losses in the polypropylene bottles were neglected, since dilute surfactant-free samples were only stored for a few hours and corresponding adsorption losses could not be distinguished from errors caused by the dilution technique and the absorbance measurements. The combined procedure of sample dilution, reagent addition and absorbance measurement typically gave a standard deviation of 1.7% and a maximum error of 8%.

APPENDIX V

ADSORPTION, FLOCCULATION AND COAGULATION DATA

Tables X through XXII contain numerical data for both the equilibrium and the nonequilibrium experiments. The coagulation results are listed in connection with the corresponding flocculation data. The following nomenclature is used:

PSL Polystyrene latex

S short tube, 0.418 m

L long tube, 0.875 m

XL extra long tube, 1.963 m

P final polymer concentration in per cent of initial concentration

N final total number concentration of flocs in per cent of initial concentration

TABLE X

EQUILIBRIUM ADSORPTION AT pH 3.0

PSL concentration: 1.50 g/L
Polymer concentration, mg/L

Initial	Final	Adsorbed	Zeta Potential, mV
	Molecular Weight: $1.3 \cdot 10^5$		
0.25	0	0.25	-49.1
0.50	0	0.50	-21.9
1.00	0.10	0.90	+36.8
2.00	0.97	1.03	+49.1
2.00	0.98	1.02	+50.8
4.00	2.65	1.35	+52.3
8.00	6.50	1.50	+54.0
	Molecular Weight: $1 \cdot 10^6$		
0.25	0	0.25	-49.1
0.50	0	0.50	-23.1
1.00	0.07	0.93	+36.8
2.00	0.95	1.05	+45.9
2.00	0.94	1.06	+52.3
4.00	2.78	1.22	+52.8
8.00	6.67	1.33	+57.9

All concentrations are based on final volumes, i.e., after mixing of PSL and polymer. Complete floc size distributions are available for all samples, but the value of N has not been calculated in the case of nearly identical floc size distributions of duplicate samples. The initial distribution at pH 3 was typically 91% singlets, 6% doublets and 3% triplets and larger flocs. At pH 10 a typical distribution had 96% singlets, 3% doublets and 1% triplets and larger flocs.

The shear rates are based on the energy dissipation calculated from the total pressure drop. Combining Eq. (3) and (25) gives

$$G = (fU^3/(2\nu D)^{1/2} \qquad (54)$$

The Blasius friction factor in Eq. (54) was determined from measurements of pressure drop *vs.* tube length for a constant flow rate. The friction factor was 0.06 for U = 0.8 m/s and 0.04 for U = 2.6 m/s.

TABLE XI

ADSORPTION AND FLOCCULATION RESULTS

pH: 3.0
Molecular weight: $1 \cdot 10^6$
PSL concentration: 1.33 g/L

Sample No.	U, m/s	G, s^{-1}	Time, s	Time, τ	PVAm Concentration, mg/L Initial	Final	Adsorbed	P, %	N, %
16A/S	0.8	1950	0.50	1.34	0.50	0.41	0.09	82.0	90.7
16B/S					0.50	0.41	0.09	82.0	
19A/S					1.00	0.87	0.13	87.0	78.7
19B/S					1.00	0.88	0.12	88.0	
20/S					2.00	—	—	--	66.9
23/S					4.00	3.71	0.29	92.8	74.3
24/S					8.00	7.75	0.25	96.9	84.2
28/S					$AlCl_3$	0.01M			55.9
29/S					$AlCl_3$	0.01M			55.2

TABLE XII

ADSORPTION AND FLOCCULATION RESULTS

pH: 3.0
Molecular weight: $1 \cdot 10^6$
PSL concentration: 1.33 g/L

Sample No.	U, m/s	G, s^{-1}	Time, s	Time, τ	PVAm Concentration, mg/L Initial	Final	Adsorbed	P, %	N, %
17A/L	0.7	1600	1.20	2.63	0.50	0.40	0.10	80.0	81.7
17B/L					0.50	0.41	0.09	82.0	
17C/L					0.50	0.39	0.11	78.0	
18/L					1.00	0.81	0.19	81.0	64.2
21/L					2.00	1.73	0.27	86.5	62.8
22/L					4.00	3.64	0.36	91.0	77.9
25/L					8.00	7.63	0.37	95.4	84.9
26/L					$AlCl_3$	0.01M			48.2

TABLE XIII

ADSORPTION AND FLOCCULATION RESULTS

pH: 3.0
Molecular weight: $1 \cdot 10^6$
PSL concentration: 4.54 g/L

Sample No.	U, m/s	G, s^{-1}	Time, s	Time, τ	PVAm Concentration, mg/L Initial	Final	Adsorbed	P, %	N, %
30A/S	0.8	1815	0.50	4.57	0.50	0.31	0.19	62.0	95.0
30B/S					0.50	0.33	0.17	66.0	94.0
31A/S					2.00	1.35	0.65	67.5	52.7
31B/S					2.00	1.43	0.57	71.5	
32A/S					8.00	6.64	1.36	83.0	67.8
32B/S					8.00	6.68	1.32	83.5	
33/S					$AlCl_3$	0.01M			26.4

TABLE XIV

ADSORPTION AND FLOCCULATION RESULTS

pH: 3.0
Molecular weight: $1 \cdot 10^6$
PSL concentration: 1.55 g/L

Sample No.	U, m/s	G, s^{-1}	Time, s	Time, τ	PVAm Concentration, mg/L Initial	Final	Adsorbed	P, %	N, %
34A/S	2.7	9000	0.16	2.28	0.50	0.38	0.12	76.0	89.3
34B/S					0.50	0.39	0.11	78.0	
35/S					1.00	0.81	0.19	81.0	75.1
36/S					2.00	1.69	0.31	84.5	56.1
37/S					4.00	3.60	0.40	90.0	56.2
38/S					8.00	7.33	0.67	91.6	69.5
39A/S					$AlCl_3$	0.01M			57.8
39B/S					$AlCl_3$	0.01M			57.8

TABLE XV

ADSORPTION AND FLOCCULATION RESULTS

pH: 3.0
Molecular weight: $1.3 \cdot 10^5$
PSL concentration: 1.08 g/L

Sample No.	U, m/s	G, s^{-1}	Time, s	Time, τ	PVAm Concentration, mg/L Initial	Final	Adsorbed	P, %	N, %
40A/S	0.8	1850	0.50	1.10	0.50	0.40	0.10	80.0	
40B/S					0.50	0.41	0.09	82.0	93.9
40C/S					0.50	0.40	0.10	80.0	
42/S					1.00	0.85	0.15	85.0	82.9
44/S					2.00	1.83	0.17	91.5	84.5
46/S					4.00	3.66	0.34	91.5	91.5
48/S[a]					8.00	6.93	1.07	86.6	94.1
50/S[a]					16.00	14.22	1.78	88.8	94.0
52/S						AlCl 0.01 M			64.2

[a]Uncertain adsorption values because of ultrafiltration losses.

TABLE XVI

ADSORPTION AND FLOCCULATION RESULTS

pH: 3.0
Molecular weight: $1.3 \cdot 10^5$
PSL concentration: 1.08 g/L

Sample No.	U, m/s	G, s^{-1}	Time s	Time, τ	PVAm Concentration, mg/L Initial	Final	Adsorbed	P, %	N, %
41A/S	2.6	8500	0.16	1.58	0.50	0.43	0.07	86.0	
41B/S					0.50	0.44	0.06	88.0	94.9
43/S					1.00	0.90	0.10	90.0	87.6
45/S					2.00	1.85	0.15	92.5	72.2
47/S					4.00	3.65	0.35	91.3	79.6
49/S[a]					8.00	7.39	0.61	92.4	88.0
51/S[a]					16.00	--	--		90.5
53/S						$AlCl_3$	0.01M		67.8
54/S						$AlCl_3$	0.01M		69.4

[a]Uncertain adsorption values because of ultrafiltration losses.

TABLE XVII

EQUILIBRIUM ADSORPTION AT pH 10.0

PSL concentration: 1.50 g/L

Polymer Concentration, mg/L Initial	Final	Adsorbed	Zeta Potential, mV
	Molecular Weight: $1.3 \cdot 10^5$		
0			-71.2
1.5	0	1.5	-60.2
4.5	0.1	4.4	-15.7
7.5	1.7	5.8	+16.2
15.0	8.3	6.7	+32.5
30.5	23.8	6.7	+30.9
	Molecular Weight: $1 \cdot 10^6$		
1.5	0	1.5	-53.3
4.5	0	4.5	- 9.5
7.5	1.0	6.5	+24.2
15.0	7.7	7.3	+28.2
30.5	23.5	7.0	+30.5

TABLE XVIII

ADSORPTION AND FLOCCULATION RESULTS

pH: 10.0
Molecular weight: $1 \cdot 10^6$
PSL concentration: 1.15 g/L

Sample No.	U, m/s	G, s^{-1}	Time, s	Time, τ	PVAm Concentration, mg/L Initial	Final	Adsorbed	P, %	N, %
55/S	0.8	1830	0.50	1.27	3.3	2.8	0.5	84.8	98.1
58/S					6.5	—	--	--	96.5
56/S					16.2	14.7	1.5	90.7	92.4
57/S					32.8	30.3	2.5	92.4	93.6
59/S					73.5	70.9	2.6	96.5	94.8
58/S	0.8	1830	0.50	1.27	6.5	—	--	--	96.5
67/L	0.7	1430	1.28	2.45	6.1	5.2	0.9	85.2	93.0
68/L	2.6	8700	0.33	3.88	6.1	5.5	0.6	90.2	95.4
66/XL	0.8	1880	2.40	6.02	6.1	5.0	1.1	82.0	83.5
63/S	0.8	1890	0.50	1.28	15.3	14.7	0.6	96.1	94.2
60/L	0.7	1570	1.21	2.52	15.7	14.4	1.3	91.7	93.5
61/XL	0.6	1070	3.49	4.97	15.7	13.8	1.9	87.9	89.5
62/XL	0.9	2100	2.22	6.24	15.7	14.1	1.6	89.8	87.7
57/S	0.8	1830	0.50	1.27	32.8	30.3	2.5	92.4	93.6
64/L	0.7	1570	1.21	2.52	31.3	30.6	0.7	97.8	94.6
65/XL	0.8	1940	2.35	6.07	31.3	30.1	1.2	96.2	92.1

TABLE XIX

ADSORPTION AND FLOCCULATION RESULTS

pH: 10.0
Molecular weight: $1 \cdot 10^6$
PSL concentration: 1.15 g/L

Sample No.	U, m/s	G, s^{-1}	Time, s	Time, τ	PVAm Concentration, mg/L Initial	Final	Adsorbed	P, %	N, %
72A/S	0.8	1840	0.52	1.26	3.00	2.53	0.47	84.3	96.8
72B/S						2.48	0.52	82.7	
71A/S	2.5	7950	0.17	1.79	3.00	2.57	0.43	85.7	
71B/S						2.56	0.44	85.3	96.9
71C/S						2.51	0.49	83.7	
69A/XL	0.9	2110	2.22	6.19	3.00	1.97	1.03	65.7	96.7
69B/XL						2.01	0.99	67.0	
70A/XL	2.5	8220	0.78	8.45	3.00	2.31	0.69	77.0	96.2
70B/XL						2.17	0.83	72.3	
73/S	0.8	1740	0.54	1.24	$AlCl_3$ 0.01M at pH 3.0				58.5
74/S	2.4	7780	0.17	1.77	$AlCl_3$ 0.01M at pH 3.0				62.9

TABLE XX

ADSORPTION AND FLOCCULATION RESULTS

pH: 10.0
Molecular weight: $1.3 \cdot 10^5$
PSL concentration: 1.15 g/L

Sample No.	U, m/s	G, s^{-1}	Time, s	Time, τ	PVAm Concentration, mg/L Initial	Final	Adsorbed	P, %	N, %
81A/S	0.8	1900	0.51	1.27	2.78	2.59	0.19	93.2	94.9
81B/S						2.51	0.27	90.3	
80A/S	2.5	7920	0.17	1.76	2.78	2.40	0.38	86.3	94.4
80B/S						2.38	0.40	85.6	
78A/XL	0.8	1890	2.39	5.90	2.78	2.32	0.46	83.5	90.9
78B/XL						2.50	0.28	89.9	
79A/XL	2.5	8070	0.79	8.33	2.78	2.26	0.52	81.3	93.3
79B/XL						2.41	0.37	86.7	
82/S[a]	0.8	1890	0.51	1.29	$AlCl_3$ 0.01M at pH 3.0				68.4
83/S[a]	2.5	8050	0.17	1.82	$AlCl_3$ 0.01M at pH 3.0				69.2
83/XL[a]	0.8	1890	2.38	6.07	$AlCl_3$ 0.01M at pH 3.0				36.2
85/XL[a]	2.4	7780	0.81	8.45	$AlCl_3$ 0.01M at pH 3.0				47.5

[a]Not completely destabilized, pH not properly adjusted.

TABLE XXI

ADSORPTION AND FLOCCULATION RESULTS

pH: 10.0
Molecular weight: $1 \cdot 10^6$, sample 75; $1.3 \cdot 10^5$, sample 76 and 86
PSL concentration: 3.35 g/L

Sample No.	U, m/s	G, s^{-1}	Time, s	Time, τ	PVAm Concentration, mg/L Initial	Final	Adsorbed	P, %	N, %
75A/S	0.8	1870	0.51	3.70	9.22	7.27	1.95	78.9	94.9
75B/S						7.53	1.69	81.7	
76A/S	0.8	1840	0.52	3.74	8.72	8.36	0.36	95.9	88.2
76B/S						8.03	0.69	92.1	
86A/S					9.00	8.28	0.72	92.0	
87B/S						8.33	0.67	92.6	
77/S	0.8	1820	0.52	3.67	$AlCl_3$	0.01M at pH 3.0			34.4

TABLE XXII

FLOCCULATION WITH POLYMER PRETREATED LATEX

PSL concentration: 1.05 g/L
Tube: S
Time: 0.5 s
G: 1800 s^{-1}
Molecular weight: H = $1 \cdot 10^6$, L = $1.3 \cdot 10^5$
U = untreated (polymer-free) latex

The polymer treatment caused some preaggregation as shown by the initial singlet concentration.

Sample No.	pH	MW	Singlets, initial %	N %	τ_α Observed	τ_α Predicted	$\Delta\alpha$ %
U	10		97				
87	10	H	83	67	0.62	0.31	100
91	10	H	84	58	0.82	0.32	156
88	10	L	75	74	0.46	0.30	53
92	10	L	75	72	0.48	0.30	60
U	3		89				
89	3	H	89	72	0.50	0.32	56
90	3	L	94	72	0.52	0.35	49

APPENDIX VI

COMPUTER PROGRAM FOR COAGULATION CALCULATIONS

The computer program gives a numerical solution of Eq. (17). The results are tabulated and plotted as floc concentration vs. time and as floc size distribution at a specified point in time. The dimensionless orthokinetic rate Eq. (17) was derived from Eq. (2):

$$dn_k/dt = 0.5 \sum_{\substack{i=1 \\ j=k-i}}^{i=k-1} \alpha(4G/3)(a_i+a_j)^3 n_i n_j - \sum_{i=1}^{\infty} \alpha(4G/3)(a_i+a_k)^3 n_i n_k \tag{2a}$$

$$dn_k/dt = 0.5 \sum_{\substack{i=1 \\ j=k-i}}^{i=k-1} \alpha(4G/3)(a_1 i^m + a_1 j^m)^3 n_i n_j 8n_o^2/(8n_o^2) - \sum_{i=1}^{\infty} \alpha(4G/3)(a_1 i^m + a_1 k^m)^3 n_i n_k 8n_o^2/(8n_o^2) \tag{2b}$$

$$dN_k/dt = (16 n_o G a_1^3/3)\left(\sum_{\substack{i=1 \\ j=k-i}}^{i=k-1} \alpha(1/8)(i^m+j^m)^3 N_i N_j - 2 \sum_{i=1}^{\infty} \alpha(1/8)(i^m+k^m)^3 N_i N_k \right) \tag{2c}$$

$$dN_k/d\tau = \sum_{\substack{i=1 \\ j=k-i}}^{i=k-1} \sigma_{ij} N_i N_j - 2 \sum_{i=1}^{\infty} \sigma_{ik} N_i N_k \tag{17b}$$

The program starts by reading the initial floc size distribution and then proceeds to calculate floc concentration as a function of time by integrating Eq. (17) using Euler's method. Euler integration gives sufficient accuracy within the experimental range. The time increment, $\Delta\tau$, is chosen small enough that a doubling of $\Delta\tau$ does not affect the result. Collision efficiencies are calculated according to Eq. (24). The upper summation limit, i.e., the largest floc size considered, was

kept as low as possible to minimize computer time but high enough to prevent loss of mass exceeding 1%. The computer program is available at the Computer Center of The Institute of Paper Chemistry.

APPENDIX VII

COMPUTER PROGRAM FOR ADSORPTION AND FLOCCULATION CALCULATIONS

This computer program is an extension of the coagulation program in Appendix VI. The orthokinetic flocculation rate Eq. (30), is identical to the coagulation rate Eq. (17), except for the surface coverage factor. The orthokinetic adsorption rate (29), is derived as follows

$$dp/dt = -\sum_{i=1}^{\infty} \alpha(1-\theta_i)(4G/3)(a_i+a_p)^3 n_i p \tag{55}$$

$$dp/dt = -\sum_{i=1}^{\infty} \alpha(1-\theta_i)(4G/3)(a_1 i^m + a_1 a_p/a_1)^3 n_i p 8 n_o p_o/(8 n_o p_o) \tag{55b}$$

$$dp/dt = -p_o(16 n_o G a_1^3/3) 2 \sum_{i=1}^{\infty} \alpha(1-\theta_1)(1/8)(i^m+r)^3 N_i P \tag{55c}$$

$$dP/d\tau = -2 \sum_{i=1}^{\infty} \alpha(1-\theta_i)\sigma_{ip} N_i P \tag{29b}$$

The rate equation for change of fractional surface coverage is solved numerically in three steps in a form that for practical reasons differs in appearance from Eq. (31). The rate of change in surface coverage due to adsorption is derived as follows, starting with a suspension where the initial polymer dose is p_o and the initial total particle concentration is n_o:

$$p_{o1}/sn_o = F_o \qquad \text{for } \theta_e = 1.0 \tag{56}$$

$$p_o/sn_o = F \qquad \text{for any value of } \theta_e \tag{57}$$

where sn_o =initial number concentration if all flocs were broken down to singlets.

By definition, θ_e = actual polymer dose divided by polymer dose required to give 100% effective surface coverage; therefore

$$F/F_o = \theta_e \tag{58}$$

The initial polymer concentration is p_o and a small change, Δp, due to adsorption gives

$$\Delta p/sn_o = - \Delta F \tag{59}$$

$$\Delta F/F_o = \Delta\theta \tag{60}$$

where $\Delta\theta$ = change in surface coverage if the adsorbed polymer is shared equally by sn_o singlets.

If the polymer, Δp, is adsorbed by flocs containing k singlets the resulting surface coverage of k-flocs is calculated as

$$\Delta p/(kn_k) = - \Delta F_k \tag{61}$$

$$\Delta F_k/F_o = \Delta\theta_k \tag{62}$$

The orthokinetic adsorption rate of polymer due to collisions with k-flocs is

$$dp/dt = - \alpha(1-\theta_k)(4G/3)(a_k+a_p)^3 n_k p \tag{63}$$

$$(dp/dt)/(kn_k) = - \alpha(1-\theta_k)(4Gn_o a_1{}^3/3k)(k^m+r)spp_o/(sn_o p_o) \tag{63B}$$

Inserting $p/(kn_k) = F_k$ and $p_o/sn_o = F$ gives

$$dF_k/d\tau = (2s/k)\ \alpha(1-\theta_k)\ \sigma_{kp} FP \tag{63c}$$

$$(dF_k/d\tau)/F = (2s/k)\ \alpha(1-\theta_k)\ \sigma_{kp} P \tag{63d}$$

Using the relations $\theta_e = F/F_o$ and $\theta_k = F_k/F_o$ gives

$$(dF_k/d\tau)/(F_o\theta_e) = (2s/k)\ \alpha(1-\theta_k)\ \sigma_{kp} P \tag{63e}$$

$$d\theta_k/d\tau = (2s\theta_e/k)\ \alpha(1-\theta_k)\ \sigma_{kp} P \tag{31b}$$

The second step in calculating the surface coverage is to determine the average fractional surface coverage of k-flocs formed during the time interval $\Delta\tau$.

$$\theta_k^f = \sum_{\substack{i=1 \\ j=k-i}}^{i=k-1} (([(1-\theta_i)\theta_j+\theta_i(1-\theta_j)]\sigma_{ij}N_iN_j)/(dN_k/d\tau)_f)(i\theta_i+j\theta_j)/(i+j)$$

$$\theta_k^f = \sum_{\substack{i=1 \\ j=k-i}}^{i=k-1} A*B \tag{64}$$

where

$(dN_k/d\tau)_f$ = formation rate of k-flocs

A = probability of forming a k-floc from an i- and a j-floc

B = average surface coverage of a k-floc formed from an i- and a j-floc

Finally the average surface coverage is calculated at a point in time equal to $\tau + \Delta\tau$

$$\theta_k\ (\tau+\Delta\tau) = [(N_k(\tau+\Delta\tau)-\Delta\tau*(dN_k/d\tau)_f)*(\theta_\kappa(\tau)+\Delta\tau*(d\theta_k/d\tau)_\tau) + \theta_k^f*\Delta\tau*(dN_k/d\tau)_f]/N_k(\tau+\Delta\tau) \tag{65}$$

$$\theta_k\ (\tau+\Delta\tau) = (C*D+E*G)/N_k(\tau+\Delta\tau) \tag{65b}$$

where

C = number concentration of k-flocs which have only experienced adsorption during the time interval

D = new fractional surface coverage of k-flocs due to adsorption at time $\tau + \Delta\tau$

E = fractional surface coverage at time $\tau + \Delta\tau$ of k-flocs which have been formed during the time interval

G = number concentration of k-flocs, which have been formed during the time interval

The dimensionless perikinetic adsorption rate is derived from Eq. (1).

$$dp/dt = -\sum_{i=1}^{\infty} \alpha(1-\theta_i)4\pi D_{ip}(a_i+a_p)n_ip \tag{66}$$

$$dp/dt = - \sum_{i=1}^{\infty} \alpha\ (1-\theta_i)4\pi D_p a_p(1/a_i+1/a_p)(a_i+a_p)n_i p$$

$$dp/dt = - \sum_{i=1}^{\infty} \alpha[(1-\theta_i)4\pi[k_B T/(6\pi\mu)](a_i+a_p)^2/(a_i a_p)]n_i p$$

$$dp/dt = - \sum_{i=1}^{\infty} \alpha[(1-\theta_i)[2k_B T/(3\mu)](i^m+r)^2/(i^m r)]n_i p n_o p_o/(n_o p_o)$$

$$dP/dt = -n_o[2k_B T/(3\mu)]16Ga_1^3 3/(16Ga_1^3 3) \sum_{i=1}^{\infty} \alpha(1-\theta_i)\beta_{ip}N_i P$$

$$dP/d\tau = -k_B T/(8\mu Ga_1^3) \sum_{i=1}^{\infty} \alpha(1-\theta_i)\beta_{ip}N_i P$$

$$dP/d\tau = -K_{Ga} \sum_{i=1}^{\infty} \alpha(1-\theta_i)\beta_{ip}N_i P \qquad (33b)$$

The dimensionless perikinetic flocculation rate and the rate of change of fractional surface coverage are derived analogously.

The program starts by reading the initial floc size distribution and the initial polymer dose expressed as θ_e. The dimensionless floc and polymer concentrations and the surface coverage are then calculated by Euler integration and the results are plotted and printed. Flocculation did not proceed very far in general and the hydrodynamic collision efficiency is therefore taken to be independent of floc size and is included in the dimensionless time.

Flocculation rates with polymer pretreated particles are calculated with a similar program including two floc size distributions, one for clean and one for polymer covered particles, but omitting the adsorption step. The computer programs are available at the Computer Center of The Institute of Paper Chemistry.